The secreted serine protease xHtrA1 is a positive feedback regulator of long-range FGF signaling

PhD Thesis

in partial fulfillment of the requirements
for the degree "Doctor of Philosophy (PhD)"
in the Molecular Biology Program
at the Georg August University Göttingen,
Faculty of Biology

submitted by

Shirui Hou

born in

Beijing, P. R. China

June, 2007

Affidavit

Herewith I declare, that I prepared the PhD thesis

"The secreted serine protease xHtrA1 is a positive feedback regulator

of long-range FGF signaling "

on my own and with no other sources and aids than quoted.

Shirui Hou   _____

Date of submission   June, 2007

List of Publications

1. Pera E. M., <u>Hou S.</u>, Strate I., Wessely O., De Robertis E. M. (2005). Exploration of the extracellular space by a large-scale secretion screen in the early *Xenopus* embryo. *Int J Dev Biol*, 49, 781-96.

2. <u>Hou S.</u>, Maccarana M., Min T. H., Strate I., Pera E. M. The secreted serine protease xHtrA1 is a positive feedback regulator of long-range FGF signaling (accepted for publication in *Dev. Cell*).

TABLE OF CONTENTS

Acknowledgments

Abstract

Fibroblast growth factors (FGFs) are important signaling molecules, whose activities need to be tightly controlled. We have recently identified the *Xenopus* homolog of HtrA1 (xHtrA1) in a direct screen for secreted proteins (Pera et al., 2005). In this thesis, we show that *xHtrA1* is co-expressed with *FGF8* in the embryo, and that its expression is activated by FGF signals, suggesting that xHtrA1 belongs to the FGF8 synexpression group. Misexpression of xHtrA1 phenocopies multiple effects of FGFs, including posterior specification, mesoderm induction, neuronal differentiation, cell motility and proliferation. Downregulation of xHtrA1 activity via an antisense morpholino oligonucleotide or a polyclonal antibody leads to an overall phenotype reminiscent of FGF loss-of-function, with enlargement of head and reduction of ventroposterior structures. *xHtrA1*-MO also impairs mesoderm formation and neuronal differentiation. xHtrA1 cooperates with FGF and requires intact FGF signaling pathway for its patterning activities. xHtrA1 stimulates FGF/ERK activity, induces the transcription of *FGF4* and *FGF8* and allows long-range FGF signaling. In biochemical experiments, we could demonstrate that Biglycan, Syndecan4 and Glypican4 are cleaved by xHtrA1. In microinjected *Xenopus* embryos, purified heparan sulfate and dermatan sulfate induce posteriorization, mesoderm induction and neuronal differentiation in an FGF-dependent manner. These findings suggest that xHtrA1 may act as a positive feedback regulator of FGF signals that through proteolytic cleavage of proteoglycans allows long-range FGF signaling in the extracellular space.

List of Figures

Abbreviation

A	Adenine
AP	Alkaline phosphate buffer
ATP	adenosine triphosphate
BCIP	5-bromo-4-chloro-3-indolyl-Phosphate
BMB	Bohringer Mannheim Blocking Reagent
BMP	bone morphogenetic protein
bp	base pairs
BSA	bovine serum albumin
C	cytosine
°C	celsius degree
cDNA	complementary DNA
CHAPS	3-(3-cholamidopropyl)dimethylammonio-1-Propansulphate
CFP	canyon fluorescent protein
ddH$_2$O	Distilled water
DIG	Digoxigenin-11-2'-deoxyuridin-5'-triphosphate
DMSO	Dimethylsulfoxide
DNA	deoxyribonucleic acid
DNase	Deoxyribonuclease
DTT	dithiothreitol
E.coli	*Escherichia coli*
EDTA	ethylendiaminetetraacetic acid
et al.	et alii
HEPES	4-(2- Hydroxyethyl)-1-piperazin
G	guanine
GPI	glycosylphosphatidylinositol
h	hours
HCG	human chorionic gonadotropin
kb	kilobase
L	liter
LB	Luria-Bertani (medium)
m	milli
μ	micro
M	molar (mol/l)
MAB	malic acid buffer
MEM	MOPS-DGTA-MgSO4-Buffer
MEMFA	MOPS-DGTA-MgSO4-Formaldehyde-Buffer
min	minutes
MOPS	4-Morpholinpropanosulfonic acid
mRNA	messenger RNA
NaAc	sodium acetate
OD	optical density
PAGE	polyacrylamide gel electrophoresis

PBS	Phosphate buffered saline
PBSw	1% Tween-20 in PBS
PDZ	PSD95/DlgA/ZO-1 homology
PCR	polymerase chain reaction
pH	preponderance of hydrogen ions
%	percent
Red-gal	5-Bromo-6-Chloro-3-indolyl-!-Dgalactopyranoside
RNA	ribonucleic acid
RT-PCR	reverse transcriptase-PCR
sec	second
SSC	standard saline citrate buffer
T	Thymine
Taq	*Thermus aquaticus*
TAE	Tris-Acetic acid-EDTA-Electrophoresis buffer
Tm	melting temperature
U	units
UV	ultra violet light
Vol.	volume
X-Gal	5-Bromo-4-Chloro-3-indolyl-!-Dgalactopyranoside
X. laevis	*Xenopus laevis*

1 Introduction

1.1 *Xenopus laevis* as model system for developmental biology

The establishment of the vertebrate body plan is a topic of considerable interest in developmental biology. The amphibian embryo has been a fruitful experimental system for these investigations because of its large egg size, its external embryonic development, and its ability to easily heal after microsurgery. These features are important prerequisites for studying the early development of the embryonic axis. Classical experimental approaches, such as fate mapping, transplantation experiments and explant cultures, together with molecular biology methods make the *Xenopus* embryo an excellent model to unravel the signaling network underlying body axis patterning. Overexpression of genes can be quickly and easily done by microinjection of *in vitro* synthesized RNA, DNA or proteins. Downregulation of gene activity can be achieved by injecting antisense morpholino oligonucleotides or, in the case of extracellularly expressed proteins, by injecting antibodies into the blastocoel cavity. In order to block a certain molecular pathway, dominant negative receptors, dominant negative signaling intermediates or pharmacological inhibitors can be injected. Animal cap explants resemble mammalian embryonic stem cells with respect to their pluripotency to give rise to derivatives of all three germ layers *in vitro*, when exposed to appropriate signaling factors, and provide a strong tool to study the molecular basis of embryonic induction and cell lineage specification.

1.2 The breakage of symmetry in *Xenopus* embryos

In *Xenopus*, the first body axis to be established is the dorsoventral (DV) axis. Upon entry of the sperm into the animal hemisphere, the outer layer of the egg rotates relative to the yolk core cytoplasm. This cortical rotation and the assembly of subcortical microtubule (MT) bundles translocate dorsal determinants from the vegetal part to the future dorsal side, which is opposite to the sperm entry site (Elinson and Rowning, 1988, review see Weaver et al., 2004). The dorsal determinants consist of Dishevelled (Dsh) and Glycogen Synthase Kinase 3 (GSK3)-binding protein (GBP). Microinjection of Dsh or GBP mRNA into early *Xenopus* embryos leads to the formation of a complete dorsal axis (Yost et al., 1998; Sokol et al., 1995). Conversely, when GBP is depleted by injecting antisense oligonucleotides into *Xenopus* oocyte, the dorsal axis fails to form (Yost et al., 1998). The dorsal determinants are transported to the future dorsal side via the track of microtubules

through interaction of GBP and kinesin light chain (KLC), which forms a heterotetrameric microtubule motor of kinesin. Both GBP and Dsh are involved in activation of the canonical Wnt pathway. GBP binds directly to Dsh, a GSK3 inhibitor that is activated by a canonical Wnt pathway (Yost et al., 1998; Li et al., 1999; Salic et al., 2000). In addition, GBP binds to GSK3 and causes the degradation of GSK3 (Dominguez and Green, 2000; Farr et al., 2000). The dorsal-localized GBP and Dsh prevent GSK3 from phosphorylating β-catenin. As a result, β-catenin is prevented from being degraded in the ubiquitin-proteasome pathway and accumulates in the nuclei on the dorsal side of the embryo. As a transcription factor, β-catenin binds to the transcriptional repressor complex containing T-cell factor/Lymphoid enhancer factor (TCF/LEF) transcription factors, converts the complex into an activator, and initiates the transcription of Wnt target genes (for review see Miller et al., 1999). The intracellular components of the Wnt pathway are clearly involved in *Xenopus* axis specification. Recently, the extracellular signal Wnt11, which is maternally enriched on the dorsal side of two-cell stage embryos (Shroeder et al., 1999), has been demonstrated to be crucial for axis formation in *Xenopus* embryos (Tao et al., 2005).

1.3   Mesoderm induction during embryogenesis

During early *Xenopus* development, the mesoderm forms in the equatorial region of the blastula embryo. Classical recombination experiments have shown that mesoderm tissue is induced in the animl cap ectoderm juxtaposed to vegetal endoderm explants (Nieuwkoop 1969; Gilbert 2003), indicating that the animal hemisphere responds to signals emitted from the underlying vegetal pole and adopts a mesoderm fate in the marginal zone. The induced mesoderm then differentiates into prechordal plate, notochord, somite, kidney, lateral plate mesoderm and ventral blood islands in a dorsal to ventral order (De Robertis and Kuroda, 2004). A variety of proteins and transcription factors have been tested for the mesoderm-inducing activity in the animal cap assays.

Members of the TGF-β superfamily have been shown to have the capability to induce mesoderm. A *Xenopus* homologue of activin A can induce animal cap explants to form several different types of mesoderm in a dose dependent manner, with low doses of activin A generating ventral mesoderm, such as mesenchyme and blood island cells, and higher doses inducing more dorsal mesoderm, such as segmented muscles, pronephros and

notochord (Smith et al., 1990; Green et al., 1990). A *Xenopus* homologue of activin B has a similar mesoderm-inducing activity like activin A (Thomsen et al., 1990), whereas, activin D is a less potent mesoderm inducer (Oda et al., 1995). The protein of activin A and B and the transcripts of activin D are found maternally before midblastula transition (Fukui et al., 1994; Dohrmann et al., 1993; Rebagliati and Dawid, 1993, Fukui et al., 1999; Oda et al., 1995), at the time when mesoderm induction takes place. However, mRNAs and proteins of all activin isoforms are ubiquitously distributed throughout the three germ layers, which cannot explain the formation of the mesoderm only in the marginal zone, suggesting that other vegetal-localized signals may be involved in the induction of mesoderm. Vg1 is a member of the TGF-β family, both mRNA and protein are maternally expressed and localized in the prospective endoderm (Weeks and Melton, 1987). Experiments with a chimeric Vg1, which can be efficiently processed *in vivo,* demonstrate that Vg1 has potent dorsal mesoderm-inducing abilities in the animal cap explants (Thomsen and Melton, 1993; Dale et al., 1993). Treating animal caps with mature Vg1 protein leads to the upregulation of *Xenopus* nodal related 1 (Xnr1), which is another mesoderm-inducing factor (Agius et al., 2000). However, the mature processed Vg1 protein is not endogenously detected before gastrulation (Tannahill and Melton, 1989). Recently, Birsoy and colleagues showed that Vg1-depleted *Xenopus* embryos exhibit lack of dorsal mesoderm structures and this effect can be partially rescued by a second allele of Vg1, which can be processed successfully *in vivo*, Overexpression of this efficiently processed Vg1 induces mesoderm marker expression in animal cap explants (Birsoy et al., 2005). Several BMPs, including BMP2, BMP4, BMP7, are abundant as maternal mRNAs in the animal hemisphere (Koster et al., 1991; Nishimatsu et al., 1992; Dale et al., 1992; Jones et al., 1992). Overexpression of BMPs in naive animal cap explants causes the formation of ventral mesoderm derivatives including mesenchyme, blood islands and muscle but not dorsal mesoderm-like notochord (Dale et al., 1992; Jones et al., 1992; Garff et al., 1994; Suzuki et al., 1994; Hemmati-Brivanlou and Thomsen, 1995). VegT is a T-box transcription factor, whose mRNA is maternally transcribed and restricted to the vegetal hemisphere of eggs and embryos (Stennard et al., 1996; Lustig et al., 1996; Zhang and King, 1996). The temporal and spatial expression pattern suggest that VegT may be one of the endogenous mesoderm-inducing signals secreted from the vegetal pole. Indeed, microinjection of synthetic *VegT* mRNA can specify mesodermal fates in animal caps (Stennard et al., 1996; Lustig et al., 1996; Zhang and King, 1996). Eliminating maternal

VegT transcripts in oocytes by antisense oligonucleotides blocks the mesoderm-inducing activity of vegetal pole explants in Nieuwkoop ectoderm-endoderm combination experiment and disrupts formation of mesoderm tissues in whole embryos (Kofron et al., 1999). These experiments suggest that VegT may act as an endogenous factor to initiate mesoderm formation in the overlying equatorial plane.

The evidence that disruption of TGF-β signaling by the dominant negative activin receptor tAR (Hemmati-Brivanlou and Melton, 1992) blocks VegT-mediated mesoderm induction, showed that the mesoderm inducing activity of VegT depends on an intact TGF-β pathway (Clements et al., 1999). After the mid-blastula transition, the maternally expressed VegT protein on the vegetal pole activates transcription of the *Xenopus* nodal-related genes Xnr 1,2,4,5,6, that all have the ability to induce mesoderm formation in animal cap explants (Hyde and Old, 2000; Clements et al., 1999; Kofron et al., 1999; Xanthos et al., 2001). On the dorsal side of the embryo, nuclear-localized β-catinin upregulates Xnr (Agius et al., 2000; Takahashi et al., 2000). Within the endoderm, the dorsal-localized β-catinin cooperates with the vegetal VegT to generate an Xnr gradient with lower Xnr activity on the ventral side and higher activity on the dorsal side. High levels of nodals induce dorsal mesoderm in the overlying equatorial zone, whereas low levels of nodal signal induce more ventral mesoderm (Agius et al., 2000). Another VegT target gene is Derrière, a vegetally expressed TGF-β family member, whose zygotic transcription is initiated by maternal VegT. Derrière was shown to be potent for mesoderm and endoderm induction. A dominant negative Derrière construct (Cm-Derrière) ablates posterior- and paraxial- mesoderm specific gene expression, suggesting that Derrière is crucial for mesoderm patterning. (Sun et al., 1999) In sum, the maternally expressed signals from the vegetal pole, such as VegT and likely also Vg1, activate the gene expression of members of the TGF-β family including Xnrs and Derrière in the endoderm after mid-blastula transition, these members together with ubiquitously expressed activin contribute to the initiation of mesoderm formation on the cells overlying endoderm.

1.4   The formation of the Spemann-Mangold organizer

Hans Spemann and Hilde Mangold reported that the dorsal blastopore lip of an amphibian gastrula embryo has the ability to induce a twin body axis, when transplanted into the ventral side of a sibling host embryo (Spemann and Mangold, 1924). Specifically, the

organizer tissue induces a central nervous system (CNS) in the ectoderm, dorsalizes the mesoderm and endoderm, and induces gastrulation movements. The dorsal accummulation of β-catenin activates the expression of Wnt target genes, such as the homeobox gene Siamois. Siamois synergizes with the vegetal-localized TGF-β family members Vg1 and Nodal-related proteins to activate the Goosecoid gene (Laurent et al., 1997; Brannon and Kimelman, 1996; Agius et al., 2000). Goosecoid is another homeobox-containing transcription factor that activates various target genes that encode antagonists against BMP, Wnt and the Nodal pathway. The group of cells in the dorsal mesoderm that receive both β-catenin signal from the dorsal side and Vg1, VegT and Nodal-related proteins from the vegetal side give rise to the Spemann-Mangold organizer.

1.5   The default model of neural induction

The CNS is derived from the dorsal ectoderm or neuroectoderm, whereas the ventral ectoderm gives rise to epidermis. The Spemann-Mangold organizer transplantation experiment showed that the dorsal blastopore lip can convert epidermis into neural tissues. Dissociated animal cap cells from *Xenopus laevis* adopt a neural fate, suggesting that a neural character could derive from ectoderm in the absence of the Spemann-Mangold organizer or other exogeneous signals (Godsave et al., 1988; Grunz and Tacke, 1990; Sato and Sargent 1989). This together with the observation that a dominant negative activin receptor (ActRIIB), which blocks the BMP pathway (Dale and Jones, 1999), induced neural tissue in animal cap explants (Hemmati-Brivanlou and Melton, 1992), leads to the idea of the default model of neural induction. This model suggests that the ectoderm by default gives rise to neural tissue rather than epidermis tissue in the absence of epidermis-inducing factors (Gilbert, 2003).

Several experiments from *Xenopus* research groups support the default model. Members of the TGF-β superfamily, such as BMP2, BMP4, BMP7 and growth and differentiation factor 6 (GDF6) were shown to repress neural-specific and induce epidermal markers in dissociated animal caps (Suzuki et al 1997; Wilson and Hemmati-Brivanlou 1995; Chang and Hemmati-Brivanlou, 1999). These factors are initially expressed ubiquitously in the ectoderm, but as gastrulation proceeds, they are excluded from the prospective neural plate (Hemmati-Brivanlou and Thomsen 1995; Hawley et al., 1995; Chang and Hemmati-Brivanlou, 1999). Activation of BMP signaling stimulates epidermal and represses neural

tissue development. Constitutively active BMP receptors, such as Alk2, Alk3, and Alk6, or of the BMP intermediates Smad1 and Smad5, induce epidermis marker in dissociated animal cap explants (Suzuki et al. 1997 a, b; Wilson et al 1997). In contrast, inhibition of the BMP pathway is sufficient to promote neural fate in ectodermal explants or whole embryos. Simultaneous depletion of endogenous BMP2, BMP4 and BMP7 by injecting antisense morpholino oligonucleotides led to embryos with significantly enlarged neural plates (Reversade et al., 2005). Quadruple knockdown of BMP2, BMP4, BMP7 and the organizer-specific TGF-β factor ADMP (anti dorsalizing morphogenetic protein) caused completly neuralized embryos devoid of any epidermis (Reversade and De Robertis, 2005). Soluble antagonists of bone morphogenetic proteins (BMPs), including noggin (Lamb et al., 1993), chordin (Sasai et al., 1995), follistatin (Hemmati-Brivanlou et al., 1994) and Xnr3 (Hansen et al., 1997) are secreted from the Spemann-Mangold organizer near the prospective neural plate. Microinjection of each of these mRNAs is able to induce anterior neural markers in animal cap explants. Connective-tissue growth factor (CTGF), which expressed in CNS derivatives, such as the floor plate, blocks BMP transduction by sequestering the ligand and preventing it from interacting with BMP receptors. Injection of *CTGF* RNA into animal cap explants induced neural marker expression (Abreu et al., 2002). Overexpression of two inhibitory Smads, Smad6 (Hata et al., 1998) and Smad7 (Souchelnytskyi et al., 1998; Casellas and Brivanlou, 1998) or injection of ectodermin, a Smad4 ubiquitin ligase involved in the degradation of Smad4 (Dupont et al., 2005), blocks BMP transduction and leads to neural tissue induction. Overexpression of Smurf1 (Zhu et al., 1999), Smurf2 (Zhang et al., 2001), which are E3 ubiquitin ligases that degrade Smad effectors in the BMP pathway, or Smad interacting protein 1 (SIP1) (Nitta et al., 2004) all antagonize BMP signaling and give rise to neural induction in animal cap tissues. The secreted protein Cerberus, which is a triple inhibitor of BMP, Wnt8 and Nodal signals, is expressed in the anterior endoderm, in close vicinity to the presumptive forebrain tissue. Microinjection of *Cerberus* mRNA led to ectopic head structure and neural tissue formation in whole embryos (Bouwmeester et al., 1996). Coco, expressed in the ectoderm until the end of gastrulation, is a maternal Cerberus/Dan like inhibitor of BMP, TGF-β and Wnt signaling. Overexpression of Coco caused neural marker induction in animal caps (Bell et al., 2003). In sum, research in *Xenopus* favors the idea that ubiquitously expressed BMPs prevent ectoderm cells from adopting their default neural fate. The inhibition of BMP signaling in the dorsal ectoderm by BMP antagonists from the ectoderm, underlying

dorsal mesoderm (Spemann-Mangold organizer) or anterior endoderm permit ectoderm cells to execute their natural tendency to generate neural tissue (for review see Vonica and Hemmati-Brivanlou, 2006).

Recent research suggests that neural induction takes place as early as the blastula stage, before the Spemann-Mangold organizer forms. At mid-blastula, the ectoderm starts to express distinct markers along the dorsal-ventral axis, suggesting that ectodermal cells are already specified (Gamse and Sive, 2001; Kroll et al., 1998). In the blastula stage, the nuclear translocation of β-catenin in the dorsal ectoderm induces the expression of BMP antagonists such as Chordin and Noggin (Wessely et al., 2001). Consequently, this dorsal ectoderm area was designated as BCNE center (Blastula Chordin and Noggin Expression center, Kuroda et al., 2004). The BCNE center has been shown to be required for neural specification, since brain formation was impaired when the BCNE center was excised. Moreover, the BCNE still formed neural tissue in embryos injected with the Nodal inhibitor Cerberus-short, indicating that the CNS develops in the absence of mesoderm. This experiment suggests that neural specification is initiated before establishment of the Spemann-Mangold organizer.

In agreement with the default model of neural induction by antagonizing BMP signaling, several pieces of evidence showed that enhancement of BMP signaling activates a number of transcription factors including Msx1, Gata1 and Vent1 and Vent2 proteins (Suzuki et al., 1997c; Xu et al., 1997; Onichtchouk et al., 1996), which act as transcriptional repressors and inhibit expression of the neural inducer SoxD (Mizuseki et al., 1998; Sasai, 1998). Conversely, blockage of BMP signal transduction relieves the repression of SoxD by downregulation of BMP target genes. Expression of SoxD leads to the induction of Ngnr1 and the onset of neuronal development (Mizuseki et al., 1998).

1.6   Other signals involved in neuralization

Studies in amphibian and amniotes suggest that the competence, specification, commitment and differentiation of neural character from naive ectoderm may not simply result from inhibiting the BMP pathway, but instead require the integration of multiple signals. Wnt signaling has been implicated in the selection of neural or epidermal fate. The acquisition of neural fate can be regarded as the dorsalization of ectoderm, which results

from dorsal-ventral axis formation soon after fertilization. The future dorsal side is determined by the nuclear accumulation of the Wnt effector β-catenin. Therefore, activation of Wnt signaling by injecting mRNAs encoding Wnt or its signal mediators into the animal hemisphere of very early embryos generates a dorsalized phenotype with ectopic neural tissues. Activation of early Wnt signaling induced neural maker gene expression in animal caps as well (Baker et al., 1999). Although early Wnt signaling is sufficient for ectopic neural induction, in later development, Wnt signaling eventually suppresses the generation of neural cells (for review see Logan and Nusse, 2004). Expression of several Wnt inhibitors induces neural markers in the animal cap assay (Glinka et al., 1997, 1998). Studies in chick indicated that in the lateral epiblast cells, where Fibroblast growth factors and Wnt exist, Wnt blocks the response of epiblast cells to FGFs, which allows BMP transcription to occur and epidermis to form. Inhibition of the Wnt pathway is sufficient and necessary to elicit epidermal lateral epiblast cells to adopt neural fate (Wilson et al., 2001).

Insulin growth factor (IGF) was shown to be both sufficient and required for the induction of ectopic head structures in whole embryos. In animal cap explants, *IGF1* and *IGF2* mRNA had the ability to induce anterior neural tissues without mesoderm formation and the neural induction by Chordin was inhibited when IGF signals were attenuated. (Pera et al., 2001; Richard-Parpaillon et al., 2002). The evidence that activation of IGF counteracted Wnt8, dominant negative GSK3 and β-catenin, but not the activated form of Tcf, suggest that IGF signals inhibit Wnt signaling downstream of β-catenin (Richard-Parpaillon et al., 2002). Activation of IGF1R by IGF1 or IGF2 can activate the Ras-MAP kinase pathway or the PI3 kinase (phosphatidylinositide-3 kinase)-Akt pathway (Blume-Jensen Hunter et al., 2001). Both an active PI3K subunit and Akt can, induce secondary axes in mRNA-injected *Xenopus* embryos and neuralization in injected animal caps. This ability was mediated by inhibiting GSK3β and therefore antagonizing the Wnt pathway (Peng et al., 2004).

It has been shown that FGF and IGF signal through receptor tyrosine kinase (RTK) and mitogen-activated protein kinase (MAPK) activation by phosphorylating the linker region of Smad1 (Pera et al., 2003). This linker phosphorylation prevents Smad1 from

translocating into the nucleus, and hence inhibits Smad activity (Kretzschmar et al., 1997; Massague, 2003). This effect counteracts the one of C-terminal Smad phosphorylation by the BMP receptor serine-threonine protein kinase and allows neural induction to occur (Pera et al., 2003). Recently, it was shown that the auto-neuralization observed in dissociated animal caps requires sustained MAPK activity, since blocking the MAPK pathway at different intracellular levels eliminated the neural marker induction and maintained the epidermal marker expression instead (Kuroda et al., 2005). The neuralization in this system also relied on the inhibition of BMP/Smad1 activity through MAPK. In sum, neural induction requires low levels of Smad1 activity, achieved by attenuating C-terminal phosphorylation mediated by BMP pathways, and elevating linker phosphorylation by FGF or IGF through MAPK (Kuroda et al., 2005).

1.7   Regional specification of the central nervous system

Nieuwkoop suggested a two-step model for the induction and regional specification of the central nervous system (Gilbert, 2003). During the first step („activation"), signals from the early invaginating endomesoderm induce neural tissue of an anterior or forebrain-like type. During the second step („transformation"), signals from later invaginating mesoderm cells convert this anterior neural tissue gradually into more posterior neural tissue, giving rise to midbrain, hindbrain and spinal cord. Studies in *Xenopus* have shown that the activation step is mediated by soluble antagonists of bone morphogenetic protein (BMP) and Wnt signals (De Robertis and Kuroda, 2004; Niehrs, 2004). Chordin, Noggin and Follistatin directly bind to and inhibit BMP ligands in the extracellular space. Frzb-1 and Dickkopf-1 specifically block Wnt signaling. The head inducer Cerberus acts as a triple inhibitor of BMP, Wnt and Nodal signals. In addition, IGFs contribute to head and neural induction through antagonizing BMP and Wnt signaling at an intracellular level (Pera et al., 2001, 2003; Richard-Parpaillon et al., 2002). The transforming step is mediated by retinoic acid, Wnt and FGF signals (Maden, 2002; Niehrs, 2004; Böttcher and Niehrs, 2005).

1.8   Fibroblast growth factor signaling

Fibroblast growth factors (FGFs) comprise a family of at least 22 secreted proteins. They signal through FGF receptors, encoded by four distinct genes *FGFR1-4* and several splicing isoforms that together form a subfamily of cell surface receptor tyrosine kinases

(RTKs). Binding of FGF ligands causes receptor dimerisation and tyrosine kinase activation, leading to the activation of phospholipase C-γ (PLC-γ), phosphatidylinositol-3-kinase (PI3K), and the Ras to extracellular signal regulated protein kinase (ERK) pathways. ERKs are a subclass of the mitogen activated protein kinases (MAPKs).

These pathways regulate a number of biological phenomena, including cell proliferation, differentiation and migration. During early vertebrate development, FGF signaling is crucial for the induction of mesoderm and endoderm, neural fate specification, axial polarity and morphogenetic movements (Böttcher and Niehrs, 2005). Studies in *Xenopus* have first demonstrated a role of FGFs in the induction and migration of mesoderm during trunk and tail development (Slack et al., 1996). In chick and *Xenopus* embryos, FGFs participate in the induction of neural fate (Hongo et al., 1999; Streit et al., 2000; Wilson et al., 2000; Hardcastle et al., 2000; Pera et al., 2003, De Robertis and Kuroda, 2004). In addition, FGFs act as posteriorizing factors during anteroposterior patterning of the central nervous system (Lamb and Harland, 1995; Cox and Hemmati-Brivanlou, 1995). Then, FGFs are involved in many later cell interactions, patterning the telencephalon and midbrain-hindbrain boundary (Dono, 2003), during limb outgrowth (Martin, 1998), bone formation (Ornitz, 2005), angiogenesis (Presta et al., 2005) and in cancer (Grose and Dickson, 2005).

1.9   FGFs in mesoderm induction

Members of FGF family are present in blastula stage embryos, suggesting an involvement in mesoderm formation (Slack et al., 1987; Kimelman et al., 1988; Isaacs et al., 1992). Purified bovine bFGF can convert animal cap explants into ventral mesoderm tissues, such as mesenchyme, mesothelium and blood cells (Kimelman and Kirschner, 1987). However, since bFGF lacks a signal sequence, it remains unclear how this protein could participate in signal transduction events (Kimelman et al., 1988). *Xenopus* embryonic FGF (XeFGF), a homologue of human FGF4, has a detectable signal peptide and can be efficiently secreted. The expression of FGF4 is maternal and increases significantly when gastrulation starts. During gastrulation, FGF4 transcripts are restricted to the mesoderm around the blastopore ring (Isaacs et al., 1992). It has been found that FGF4 has robust mesoderm-inducing activity in mRNA-injected animal caps (Isaacs et al., 1994). FGF4 has been shown to generate a positive autoregulatory loop with the T-box transcription

factor Xbra, in which each factor activates the transcription of the other, hence stabilizing mesoderm formation in the marginal zone (Isaacs et al., 1994). Exogenously added bFGF, FGF4 or activated Ras induces ectopic expression of mesodermal marker genes in vegetal explants where the activin-like signal exists (Cornell et al., 1995). This experiment suggest FGF act as a competence factor in the marginal zone, allowing marginal zone cells to respond to the activin-like signal and form mesoderm.

Several pieces of evidence support that FGF signals are essential for mesoderm induction. Inhibition of FGF signaling by a dominant inhibitory FGFR1 construct (XFD) results in the blockage of mesoderm, including notochord, muscle and ventral mesoderm, and prevents posterior cells from undergoing proper gastrulation movements (Amaya et al, 1991, 1993). XFD, or two dominant negative effectors of the MAPK pathway, c-Ras and c-Raf, inhibit the ability of activin to induce both dorsal and ventral mesoderm markers, suggesting the requirement of FGF signals for mesoderm induction by activin. Therefore FGF signaling appears to be a permissive signal to permit activin-mediated mesoderm induction (LaBonne and Whitman 1994; Cornell et al., 1995). In mice, FGF4 and FGF8 are required for the migration of cells out of the primitive streak and thus for the formation of mesoderm (Sun et al., 1999). FGF signals are also essential for the migration and patterning of mesoderm in *Drosophila* (Huang and Stern, 2005).

1.10   FGFs in neural induction

A role of FGFs has been suggested during neural induction. Basic FGF can induce gastrula stage ectoderm cells to express neural markers along the anterior-posterior axis in a dose-dependent manner, with lower doses inducing anterior neural marker genes and higher doses more posterior neural markers. This neural inducing activity is direct, since the applied dosis of basic FGF was 50 fold lower than that required to induce mesoderm, and did not induce transcription factors expressed in the Spemann-Mangold organizer (Kengaku and Okamoto, 1993, 1995). Basic FGF induced pan-neural marker gene expression in early to late gastrula ectoderm without mesoderm formation. Moreover, the anterior-posterior neural character induced by bFGF also depended on the age of gastrula ectoderm, with early gastrula ectoderm expressing posterior neural markers and older ectoderm being competent to form more anterior neural markers (Lamb and Harland 1995). A constitutively active chimeric FGFR1 induced the upregulation of posterior

11

neural markers such as Krox20 and HoxB9 in animal caps neuralized by dominant negative type II activin/BMP4 receptor (ActRIIB). When a constitutively active FGFR4 was injected into ectoderm that had been neuralized by ActRIIB, more anterior midbrain markers such as En2 and Wnt1 were induced. This inducing activity required the PLC-γ pathway, since a FGFR4 mutant, in which a conserved tyrosine residue was mutated and cannot bind to PLC-γ, completely blocked induction of these midbrain markers (Umbhauer et al., 2000). FGF8 mRNA injection was shown to induce ectopic neural markers in whole embryos (Hardcastle et al., 2000).

Intact FGF signaling is required for neural induction. Overexpression of a dominant negative FGFR4a construct (DnFGFR4a), which lacks the intracellular tyrosine kinase domain, led to the loss of telencephalon and eye structures. Furthermore, the DnFGFR4a inhibited neural marker gene expression induced by the Spemann-Mangold organizer or prolonged dissociation of ectodermal explants (Hugo et al., 1999). Similarly, neural induction and neural differentiation was diminished by DnFGFR4a, as judged by the loss of the early pan-neural marker Sox2 and the neuronal marker N-tubulin (Hardcastle et al., 2000; Delaune et al., 2005). Overexpression of another dominant negative FGFR1 (XFD) blocked neural induction in animal cap explants that had been injected with Noggin or Chrodin (Launay et al., 1996; Sasai et al., 1996), or recombined with Spemann-Mangold organizer (Launay et al., 1996). The FGFR1 inhibitor SU5402 induced defects including impairment of neural tissues and loss of axial tissue from posterior to anterior in a dose-dependent manner. SU5402 prevented neural induction of ectodermal explants by the Spemann-Mangold organizer, or by Noggin, dominant negative BMP receoptor (tBR) and Smad6 mRNA injection (Delaune et al., 2005). Similarly, in chick embryos, FGF signaling is also required for neural induction. At the blastula stage, FGF3 is expressed in the neurogenic medial ectoderm. When a medial ectoderm explant was treated with the FGFR1 antagonists SU5402, BMP transcription was upregulated and the tissue acquired an epidermal fate, suggesting that endogenous FGF signals may attenuate BMP signals (Wilson et al., 2000). The observation that addition of BMP antagonists can restore neural fate of medial epiblast explants that have been treated with low but not with high doses of the FGFR antagonist suggested that apart from merely inhibiting BMP transcription, FGFs activate an independent pathway to promote neural fate (Wilson et al., 2000, 2001).

1.11   FGFs in posterior development

Apart from its ability to initiate a neural character, FGFs have also been shown to caudalize neural tissues (for review see Doniach, 1995). In *Xenopus*, the cement gland is the rostal-most structure at the anterior ridge of the neural plate (Sive and Bradley, 1996), which responded to very low BMP activity and was detected in dissociated animal cap explants. Addition of bFGF protein transformed dissociated ectoderm explants into more posterior structures (Lamb and Harland, 1995). Similarly, the transcription factor Sox2 can induce cement gland differentiation in ectoderm explants, and supplemented bFGF induced neural tissue (Mizuseki et al., 1998a). Anterior neural tissues induced in animal caps by BMP antagonists such as Noggin, Follistatin or Chordin were converted to form posterior neural tissues in the presence of bFGF proteins (Lamb and Harland, 1995; Cox and Hemmati-Brivanlou, 1995; Sasai et al., 1996). Applying bFGF protein to presumptive hindbrain tissues induced spinal cord marker gene expression (Cox and Hemmati-Brivanlou, 1995). In whole embryos, FGF8 induced a transformation of the caudal diencephalon to more posterior midbrain structures. When FGF4- or FGF8- soaked beads were implanted into the prospective forebrain regions of neurula or tailbud stage *Xenopus* embryos, ectopic expression of the midbrain markers En2 and Wnt1 was observed (Riou et al., 1998). A similar posteriorizing effect of FGF8 was observed in chick embryos (Crossley et al., 1996). In addition, FGF8 mutants in mouse and zebrafish lack posterior midbrain and cerebellar tissues (Meyers et al., 1998; Reifers et al., 1998), pointing towards a pivotal role of FGF8 in the development of the midbrain in vertebrate embryos.

1.12   Proteoglycans as regulators of FGF signaling

Proteoglycans are abundant extracellular molecules that consist of a protein core to which highly sulfated glycosaminoglycan (GAG) residues are covalently attached. According to their sugar composition, the GAG chains are classified as heparan sulfate, chondroitin sulfate or dermatan sulfate (Iozzo, 1998; Bernfield et al., 1999; Buelow and Hobert, 2006). Glypicans and Syndecans are two major cell surface heparan sulfate proteoglycans. Members of the small leucine-rich proteoglycan family, such as Decorin and Biglycan, are associated with the cell surface or pericellular matrix, and belong to the chondroitin or dermatan sulfate proteoglycans. Biochemical and cell culture experiments have identified proteoglycans as co-regulators of several growth factors, among them FGFs. Binding of FGFs to heparin or heparan sulfate is crucial for efficient receptor stimulation (Lin et al.,

1999; Schlessinger et al., 2000). Similarly, dermatan sulfate binds to FGFs and potentiates their activity (Penc et al., 1998; Trowbridge et al., 2002; Taylor et al., 2005). In genetic analyses, mutations in the enzymes responsible for the biosynthesis of GAG chains have demonstrated the importance of proteoglycans for FGF signalling during development (Lin, 2004; Buelow and Hobert, 2006). For example, mice mutated in UDP-glucose dehydrogenase (Ugdh), an enzyme required for GAG biosynthesis, arrest during gastrulation and display defects in mesoderm and endoderm migration reminiscent of mutants in the FGF pathway (Garcia-Garcia and Anderson, 2003). In the *Ugdh* mutant embryos, FGF signaling is specifically blocked. In *Drosophila*, *Ugdh* mutants also exhibit phenotypes similar to FGFR mutants (Lin et al., 1999), suggesting an evolutionarily conserved function for HSPGs (Heparan sulfate proteoglycans) in FGF signaling.

1.13 HtrA superfamily

HtrA1 belongs to the HtrA (High temperature requirement) family of serine proteases that is well conserved from bacteria to humans (for review, see Clausen et al., 2002). The defining structural feature is the combination of a catalytic domain ressembling trypsin with one or more C-terminal peptide binding (PDZ) domains. The founding member of the family has been identified as a heat shock protein in *Escherichi coli* (HtrA, DegP) and is a key factor in the control of protein stability and turnover. In mammals, four homologs have been reported (HtrA1-4). Mitochondrial HtrA2 (Omi, Prss25) is the best characterized and involved in programmed cell death (Li et al., 2002) and neuromuscular disorder (Jones et al., 2003). In contrast with HtrA2, the mammalian HtrA1 and its close family members, HtrA3 and HtrA4, are secreted proteins that contain an aminoterminal signal peptide, an insulin-like growth factor binding domain, and a Kazal-type serine protease inhibitor domain upstream of the HtrA homology region. HtrA1 (L56, Prss11) was originally isolated as a gene down-regulated in simian virus 40-transformed human fibroblasts (Zumbrunn and Trueb, 1996), and recent studies showed that HtrA1 is either absent or significantly downregulated in various tumors (Shridhar et al., 2002; Baldi et al., 2002; Chien et al., 2004). In addition, overexpression of HtrA1 inhibits proliferation and tumor growth and causes apoptosis, suggesting that HtrA1 is a candidate tumor suppressor. HtrA1 has also been implicated in osteoarthritis (Hu et al., 1998) and more recently in Alzheimer's disease (Grau et al., 2005). More recently, a single nucleotide polymorphism in the HtrA1 promoter has been presented as a major risk factor for aged-

related macular degeneration (DeWan et al., 2006; Yang et al., 2006). HtrA1 binds to and inactivates members of the TGFb family (Oka et al., 2004) and modulates insulin-like growth factor (IGF) signals (Hou et al., 2005), but its biological function is not yet known.

1.14 Aim of the study

We have recently identified the *Xenopus* homolog of HtrA1 (xHtrA1) in a direct screen for secreted proteins (Pera et al., 2005). Here, we introduce xHtrA1 as a novel modulator of FGF signalling that participates in axial development, mesoderm formation and neuronal differentiation. xHtrA1 is activated by FGF signals and induces ectopic *FGF4* and *FGF8* transcription. We could identify Biglycan, Syndecan-4 and Glypican-4 as proteolytic targets of xHtrA1 and show that pure heparan sulfate and dermatan sulfate phenocopy xHtrA1 and FGF activities in *Xenopus* embryos. The results suggest that xHtrA1 acts as a positive feedback regulator of FGF signals and through proteolytic cleavage of proteoglycans allows long-range FGF signalling in the extracellular space.

2. Materials and methods

2.1 Materials

2.1.1 Solutions

Human chorionic gonadotropin (HCG)

Resuspend in 5 ml dH2O to make a stock solution of 2000 U/ml, aliquot in fractions of 1 ml each, and store at − 20 °C.

5 X MBS (Modified Barth Solution)

440 mM NaCl, 12 mM NaHCO$_3$, 5 mM KCl, 50 mM HEPES (pH 7.0), 4.1 mM MgSO$_4$, 2.05 mM CaCl$_2$, 1.65 mM Ca(NO$_3$)$_2$, adjust pH to 7.4.

L-Cystein hydrochloride 2 %

10 g L-Cystein hydrochloride, dissolve in 500 ml ddH2O and adjust pH to 7.8 – 8.0

Ficoll 10 %

10 g Ficoll in 100 ml ddH2O, filter through 45μl filter and store at 4 °C.

Injection buffer

1 % Ficoll in 1 X MBS,

10 X MEM

1 M MOPS, 20 mM EDTA, 10 mM MgSO$_4$ in 500 ml ddH2O and autoclave

1 X MEMFA

10 ml 10 X MEM, 10 ml 37 % Formaldehyde in 80 ml ddH2O

10x PBS

80 g NaCl, 2 g KCl, 14.4 g Na$_2$HPO$_4$, 2.4 g KH$_2$PO$_4$, dissolved in 800 ml distilled water, adjust pH to 7.4, add distilled water to 1 L and autoclave.

X-Gal staining solution

100 μl (0.1M) K$_3$Fe(CN)$_6$, 100 μl (0.1M) K$_4$Fe(CN)$_6$, 4 μl MgCl$_2$, 50 μl (40 mg / ml) XGal in DMSO in 1.75 ml PBS

Red-Gal staining solution

100 μl (0.1M) K$_3$Fe(CN)$_6$, 100 μl (0.1M) K$_4$Fe(CN)$_6$, 4 μl MgCl$_2$, 10 μl Red-Gal (40 mg / ml in DMSO) in 1.75 ml PBS

PBSw

PBS with 0.1% Tween-20

PBSw / Proteinase K solution

20 μl (20 mg / ml) Proteinase K in 20 ml PBSw

5 X MAB solution

500 mM Maleic acid, 750mM NaCl, adjust pH to 7.5 and autoclave.

20x SSC

175.3 g NaCl, 88.2 g sodium citrate, dissolve in 800 ml distilled water, adjust pH to 7.0, add distilled water to 1 L and autoclave.

Boehringer Block (BMB) 10 %

1 X MAB, 10 % BMB, dissolve at 60 °C and autoclave, then store at – 20 °C.

Hybridisation solution

10 g Boehringer block, 500 ml formamide, 250 ml 20x SSC, heat at 65 ºC for 1 hour, 120 ml DEPC treated water, 100 ml Torula RNA (10 mg/ml filtered), 2 ml Heparin (50 mg/ml in 1xSSC), 5 ml 20 % Tween-20, 10 ml 10 %CHAPS, 10 ml 0.5 M EDTA.

Antibody buffer

10 % heat inactivated horse serum, 1 % Boehringer block, 0.1 % Tween-20, dissolve in PBS at 70 ºC vortexing frequently.

AP buffer

100 mM Tris-HCl, pH 9.5, 50 mM $MgCl_2$, 100 mM NaCl, 0.1 % Tween-20, prepare just before use.

Staining solution

NBT 1.75μl, BCIP 3.5μl per 1 ml AP buffer

Loading buffer

0.5 ml Tris-HCl (1 M pH7.5), 0.1 ml EDTA (0.5M), 0.025 % Bromophenol Blue, 0.025 % Xylencyanol, 30 % Glycerol, add ddH_2O to 50 ml

TE buffer

10mM Tris-HCl (pH7.5), 1m M EDTA, add ddH_2O to 100ml and adjust pH to 8

Tris buffer (pH 9.5)

121.1 g Tris-HCl in 1 L ddH_2O, adjust pH to 9.5 and autoclave

Diethylpyrocarbonat (DEPC) – dH2O

0.1 % Diethylpyrocarbonat, 500 ml dH2O, Incubate for 2 h at 37 °C and autoclave.

2.1.2 Media

Luria-Bertani (LB) medium:

20 g LB was dissolved into 1L ddH$_2$O and autoclaved for more than 20 min at 121ºC, stored at 4ºC.

Luria-Bertani (LB) agar plate:

1.5% (w/v) agar and 20 g LB were dissolved in 1 L sterile water and autoclaved for at least 20 min at 121°C then cooled to around 50°C before the antibiotic was added and the plates were poured in a sterile hood.

2.1.3   Kits

The following kits were used in this study, according to manufacturers instructions:

SP6 Message Machine *in vitro* transcription Kit (Ambion)

Qiagen Plasmid Midi Kit (Qiagen)

QIAquick Purification Kit (Qiagen)

QIAprep Spin Miniprep Kit (Qiagen)

RNeasy Mini Kit (Qiagen)

In vitro transcription Kit (Stratagene)

Quickchange Site-directed Mutagenesis Kit (Stratagene)

2.1.4   Equipment

Gastromaster (XENOTEK)

TRIO Thermoblock (Biometra)

Microinjector (Eppendorf)

Pneumatic PicoPump PV820 (world Precision Instruments)

PN30 needle puller (Narishige)

2.1.5   Experimental Organism

The African clawed frog *Xenopus laevis* was used as experimental organism during this study. Frogs were purchased from Nasco (Ft. Atkinson, USA). The embryonic staging was based on Nieuwkoop und Faber (1967).

2.1.6 Constructs

pCS2+*xHtrA1*

A full-length cDNA clone of xHtrA1 in pcDNA3 was obtained by secretion cloning (Pera et al., 2005). The xHtrA1 cDNA was then subcloned into the EcoRI/XhoI sites of the pCS2+ vector. For sense RNA synthesis, the construct was linearized with NotI and RNA transcribed with SP6 RNA polymerase.

pBluescript II KS+ *xHtrA1*

A full-length cDNA clone of xHtrA1 in pCS2+xHtrA1 was excised and cloned into the EcoRI/XbaI sites of pBluescript II KS+ vector. For antisense RNA synthesis, the construct was linearized with EcoRI and transcribed with T7 RNA polymerase.

pCS2+ *xHtrA1ΔGC*

The full-length sequence of pCS2+*xHtrA1* without the CGCCSVC sequence was amplified with the forward primer (AflII) 5'- TTTCTTAAGAGCTGCTGCCGAGAATGAGCGCTGCG-3' and reverse primer (Afl II) 5'-TTTCTTAAGGCCGTCTCCCCCGACTGGCAGTTG-3'. The PCR product was digested with Afl II and religated. For sense RNA synthesis, the construct was linearized with NotI and transcribed with SP6 RNA polymerase.

pCS2+ *xHtrA1ΔPDZ*

The open reading frame (ORF) of xHtrA1 lacking the PDZ domain was PCR-amplified with the forward primer (ClaI) 5'- AAAATCGATGTGCTGAGGACACAGAGG-3' and reverse primer (XhoI) 5'-AAACTCGAGTTACTGCCTGTTGTGCGACTC-3' and cloned into the ClaI/XhoI sites of the pCS2+ vector. For sense RNA synthesis, the construct was linearized with NotI and transcribed with SP6 RNA polymerase.

pCS2+*xHtrA1Δtrypsin*

To generate pCS2-*xHtrA1Δtrypsin* (deletion of amino acids 151-343), the cDNA sequences upstream and downstream of the trypsin domain including the vector sequence of pCS2-xHtrA1 were PCR amplified using the forward primer (NheI) 5'-AAA GCT AGC GAG TCG CAC AAC AGG CAG-3' and reverse primer (NheI) 5'- AAA GCT AGC GAA GTT GTA CTT GTA GCG CG-3'. The product was digested with NheI and religated. For sense RNA synthesis, the construct was linearized with NotI and RNA transcribed with SP6 RNA polymerase.

pCS2+*xHtrA1S307A*

For pCS2+*xHtrA1S307A*, a single point mutation was made in xHtrA1 to replace serine in

position 307 by alanine using the QuikChange Site-Directed Mutagenesis Kit (Stratagene) with the forward primer 5'- TCAATTATGGAAACGCTGGGGGCCCGCTC-3' and reverse primer 5'- GAGCGGGCCCCCAGCGTTTCCATAATTGA-3'. For sense RNA synthesis, the construct was linearized with NotI and RNA transcribed with SP6 RNA polymerase.

pCS2+*xHtrA1*

To obtain pCS2-*xHtrA1**, the xHtrA1 open reading frame (ORF) lacking the signal peptide was PCR-amplified with the forward primer (XhoI) 5'-AAACTCGAGGCTCTTCTCCCCACATCC-3' and reverse primer (XbaI) 5'-AAATCTAGATTAAAATTCTATTTCCTTGGGTG-3' and cloned into the XhoI/XbaI sites downstream of the chordin signal peptide and Flag tag sequence of pCS2-Chd-Flag vector (gift of S. Piccolo, University of Padua, Italy). For sense RNA synthesis, the construct was linearized with NotI and RNA transcribed with SP6 RNA polymerase.

pGEX-5X-1 *xHtrA1-PDZ*

To generate the GST-tagged xHtrA1-PDZ construct, the PDZ domain of xHtrA1 (amino acids 344-481) was amplified by PCR with the forward primer (BamHI) 5'-AAAGGATCCACAACAGGCAGTCCACAGG-3' and reverse primer (XhoI) 5'-AAACTCGAGGAAACCAGCTCATTTCTCCC-3' and cloned into the BamHI/XhoI sites of pGEX-5X-1 (Stratagene).

pCS2+*eFGF-GFP*

The ORF of Xenopus embryonic FGF (eFGF, FGF4) without stop codon (gift of J. Slack, University of Bath, UK) was amplified by PCR using the forward primer (BamHI) 5'-AAAGGATCCATGACTGTTCCATCGGC-3' and reverse primer (XbaI) 5'-AAATCTAGATATCCGTGGCAAGAAATGG-3',
and inserted into the BamHI/XbaI sites of pCS2+Myc tag GFP (gift from Klymkowsky). For sense RNA synthesis, the construct was linearized with NotI and RNA transcribed with SP6 RNA polymerase.

pCS2+*FGF8-GFP*

The ORFs of Xenopus FGF8 without stop coden (gift of J. Slack, University of Bath, UK) was PCR amplified with the forward primer (ClaI) 5'-AAAATCGATATGAACTACATCACCTCCATC-3' and reverse primer (XbaI) 5'-AAATCTAGACCGAGAACTTGAATATCGAG-3' and inserted into pCS2+ Myc tag GFP vector. For sense RNA synthesis, the construct was linearized with NotI and RNA

transcribed with SP6 RNA polymerase.

pCS2+ *Flag FGF4*

The ORF without signal peptide of *Xenopus* FGF4 (gift of J. Slack, University of Bath, UK) was amplified with the forward primer (XhoI) 5'-AAA<u>CTCGAG</u>CTGCCGCTTTCTTTCCAGAG-3' and reverse primer (XbaI) 5'-AAA<u>TCTAGA</u>TCATATCCGTGGCAAGAAATG-3' and cloned into the XhoI/XbaI sites of the pCS2-chd-Flag vector (gift of S. Piccolo, University of Padua, Italy).

pCS2+ *Flag FGF8*

The ORF lacking the signal peptide of *Xenopus* FGF8 (gift of J. Slack, University of Bath, UK) was amplified with the forward primer (XhoI) 5'-AAA<u>CTCGAG</u>CAGCATGTGAGGGAGCAGAG

-3' and reverse primer (XbaI) 5'-AAA<u>TCTAGA</u> CTACCGAGAACTTGAATATC

-3' and cloned into the XhoI/XbaI sites of the pCS2-Chd-Flag vector (gift of S. Piccolo, University of Padua, Italy).

pCS2+ *Flag Syn1*

The ORF of *Xenopus* Syndecan-1 (gift from J. Yost, University of Minnesota, U.S.A) lacking signal peptide was generated by PCR with the forward primer (SalI) 5'-AAA<u>GTCGAC</u> GATGTGAGCGTGAGATCC-3' and reverse primer (NheI) 5'-AAA<u>GCTAGC</u> CTACGCGTAGAATTCCCGTTGTGCACG-3' and inserted into the XhoI/XbaI sites of the pCS2-*Chd*-Flag vector (gift of S. Piccolo, University of Padua, Italy) to introduce a chordin signal peptide and a Flag tag at the N-terminus of the mature syndecan1 protein.

pCS2+ *Flag Syn2*

The ORF of *Xenopus* Syndecan-2 (gift from J. Yost, University of Minnesota, U.S.A) lacking signal peptide was generated by PCR with the forward primer (XhoI) 5'-AAA<u>CTCGAG</u>CAAGCTGACAGAGACCTATATC

-3' and reverse primer (XbaI) 5'- AAA<u>TCTAGA</u>TTACGCGTAAAACTCTTTAG

-3' and inserted into the XhoI/XbaI sites of the pCS2-*Chd*-Flag vector (gift of S. Piccolo, University of Padua, Italy).

pCS2+ *Flag Bgn*

The ORF of *Xenopus* Biglycan (gift of J. Larrain, Universidad Catolica de Chile, Chile) lacking signal peptide was generated by PCR with the forward primer (SalI) 5'-AAA<u>GTCGAC</u>CTGCCTTTTGAACAGAGAGG

-3' and reverse primer (XbaI) 5'- AAA<u>TCTAGA</u>TTACTTCCTGTAATTGCCAAACTG -3' and cloned into the XhoI/XbaI sites of the pCS2-*Chd*-Flag vector (gift of S. Piccolo, University of Padua, Italy). For sense RNA synthesis, the construct was linearized with NotI and transcribed with SP6 RNA polymerase.

pCS2+ *Flag Glypican4*

The ORF of *Xenopus* Glypican4 lacking the signal peptide was PCR-amplified with the forward primer (XhoI) 5'-AAA<u>CTCGAG</u>GATCTCAAGTCCAAGAGTTG-3' and the reverse primer (XbaI) 5'-AAATCTAGATTATCTCCATTGCCTCACC-3' and cloned into the XhoI/XbaI sites of the pCS2-chd-Flag vector (gift of S. Piccolo, University of Padua, Italy).

pCS2+ *Glypican-4 Flag*

The amino acids 1-539 of the *Xenopus* Glypican-4 ORF were amplified with the forward primer (EcoRI) 5'-AAA<u>GAATTC</u>ATGCTTTGGATCTCCTTTTAC-3' and reverse primer (XbaI) 5'-AAA<u>TCTAGA</u>CTACTTGTCATCGTCGTCCTTGTAGTCAACACTGTTGGAAGAGGCTG-3' and cloned into the EcoRI / XbaI sites of the pCS2+ vector.

Other constructs, which have been used in this study, are as follows:

pCS2+*Flag Syn4* (provided by J. Larrain, Universidad Catolica de Chile, Chile.).

pSP64T *BMP4* (gift from W. Knöchel, University of Ulm, Germany). For mRNA sythesis, digested with BamHI and transcribed with SP6 RNA polymerase.

pXFD/Xss (gift from E. Amaya, Wellcome /CRC Institute, Cambridge, UK). For mRNA synthesis, digested with EcoRI and transcribed with SP6 RNA polymerase.

pSP64T *DN-FGFR4a* (gift from H. Okamoto, AIST Institute, Japan). For mRNA synthesis, digested with *SalI a*nd transcribed with SP6 RNA polymerase.

nlacZ mRNA from pXEXβgal (gift from R. Harland, University of California, Berkley, USA). For mRNA synthesis, digested with XbaI and transcribed with T7 RNA polymerase.

pSP64T *CFP-GPI* (gift from J. Smith, Wellcome /CRC Institute, Cambridge, UK). For mRNA synthesis, digested with EcoRI and transcribed with SP6 RNA polymerase.

pBluescript KS *Shh* For antisense RNA synthesis, digested with XbaI and transcribed with T3 RNA polymerase.

pSP73-*MyoD* For antisense RNA synthesis, digested with BamHI and transcribed with SP6 RNA polymerase.

PCS2+*GFP* For mRNA synthesis, digested with NotI and transcribed with SP6 RNA polymerase.

pCS2+*BF1* For antisense RNA synthesis, digested with XhoI and transcribed with SP6 RNA polymerase.

pGEM-T-*Rx2a* For antisense RNA synthesis, digested with NcoI and transcribed with SP6 RNA polymerase.

pGEM-*Krox20* For antisense RNA synthesis, digested with EcoRI and transcribed with T7 RNA polymerase.

pGEM-3ZF-*NKx2.5* For antisense RNA synthesis, digested with HindIII and transcribed with T7 RNA polymerase.

pCDNA3-*Sizzled* For antisense RNA synthesis, digested with BamHI and transcribed with SP6 RNA polymerase.

pBSt-SK-*Otx2* For antisense RNA synthesis, digested with NotI and transcribed with T7 RNA polymerase.

pSP73-*Xbra* For antisense RNA synthesis, digested with BglII and transcribed with T7 RNA polymerase.

Sox2 For antisense RNA synthesis, digested with EcoRI and transcribed with T7 RNA polymerase.

pGEM-*Cytokeratin* For antisense RNA synthesis, digested with EcoRI and transcribed with SP6 RNA polymerase.

Slug For antisense RNA synthesis, digested with ClaI and transcribed with SP6 RNA polymerase.

N-tubulin For antisense RNA synthesis, digested with BamHI and transcribed with T3 RNA polymerase.

pBSt-KS-*En2* For antisense RNA synthesis, digested with XbaI and transcribed with T3 RNA polymerase.

pBSII-KS+*FGF4* For antisense RNA synthesis, digested with EcoRI and transcribed with T3 RNA polymerase.

FGF8 For antisense RNA synthesis, digested with Xba and transcribed with T3 RNA polymerase.

2.1.7 Morpholino oligonucleotides

Morpholino antisense oligomers were obtained from Gene Tools Inc. and had the following sequences: *xHtrA1*-MO 5'-ACACCGCCAGCCACAACATGGTCAT-3' and standard control-MO 5'-CCTCTTACCTCAGTTACAATTTATA-3'. The morpholino oligomers were resuspended to 1 mM and further diluted in ddH2O to give a working solution, which was incubated at 65°C for 5 minutes before use.

2.2 Method

2.2.1 *In vitro* synthesis of sense RNA for microinjection

To prepare synthetic capped mRNA , the SP6 mMessage-mMachine™ Kit (Ambion) was used according to the manufacturer's protocol..A 20 µl

reaction contains 1-1.5 µg linearized plasmid, 2 µl 10 x reaction buffer, 10 µl 2 x NTPs/ Cap, 2 µl enzyme mix . Transcription was carried out at

37°C for 2.5 hours. The DNA template was removed by addition of 2 U

DNaseI and incubated at 37°C for 30 min. The mRNA was purified with the RNeasy Mini Kit (Qiagen) accoding to the manufacture's protocol, eluted in 20 µl

RNase-free H2O. The concentration of mRNA was determined using the Nano drop ND-1000 (Nano Drop) and the quality assayed on an 1% agarose gel. mRNA was stored in aliquots at -20°C.

2.2.2 *In vitro* synthesis of antisense RNA for *in situ* hybridization

To prepare antisense RNA, a 25 µl reaction mixture was used that contains: 1-1.5 µg linearized template, 5 µl 5 x Transcription buffer (Fermentas), 2 µl 0.1 M DTT, 0.5 µl RNase out (Invitrogen), 1 µl RNA polymerase (Fermentas), 0.5 µl pyrophospatase (Fermentas) and 4 µl Digoxigenin-Mix (5 µl 100 mM ATP, 5 µl 100 mM GTP, 5 µl 100 mM CTP, 3.25 µl 100 mM UTP, 17.25 µl Dig-11-UTP (Roche), 14.5 µl RNase-free H2O). The reaction was incubated at 37°C for 2.5 hours, and the DNA template was destroyed by adding 2 µl DNaseI (Fermentas) and incubated at 37°C for 30 min. Antisense RNA probe was purified with the RNeasy Mini Kit (Qiagen) according to the manufacture's protocol and eluted with 35 µl RNase-free H2O. The purified RNA probe was mixed with 30 µl formamide and 1150 µl hybridization solution and stored at -20°C. This antisense RNA probe was then diluted in hybridization solution according to the intensity of the *in situ* hybridization signals.

2.2.3 *Xenopus* embryo microinjection

Pigmented and albino *Xenopus laevis* frogs were purchased from Nasco (Ft. Atkinson, USA). Ovulation was stimulated by injection of 1000 IU human chorionic gonadotropin (hCG, Sigma) into the dorsal lymph sac of female frogs on the evening before egg collection. Eggs were fertilized *in vitro* with minced testes in 0.1 x MBS, dejellyed with 2% cystein hydrochloride (2% L-cystein hydrochloride in 0.1 x MBS, pH 7.8-8.0) and cultured in 0.1 x MBS buffer. Albino embryos were stained with Nile Blue sulphate (0.1 g Nile blue, 89.6 ml 0.5 M Na_2HPO_4, 10.4 ml NaH_2PO_4, filled to 1 L with ddH_2O, pH7.8). Embryos were staged according to Nieuwkoop and Faber (1967).

The microinjection needles were prepared from glass capillaries (Harvard apparatus, U.S.A) using the P-97 Flaming/ brown micropipette puller (Sutter instrument, U.S.A). The needles were back-filled using microloaders (Eppendorf). For the injection, a pneumatic PicoPump PV820 injector (Helmut Saur Laborbedarf, Reutlingen, Germany) was used. A volume of 4 nl for RNA or DNA and 10 nl for morpholino oligonucleotides was injected. Embryos were arranged on a glass slide in injection buffer (1% Ficoll, 1 x MBS). Following injection, the embryos were cultivated in injection buffer for 30-45 min and transferred into Petri dishes with 0.1 x MBS.

Embryos were fixed at the desired developmental stage in MEMFA (0.1 M MOPS, 2 mM EGTA (pH 8.0), 1 mM $MgSO_4$, 4% formaldehyde, pH7.4) overnight at 4 °C. After fixation, the embryos were washed twice with 1 x PBS, dehydrated via the ethanol series in 1 x PBS (25% EtOH, 50% EtOH, 75% EtOH, 2x 100% EtOH) and stored in 100% EtOH at –20 °C.

2.2.4 *Xenopus* explant assays and confocal microscopy

For the neural plate explant assay, *Xenopus* embryos were injected with 5 pg *xHtrA1* mRNA into each blastomere at the 4-cell stage. When the embryos reached stage 13, neural plate explants together with underlying mesoderm and endoderm were excised in 0.8xMBS using the gastromaster (Xenotec), dissected into four sections roughly

corresponding to forebrain, midbrain, hindbrain and spinal cord, cultured until sibling embryos reached stage 28 and processed for RT-PCR (five explants per sample).

For the Einsteck experiment, dorsal marginal zone explants were isolated from *xHtrA1* mRNA-injected stage 10.25 and *xHtrA1*-MO injected stage 13 embryos in Steinberg solution (600 mM NaCl, 6.7 mM KCl, 3.4 mM Ca(NO3)2, 8.3 mM MgSO4, 100 mM HEPES) and transplanted into the blastocoel cavity of stage 10.25 host embryos. After 1-2 hours of healing in Steinberg solution, transplanted embryos were transferred into 0.1xMBS and cultured until stage 42.

Animal cap conjugates were prepared and processed as described (Williams et al., 2004) with the modification that *nlacZ* mRNA was used as lineage tracer. The *Xenopus* embryos were microinjected with the indicated mRNAs into each blastomere at the 4-cell stage. In 0.8xMBS, animal cap explants from stage 8 embryos were dissected and juxtaposed in pairs with the inner sides facing each other. When sibling embryos reached stage 11, the animal cap conjugates were fixed in MEMFA solution at room temperature for 45 min and processed for X-gal staining. Subsequently, animal cap conjugates were re-fixed in MEMFA at 4ºC overnight, dehydrated through the ethanol series to 100% ethanol and stored at -20ºC before subjecting to *in situ* hybridization with the *Xbra* antisense probe.

For the confocal microscopy experiment, *Xenopus* embryos were microinjected with *FGF8-GFP/FGF4-GFP* alone or in combination with *xHtrA1* mRNA. Another group of embryos were injected with *CFP-GPI* mRNA, Animal cap explants from injected embryos were dissected at stage 9.5-10.5 in 0.8xMBS and immediately transferred onto fibronectin-coated glass slides (Sigma, Gurdon et al., 1999). To allow stable contact between two adjacent caps, one small circular animal cap explant injected with FGF-GFP was surrounded by a second ring-shaped animal cap explant injected with *CFP-GPI* mRNA. The tissue explants were overlaid with coverslips, with small pieces of broken glass slide as spacers in between glass plates and coverslips. Fluorescent signals were analyzed using a confocal laser scan Axiolpan2, LSM510 microscope (Zeiss, Germany).

In an independent experiment, GFP-labelled FGF8 protein was soaked in heparin bead (Sigma) and used as FGF ligand source. FGF8b recombinant protein (R&D; 1 mg) was

dissolved in 100 μl 0.1 M NaHCO3, pH9.0. Alexa Fluor 488 fluorescent dye (Invitrogen; 0.2 mg) was dissolved in 20 μl DMSO. The fluorescent dye solution was slowly added into FGF8b protein solution. The mixture was incubated at room temperature for 2 hours on a shaker to allow binding of the fluorescent dye to the recombinant protein. In order to remove unbound fluorescent dye, the reaction mixture was transferred into Slide-A-Lyzer Mini dialysis units (Pierce) and dialyzed against 1x PBS (3 x 1 L, 4 ºC overnight in dark). The fluorescent dye-labelled FGF8b protein was stored in aliquots at -20 ºC. Heparin-acrylic beads (Sigma) were soaked in fluorescence-conjugated FGF8b proteins (30 min on ice) and used as carriers for FGF8b proteins. Animal cap explants injected with *CFP-GPI* alone or in combination with *xHtrA1* were transferred to fibronectin-coated glass slides with the inner side facing upwards. After briefly washing away unbound proteins, an individual heparin bead was carefully transferred into a preformed hole at the center of the animal cap explant, and the conjugate was covered with a coverslip. Fluorescence signals were analysed using a con-focal laser scan microscope (Leica).

2.2.5 Whole mount *in situ* hybridization

The whole-mount *in situ* hybridization was performed as described (Hollemann et al., 1998) over a period of three days.

Day 1:

Embryos were rehydrated through the ethanol series (75%, 50%, 25% in PBS), 5 min for each step. Afterwards, embryos were washed with PTw (0.1% Tween-20 in 1x PBS, (4 x 5 min). Embryos were then digested with 0.5μl/ml Proteinase K (Sigma) in PTw (room temperature, 5-8 min). Subsequently, embryos were washed with 0.1M triethanolamine, pH7.5 (2 x 5 min) and acetylated by addition of 12.5 μl acetic anhydrite into 4 ml 0.1 M triethanolamine (2 x 5 min). Embryos were washed with PTw (2 x 5 min) and refixed with 4% formaldehyde in 1x PTw (room temperature, 20 min). Afterwards, embryos underwent wash steps as follows: PTw (5 x 5 min); 1.25 ml of 80% PTw, 20% hybridization mix; 500 μl hybridization mix (65 ºC, 10 min); 1 ml hybridization mix (65 ºC, 5 hours). Embryos were then hybridized overnight at 65 ºC in 1 ml hybridization solution containing the appropriate amount of antisense probe.

Day 2:

The probe/hybridization mix was removed, stored at -20° for later use, and replaced with 1 ml hybridization mix (60 ºC, 10 min). Embryos were then washed with 4 ml of 2 x SSC (pH 7.0) at 60 ºC, 3 x 15 min. Unspecifically bound antisense probe was digested by RNase Mix (10 µl/ml RNase A, 0.01 u/ml RNase T1 in 2x SSC) at 37 ºC, 30-60 min. Embryos underwent the following processes: 2x SSC (10 min); 0.2x SSC (60 ºC, 2 x 30 min); 1x MAB (2 x 15 min); 2% BMB in 1x MAB (20 min); 2% BMB, 20% horse serum in 1x MAB (60 min); 1/5000 anti-digoxigenin- alkaline phosphatase conjugated antibody (Sigma), 2% BMB, 20% horse serum in 1x MAB (4 hours); 1x MAB (3 x 10 min); 1x MAB (4 ºC, overnight).

Day 3:

Embryos underwent several washing steps: 1x MAB (5 x 5 min); APB (100 mM Tris, pH 9.0; 50 mM MgCl2; 100 mM NaCl; 0.1% TWEEN-20) (4 ºC, 2 x 5 min).

Two different protocols for the staining reaction were applied. First, APB was substituted with an NBT/BCIP solution (1.75 µl/ml NBT (Fermentas), 3.5 µl/ml BCIP (Fermentas) in APB) Alternatively, embryos were washed with 0.1M Tris (pH 8.2) for 2 x 15 min and incubated with Fast Red (Roche; 1 tablet / 2 ml) in 0.1M Tris (pH8.2). Embryos were incubated on ice under dark conditions, until the desired staining was reached. The staining reaction was stopped by directly exchanging the staining solution with methanol. Subsequent exchange against fresh methanol helped to lower the background. Embryos were then transferred through a methanol series (75%, 50%, 25%, 5 min each step) and stored in MEMFA solution at 4 ºC.

2.2.6   RT-PCR

Fifteen animal caps or 3 whole embryos were harvested in 400 µl Trizon (Invitrogen). Tissues were homogenized by first pipetting up and down using 1000 µl- and then 200 µl-pipet tips, followed by vortexing . At this step, the samples could be frozen at -20 ºC. The tissues were thawed and vortexed again for 30 seconds, then 80 µl chloroform was added. The mixture was vortexed for 30 seconds and centrifuged in a table centrifuge at maximum speed (13.000 rpm) for 15 min at 4 ºC. The upper phase was recovered and transferred into a new microfuge tube. Sebsequently, 200 µl chloroform was added and centrifuged for

5 min. The upper phase solution was transferred again into a new eppendorf tube and mixed with 200 μl isopropanol, after precipitated at -20 ℃ for 30 min. Total RNAs were centrifuged down at maximum speed at 4 ℃ for 30 min. The pellet was washed with 400 μl 75% ethanol. After centrifuge for 5 min, ethanol was removed and the pellet was dried. The RNA was eluted in 30 μl, 60 °C pre-heated elution buffer.

The reverse transcriptase-polymerase chain reactions (RT-PCR) was used to analyze the gene expression level in embryonic explants or whole embryos. A standard 10 μl reverse transcription reaction consisted of: 2 μl 25 mM MgCl$_2$, 1 μl 10 x PCR buffer II (QBiogene), 1 μl 10 mM dATP, 1 μl 10 mM dGTP, 1 μl 10 mM dCTP, 1 μl 10 mM dTTP, 0.5 μl Random Hexamer (50 ng/μl, Invitrogen), 0.4 μl Reverse Transcriptase (Invitrogen), 0.2 μl RNase out (Invitrogen), 1.5 μl 30 ng/μl RNA, 0.4 μl DEPC water.

RT reaction follows the Perkin Elmer protocol: 22 ℃, 10 min; 42 ℃, 50 min; 99 ℃, 5 min. A standard 25 μl of PCR reaction contained 5 μl cDNA obtained from RT reaction, 0.5 μl 25 mM MgCl$_2$, 2μl 10x PCR buffer II, 0.75 μl gene specific primer (forward and reverse, 7.5μM each), and 0.1 μl Taq polymerase (5 u/μl, QBiogene) and 16.75 μl HPLC water. PCR program was designed as follows: pre-denaturation at 94 ℃ for 2 min, 28 cycles of denaturation at 94℃ for 45 sec, annealing at 56 ℃ for 45 sec and extension at 72 ℃ for 45 sec, followed by final extension at 72 ℃ for 5 min.

The following primers, annealing temperatures and cycle numbers were used: *Histone H4* (forward primer 5'-CGGGATAACATTCAGGGTATCACT- 3' and reverse primer 5'-CATGGCGGTAACTGTCTTCCT-3', 56 °C, 24 cycles); *Xbra* (forward primer 5'-GGATCGTTATCACCTCTG-3' and reverse primer 5'-GTGTAGTCTGTAGCAGCATGCTGCTAC-3', 56°C, 28 cycles); *xHtrA1* (forward primer 5'-TGTTGTGGCTGGCGGTGTTACTG-3' and reverse primer 5'-TCCATCCTCCGACACAATGAATCC-3', 57°C, 43 cycles); *Rx2a* (forward primer 5'-CAACAGCCCAAGAAGAAACACAG-3' and reverse primer 5'-GAGGGCACTCATGGCAGAAGG-3', 56°C, 28 cycles); *Otx2* (forward primer 5'-CCAGTCATCTCGAGCAGCACA-3' and reverse primer 5'-CAGGAGGCCGTTTGGTCTTTG-3', 56°C, 28 cycles); *Krox20* (forward primer 5'-CGCCCCAGTAAGACC-3' and reverse primer 5'-TCAGCCTGTCCTGTTAG-3', 56°C,

30 cycles); *HoxD1* (forward primer 5'-CAGCCCCGATTACGATTATTATGG-3' and reverse primer 5'-CCGGGGAGGCAGGTTTTG-3', 56°C, 30 cycles); *HoxB9* (forward primer 5'-GCCCCTGCGCAATCTGAAC-3' and reverse primer 5'-CAGCAGCGGCTCAGACTTGAG-3', 56°C, 28 cycles); *Xcad3* (forward primer 5'-GGATCACCGAGGGAGGAATG-3' and reverse primer 5'-TAAGAGCGCTGGGTGAGTTGG-3', 56°C, 28 cycles). The PCR products were separated on 2% agarose gels.

2.2.7   Cell culture and transfection

HEK293 cells were splitted, stored and cultured according to product sheet (Invitrogen). At 50-60% confluency, cells were transfected. Plasmid DNA (3 μg) of substrate candidate constructs such as Flag-Biglycan, Flag-Syndecan4 and Glypican4-Flag alone or together with xHtrA1 DNA (2.5 μg) were added into 250 μl DMEM with 2 mM L-glutamine. One tenth of pAdvantage plasmid DNA was added to increase transfection efficiency (Pera et al., 2005). Add 2.5 μl lipofectamine 2000 (invitrogen)/ per μg DNA into another 250 μl DMEM with L-glutamine and incubate at room temperature for 5 min. These above two solutions were then mixed well and incubated at room temperature for 20 min. In 6-well plate, the culture medium was exchanged with 2 ml DMEM with L-glutamine, 10 % Horse serum. The DNA and lipofectamine complexes were then added and mixed well. One day afterwards, culture medium was substituted with 1 ml DMEM with 2 mM L-glutamine. Three days after transfection, cells were harvested with cell scrapers and lysed in 200 μl RIPA buffer on ice.

2.2.8   Antibody production and immunopurification

pQE32-His-xHtrA1-PDZ and pGST-xHtrA1-PDZ were electroporated into SG1300 (Qiagen) and BL21 bacteria (Stratagene), respectively. Expression of recombinant protein was induced with 1 mM IPTG in LB medium containing 50 ug/ml carbenicillin. After 6 hours incubation at 220 rpm and 30°C, the bacteria were spinned down at 6000 rpm and 4°C for 10 minutes and frozen at -80°C. The bacterial pellet was then thawed and resuspended on ice in lysis buffer (50 mM NaH_2PO_4, 300 mM NaCl, 20 mM imidazole, 10% glycerol, 0.4% Triton-X-100, 0.1 mM PMSF, complete EDTA-free protease inhibitor cocktail (Roche)) and sonicated for 20 minutes with Sonifier 450 (G. Heinemann). The

bacterial lysate was centrifuged at 10.000 rpm at 4°C for 30 minutes and the supernatant was harvested for purification.

His-tagged xHtrA1-PDZ was purified under native conditions with Ni-NTA Agarose (Qiagen) and GST-tagged xHtrA1-PDZ was purified using Glutathione immobilized on cross-linked 4% beaded agarose (Sigma) according to the manufacturer's protocols. Polyclonal antibodies against the recombinant xHtrA1-PDZ proteins were independently raised in rabbits (Bioscience, Göttingen). The pre-serum and immunized serum from the third bleeding was subjected to immunoaffinity purification using the AminoLink Plus Immobilization Kit (Pierce). The concentration of IgG was measured with the Bradford reagent (Sigma).

2.2.9   Whole mount immunohistochemistry with pH3 and dpERk

Whole-mount immunostaining was done using the protocol modified from Christen and Slack, 1999; Saka and Smith, 2001) using anti- phosphorylated histone3 (pH3, 1:200, Upstate Biotechnology) and anti-phospho-p44/42 MAP Kinase, Thr202/Tyr204 (dpERK, 1:200, Cell Signaling). Goat anti-rabbit antibody coupled with alkaline phosphatase (1:2000; Sigma) was used as secondary antibody.

Embryos were transferred from ethanol to methanol, and kept in Dents solution (80% methanol, 20% DMSO) at -20 °C overnight. Embryos were rehydrated through methanol series (100%, 75%, 50%, 25%, 5 min each step), washed with 1x PBS (2 x 10 min). The vitelline membranes were removed by digesting with 0.5 µl/ml Proteinase K in PBS (room temperature, 5-8 min) and the reaction was stopped by washing with 1x PBS (2 x 5 min). Unspecific binding was blocked by incubating embryos with 20% horse serum in 1x PBS (room temperature, 2 hrs). Embryos were incubated with appropriate dilution of 1st antibody in 20% horse serum, 1x PBS (room temperature, 5 hrs). Unbound antibody was washed through series steps: PBS-TB (0.05% Tween-20, 0.2% BSA in 1x PBS) (2 x 2 hrs); PBS-TBN (0.3 M NaCl in PBS-TB) (2 hrs); PBS-TB (5 min). Then embryos were incubated with the 1/ 2000 dilution of 2nd antibody in 20% horse serum in 1x PBS (5 hrs). After several wash steps: PBS-TB (2 x 30 min); PBS-TBN (30 min); PBS-TB (3 x 10 min), APB (2 x 5 min, 4 °C), embryos were incubated in color reaction solution (1.75

μl/ml NBT, 3.5μl/ml BCIP in APB) (4 °C in dark). The background of staining was removed by washing with methanol for several times.

2.2.10 Immunoblotting

For immunoblotting, embryo lysates were prepared as described (Pera et al., 2003). Proteins were separated by 12% SDS-PAGE and Western blots performed using purified polyclonal antibodies against xHtrA1-PDZ (1:400) and GAPDH (1:2500, Abcam). Goat anti-rabbit antibody coupled with horseradish peroxidase (1:10,000; Cell Signaling) was used as secondary antibody.

2.2.11 Dermatan sulfate preparation (done by Prof. Dr. Anders Malmström and Dr. Marco Maccarana)

Bovine lung dermatan sulfate was prepared by precipitation with cetylpyridium chloride in 0.5 M NaCl. The crude polysaccharide was further purified by repetitive precipitation as copper complex (Stern et al., 1968). To be certain that heparin and heparan sulfate would not be present as contaminants, deamination at pH 1.5 (Shively and Conrad, 1976) was performed and dermatan sulfate reisolated after ethanol precipitation. The absence of heparin/heparan sulfate was confirmed by lacking of 232 nm absorbance following extensive heparinase treatment.

2.2.12 Proteoglycan isolation and lyase treatment (done by Dr. Marco Maccarana)

Proteoglycan were extracted at 4°C from embryos adding 5 volumes of guanidine extraction buffer (50mM acetate pH 5.5, 4M guanidine/HCl, 10 mM EDTA, 2%Triton X-100, DTT 1mM, PMSF 1 mM, aprotinin, leupeptin, pepstatin, each at 1 μg/ml) and homogenizing by Potter. The homogenate was diluted 1:20 with buffer A (50 mM acetate pH 5.5, 6M urea, 1mM EDTA, 0.1% Triton X-100, DTT 1mM, PMSF 1 mM, aprotinin, leupeptin, pepstatin, each at 1 μg/ml) and applied to 1 ml DE52 anion-exchange column, operated at 4°C. The column was washed with buffer A containing 0.1M NaCl, and eluted with 10 volumes of buffer (2M acetate pH 5.5, 6M urea, 1mM EDTA, 0.1% Triton X-100, DTT 1mM, PMSF 1 mM, aprotinin, leupeptin, pepstatin, each at 1 μg/ml). Proteoglycans were precipitated by addition of 4 volumes of ethanol, re-precipitated with ethanol, 1.4% Na-Acetate, liophilized, and finally re-dissolved in TBS, containing 0.1% Triton X-100,

DTT 1mM, PMSF 1 mM, aprotinin, leupeptin, pepstatin, each at 1 µg/ml. Soluble material after 20,000g X 30 min was used for lyase treatment and Western blot analysis.

Twenty µl of the above anion-exchange purified material was diluted 1:3 with Tris 20 mM pH 7.5, NaCl 50 mM, $CaCl_2$ 4 mM, followed by addition of 0.5 mU Chondroitinase B (Seikagaku, Japan), or mock-treatment. After overnight incubation at 37°C, the reaction was stopped by Laemmli buffer, and the samples were subjected to Western blot analysis on pre-made 4-12% acrylamide mini-gel (NuPAGE, Invitrogen). Flag-Biglycan was decorated by anti-Flag antibody HRP-conjugated (1:1000; Sigma, A8592), and detected by ECL (AmershamBioscience, Sweden).

2.2.13   Paraffin section

Embryos were fixed in MEMFA solution (room temperature, 1 hour), washed in 1 x PBS (3 x 5 min) and then gradually transferred into 100% ethanol for storage. For paraffin embedding, embryos were transferred to chloroform and then to xylene (2 x 20 minutes). Subsequently, embryos were incubated in 60°C melting paraffin (2 x 1 hour) and then embedded in paraffin. A microtome was used to prepare 10 µM tissue sections and fixed onto glass slides. Let the section slides dry on 40°C heater for overnight.

2.2.14   Hematoxylin eosin staining

Embryonic section slides was washed with xylene (2 x 5min), and then transferred gradually through ethanol gradient series (100%, 2 x 3 min; 95%, 3 min; 70%, 3 min) into distilled water (3 min). The sections were stained in Hematoxylin solution (10 sec). The excessive staining was washed away first by tap water (2 x 10 shakes), then by Scott's tap water (10 g $MgSO_4$, 2 g $NaHCO_3$ in 1 L ddH_2O; 2 min), followed by ddH_2O (2 min). The section slides were transferred into 70% ethanol (3 min) and stained with eosin solution (50 mg eosin Y, 350 µl glacial acetic acid in 100 ml 95% ethanol; 3-5 min). The sections were then washed with 95% ethanol until unspecific staining being removed. The slides underwent decreasing concentration of ethanol series to 1 x PBS and then can be mounted in Mowiol solution (5 g Mowiol, 10 ml glycerol in 20 ml PBS, pH~7.0. Not dissolved Mowiol removed by centrifugation).

3. Results

3.1 Identification of *Xenopus* HtrA1

We isolated a full-length cDNA clone of *Xenopus* HtrA1 (xHtrA1) by secretion cloning from UV-ventralized gastrula embryos (Pera et al., 2005). xHtrA1 was identified as a 50 kD secreted protein in the supernatant of transfected and metabolically labeled human embryonic kidney (HEK) 293T cells (data not shown). The xHtrA1 cDNA clone (GenBank accession number EF490997) encompasses a 303 bp 5' untranslated region (5' UTR), a 1379 bp open reading frame (ORF) followed by a 109 bp 3' UTR. At its amino terminus, predicted by Psort software (http://psort.nibb.ac.jp), *Xenopus* HtrA1 (xHtrA1) has a 16 amino acids cleavable signal peptide. The mature protein contains an IGF binding domain, a Kazal-type serine protease inhibitor domain, a trypsin-like serine protease domain and a PDZ (PSD95/DlgA/ZO-1 homology) protein-protein interaction domain (Fig. 1; Hou, 2004). xHtrA1 homologues also exist in human (68% amino acid identity; Zumbrunn and Trueb, 1996; Hu et al., 1998), mouse (68% amino acid identity; Oka et al., 2004) and have the same modular composition as xHtrA1. In addition, related proteins are found in *Drosophila melanogaster* (46% amino acid identity) and *Escherichia coli* (40% amino acid identity; Lipinska et al., 1990), that share a signal peptide, a trypin domain and one (*Drosophila*) or two copies (*E. coli*) of the PDZ domain.
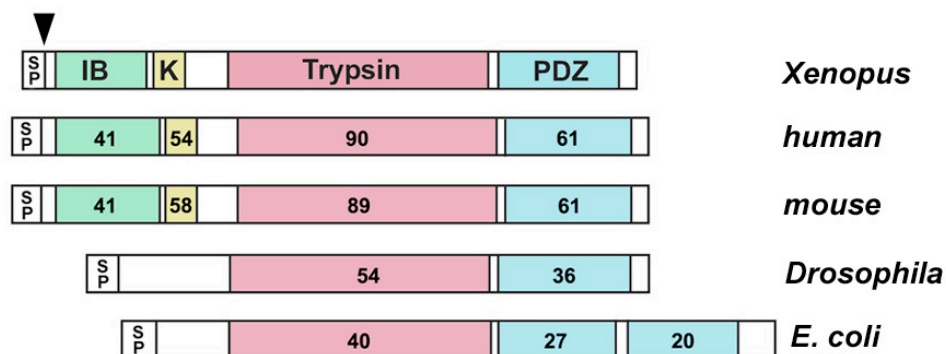
Figure 1. Protein structure of *Xenopus* HtrA1

Schematic structures of xHtrA1 and related homologues. The GenBank accession numbers for the listed proteins are *Xenopus* HtrA1 (EF490997), human HtrA1 (NP 002766), mouse HtrA1 (AAH13516), *Drosophila* serine protease (NP 650366) and *E. coli* HtrA/DegP (X12457). The positions of signal peptides (SP) are predicted by PSORT II program (http://psort.nibb.ac.jp) and the domain annotations derived from NCBI Conserved Domain Search. IB, Insulin-like growth factor binding domain; K, Kazal type serine protease inhibitor domain; Typsin, trypsin-like serine protease domain and PDZ, PSD95 (post synaptic density protein) DlgA (Drosophila disc large tumor suppressor) ZO1 mammalian tight junction protein domain. The numbers indicate the percentages of amino acid identity with the corresponding domains in xHtrA1. Figure modified from Hou, 2004.

Master Thesis.

3.2   Expression of *xHtrA1*

We analysed the expression of *xHtrA1* in early *Xenopus* embryos (Fig. 2). Reverse transcription polymerase chain reaction (RT-PCR) analysis showed that *xHtrA1* gene transcripts were not detected in unfertilized eggs or embryos younger than mid-blastula transition (MBT), indicating that *xHtrA1* is not maternally expressed (Fig.2A). *xHtrA1* gene transcripts were detected in early and mid gastrula stage (stage 10 and 11). The expression of *xHtrA1* reached its peak at late gastrula (stage 12) and early neurula (stage 13). Subsequently, *xHtrA1* gene expression decreased at open neural plate stage (stage 14 and 15) and then enhanced again at mid neurula stage (stage 16). The transcripts were too weak to be observed at tadpole stage (stages older than 20).

Whole mount *in situ* hybridization at the early gastrula stage (stage 10) revealed ubiquitous expression of *xHtrA1* in the ectoderm and mesoderm but not endoderm (Fig. 2B). Since the yolk in the vegetal part of the embryo may quench *in situ* hybridization signals, RT-PCR analysis was performed on ectodermal, mesodermal and endodermal explants of stage 10 embryos (Fig. 2C,D). *xHtrA1* transcripts exhibited highest levels in mesoderm and intermediate levels in ectoderm, but only very weak expression in endoderm explants (Fig. 2D), confirming the result of the whole mount *in situ* hybridization (Fig. 2B). As gastrulation proceeded, distinct expression was seen in a ring around the blastopore with higher intensity in the dorsal mesoderm (Fig. 2E). In late gastrula embryos, this periblastoporal expression domain became located to the posterior end, while an additional expression domain appeared in the anterior neural plate (Fig. 2F). During neurulation, *xHtrA1* expression further strengthened in the rostral CNS exhibiting high levels in the prospective eye field and in bilateral spots at the level of the midbrain-hindbrain boundary, at this stage, a new expression domain appeared in the neural folds (Fig. 2G). At the tail bud stage, transcripts were restricted to neural crest-derived cells of the facial mesenchyme and branchial arches (Fig. 2H and data not shown).

The expression pattern of *xHtrA1* shows similarities to sites of FGF signaling in the early embryo (Christen and Slack, 1997; 1999; Fig. 2I-L). Overlapping expression domains with *FGF8* include the blastopore ring (Fig. 2I), anterior neural plate, early midbrain-hindbrain

boundary, posterior mesoderm (Fig. 2J,K), and the branchial arch region (Fig. 2L). In addition, the expression of *xHtrA1* matches with ERK activation in the neural folds (Christen and Slack, 1999).
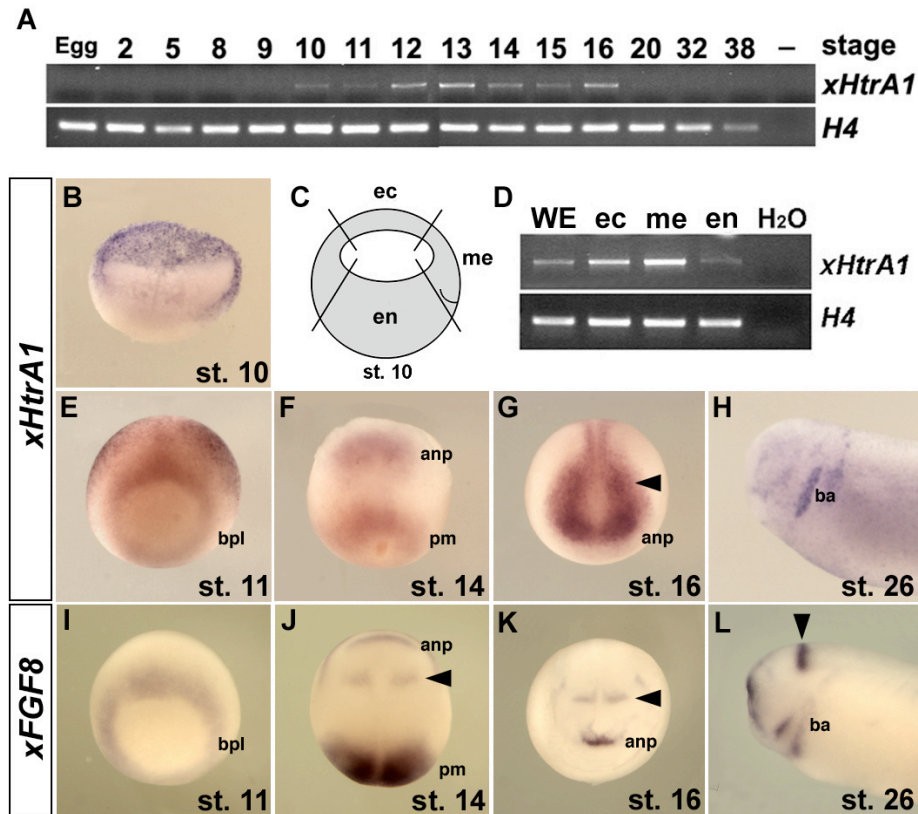
Figure 2. Gene expression of *Xenopus HtrA1*
(A) RT-PCR analysis of *xHtrA1* transcripts in the unfertilized egg and whole embryos. Staging of embryos according to Nieuwkoop and Farber (1994). *Histone4* (*H4*) was used as RNA loading control. Note abundant *xHtrA1* expression during the gastrula and neurula stages. (B) Lateral view of a hemi-sectioned early gastrula embryo (stage 10) after whole mount *in situ* hybridization with antisense *xHtrA1* RNA probe. (C) Diagram of stage 10 embryo dissected into ectoderm (ec), mesoderm (me), and endoderm (en). (D) RT-PCR analysis of embryo explants from (C). *xHtrA1* transcripts are abundant in ectoderm and mesoderm but hardly detectable in endoderm. (E-L) Whole mount *in situ* hybridization of *xHtrA1* (E-H) and *xFGF8* (I-L). *Xenopus* embryos at late gastrula stage, (E,I; dorso-vegetal view), early neurula stage (F,J; dorsal view), mid-neurula stage, (G,K; anterior view), tailbud stage (H,L; lateral view). The arrowhead indicates the midbrain-hindbrain boundary; bpl, blastopore lip; anp, anterior neural plate; pm, posterior mesoderm; nf, neural fold; fb, forebrain; ba, branchial arch.

3.3   Regulation of *xHtrA1* transcription by FGF signals

An animal caps experiment was performed to test the regulation of *xHtrA1* expression by FGF signaling (Fig. 3A). To this end, synthetic mRNAs of *Xenopus FGF8* and *FGF4* (also called *embryonic FGF, eFGF*) were microinjected into the animal pole of each

blastomere of the four-cell stage embryo. Animal caps were excised from stage 9 blastula embryos and cultured until sibling embryos reached stage 18. RT-PCR was performed to assay endogenous *xHtrA1* transcription and mesodermal *Xbra* gene expression was used as control. Uninjected animal caps neither expressed *xHtrA1* nor *Xbra* (Fig. 3A, lane 2). Injection of *FGF8* mRNA upregulated *xHtrA1* transcription in a concentration dependent manner (Fig. 3A, lane 3-5). In the same explants, *Xbra* gene transcription was induced at low dosis of *FGF8* and downregulated at higher dosis of *FGF8* (Hardcastle et al., 2000). *xHtrA1* was also upregulated in animal caps injected with *FGF4* mRNA (Fig. 3A, lanes 6-8), concomitant with a robust activation of *Xbra* (Isaacs et al., 1999). The activation of *xHtrA1* by members of the FGF family was specific, as *BMP4* mRNA failed to induce *xHtrA1* (Fig. 3A, lane 9), even though a dosis of *BMP4* mRNA was injected that robustly induced *Xbra* expression.

We also tested whether FGF signaling is required for *xHtrA1* transcription, using marginal zone explants from gastrula embryos (Fig. 3B). Four-cell stage embryos were microinjected into the marginal zone of each blastomere with different doses of mRNAs encoding a dominant negative FGF receptor-4a (DnFGFR4a; Hongo et al., 1999) or dominant negative FGFR-1 (XFD; Amaya et al., 1991). At stage 10, marginal zone regions were dissected and cultured for 2 hours, until sibling embryos reached stage 11. Marginal zone explants from uninjected embryos showed robust expression of *xHtrA1* and *Xbra* (Fig. 3B, lane 2). However, microinjection of *DnFGFR4a* or *XFD* mRNAs did not reduce *xHtrA1* mRNA levels, even at doses that significantly lowered or completely erased *Xbra* expression (Fig. 3B, lanes 3-6). We conclude that FGF signaling is sufficient, but not required for *xHtrA1* transcription. The overlapping expression between *xHtrA1* and *FGF8* sites and the finding that *xHtrA1* is activated by FGF signals suggest that *xHtrA1* may belong to the *FGF8* synexpression group.

37
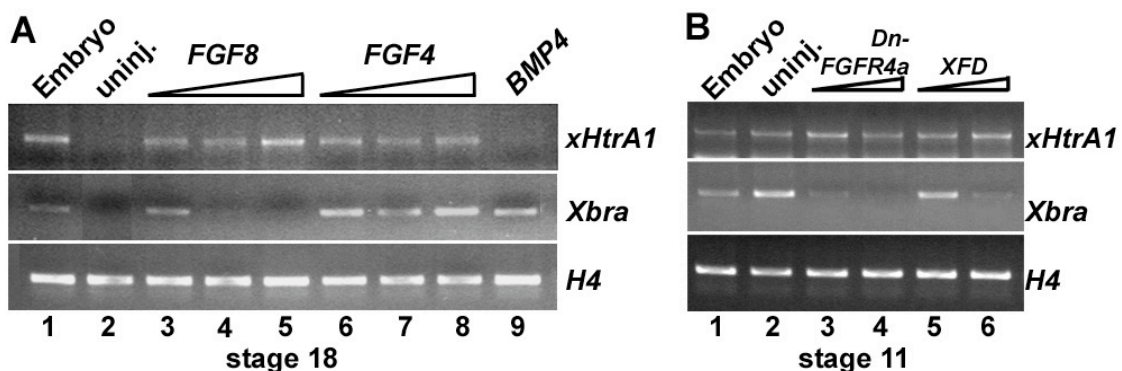
Figure 3. *FGF* is sufficient, but not required to induce *xHtrA1*

(A) Four-cell stage embryos were injected into the animal pole of each blastomere with *FGF8* mRNA (50, 150, 450 pg per embryo), *FGF4* mRNA (3, 6,12 pg per embryo) or *BMP4* mRNA (200 pg per embryo). Animal cap explants were cut from stage 9 embryos and analyzed at stage 18 by RT-PCR for expression of *xHtrA1* and *Xbra*. (B) Four-cell stage embryos were injected into the marginal zone of each blastomere with *DnFGFR4a* mRNA (400 pg, 4 ng per embryo) or *XFD* mRNA (2 ng, 6 ng per embryo). Marginal zone explants were excised from stage 10 embryos, and analyzed at stage 11 by RT-PCR for gene expression.

3.4   xHtrA1 blocks head formation and induces ectopic tails in a non-cell autonomous manner

To investigate the activity of xHtrA1, synthetic mRNA was injected into the animal pole of one ventral blastomere at the four-cell stage (Fig. 4; Hou, 2004). Embryos were first analyzed at the early tailbud stage, when the pigmentation of the closing neural folds demarcates the anteroposterior body axis (Fig. 4A). Microinjection of *xHtrA1* mRNA caused an overall shortening of the embryo and formation of a secondary body axis (Fig. 4B). Interestingly, the xHtrA1-induced ectopic axis was fused with the primary axis at the anterior end of the embryo. This phenotype is clearly distinct from a secondary axis induced by ventral injection of Wnt/β-Catenin signals or BMP antagonists, which converges with the primary embryonic axis at the posterior end (Moon and Kimelman, 1998). At the swimming tadpole stage, injection of *xHtrA1* mRNA caused the loss of head structures, including cement gland and eyes, and induced the formation of ectopic tail-like outgrowths (Fig. 4C,D; Hou, 2004). The induced tails consisted of dorsal and ventral fins also found in the primary tails. Histological analyses of *xHtrA1*-injected embryos showed that the secondary tail-like structures contained spinal cord, notochord and somite tissue (Fig. 4E). A single injection of *xHtrA1* mRNA induced ectopic expression of the neuronal marker *N-tubulin* (Fig. 4F,G; Hou, 2004), the axial marker *Sonic Hedgehog* (Fig. 4H,I; Hou, 2004) and the paraxial mesoderm marker *MyoD* (Fig. 4J,K; Hou, 2004) at sites where secondary axes formed. These findings indicate that the supernumerary tail structures induced by *xHtrA1* misexpression are of high complexity and contain all elements characteristic of endogenous tails. To determine whether xHtrA1 can induce ectopic structures on neighboring cells, we used the green fluorescent protein (GFP) as a lineage marker. After co-injection of *xHtrA1* and *GFP* mRNA into one ventral blastomere, GFP-positive cells were found predominantly in the secondary tail region (25%; Fig.

4L,L'). Injection of *xHtrA1* and *GFP* mRNA into one dorsal blastomere also generated secondary tail-like structures (11%; Fig. 4M,M'), abeit with lower frequency. Interestingly, the ectopic tail outgrowths were devoid of any GFP expression, suggesting that xHtrA1 recruited non-injected neighboring cells into the induced structures. The results demonstrate that xHtrA1 has non-cell autonomous activity and signals at long-range in the embryo.
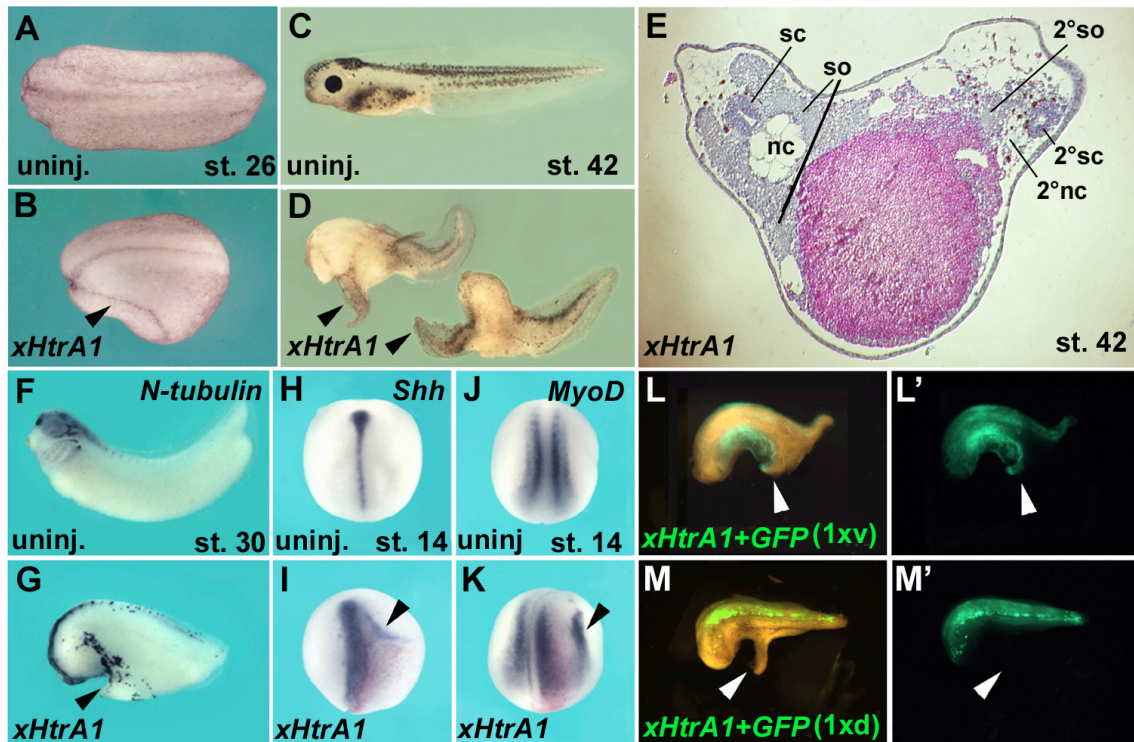
Figure 4. xHtrA1 induces ectopic tail-like structures in a non-cell autonomous way

(A) An uninjected tailbud embryo in dorsal view, anterior to the left. (B) Sibling embryo injected with 80 pg *xHtrA1* mRNA into one ventral blastomere at the four-cell stage. Note the secondary axis (arrowhead) fused with the primary body axis at the anterior end (21/88). (C) Uninjected embryo at swimming tadpole stage. (D) Reduction or loss of head structures (186/203) and ectopic tails (61/203; arrowhead) induced by a single ventral injection of *xHtrA1* mRNA. (E) Histological section of *xHtrA1*-injected embryo; secondary spinal cord (sc), notochord (nc) and somites (so) can be seen. (F-K) Ectopic expression domains of *N-tubulin* (differentiated neurons; 15/18), *Shh* (axial midline; 3/15), and *MyoD* (paraxial mesoderm; 6/19) induced by *xHtrA1* mRNA in tailbud (F,G; lateral view) and neurula embryos (H-K; dorsal view). Note that ectopic gene expression (arrowheads) in (I) and (K) arises adjacent to cells co-injected with *xHtrA1* and nuclear *lacZ* mRNA (red nuclei). (L,L',M,M') Lineage tracing of *xHtrA1* mRNA-injected cells using green fluorescent protein (GFP). Tailbud stage embryos in bright and darkfield views (merged pictures, L,M) or darkfield view alone (L',M'). (L,L´) After a single ventral injection of *xHtrA1* and *GFP* mRNA, injected cells populate the ectopic tail structure (arrowhead; 3/12). (M,M´) Co-injection of *xHtrA1* and *GFP* mRNA into one dorsal blastomere induces ectopic tail outgrowths (arrowhead) distant to the injection site

39

(4/37). Amounts of mRNA injected per blastomere were *xHtrA1* (80 pg), *nlacZ* (50 pg), *GFP* (320 pg). Panels C-D, F-K as in Hou, 2004. Master Thesis.

3.5 Proteolytic activity is required for xHtrA1 effects

To investigate the role of individual domains in the HtrA1 protein, a series of mutant constructs were generated and studied in *Xenopus* embryos (Fig. 5A; Hou, 2004). Microinjection of wild type *xHtrA1* mRNA into one ventral blastomere at the four-cell stage caused anencephaly and secondary tail formation in embryos at the advanced tail bud stage (Fig. 5C; Hou, 2004). The IGF binding domain of xHtrA1 contains a consensus CGCCXXC sequence (X, variable amino acid), characteristic of most members of the Insulin-like growth factor binding protein (IGFBP) superfamily. A deletion mutant lacking this consensus sequence (*xHtrA1ΔGC*) caused anencephaly and ectopic tail formation at a frequency similar to the wild type *xHtrA1* (Fig. 5D), indicating that the CGCCXXC sequence is not crucial for the xHtrA activity. Next, the entire trypsin-like serine protease domain was deleted (*xHtrA1Δtrypsin*). Microinjection of *xHtrA1Δtrypsin* mRNA gave rise to normally developed embryos (Fig. 5E), indicating that trypsin domain may be essential for the xHtrA1 activity. Since the trypsin domain comprises nearly two fifth of the mature protein, its deletion may change the overall conformation or interfere with a possible oligomerization of the protein. It has been reported that a mutational alteration of the active site serine to alanine in *E. coli* HtrA/DegP and in human HtrA1 results in loss of the proteolytic activity (Skorko-Glonek et al., 1995; Hu et al., 1998). We therefore substituted in *xHtrA1* the catalytic serine at position 307 with alanine (*xHtrA1S307A*). Microinjection of *xHtrA1S307A* mRNA failed to show any effect (Fig. 5F; Hou, 2004), suggesting that the proteolytic activity is required for the activity of xHtrA1. The PDZ protein-protein interaction domain has been shown to bind to substrates of mouse HtrA1 and thereby regulates its proteolytic activity (Murwantoko et al., 2004). A PDZ deletion mutant (*xHtrA1ΔPDZ*) failed to exhibit anencephalic or tail-like outgrowth phenotype caused by wild type *xHtrA1* (Fig. 5G), demonstrating the requirement of PDZ domain.

To ensure that the wild type and mutant proteins were properly synthesized *in vivo*, we performed a Western blot analysis of lysates from uninjected and mRNA-injected embryos at the late blastula stage (Fig. 5H), using an immunopurified antibody against the carboxyterminal PDZ domain of the xHtrA1 protein (see Materials and Methods). This

analysis showed that wild type *xHtrA1, xHtrA1ΔGC, xHtrA1Δtrypsin* and *xHtrA1S307A* generated comparative amount of proteins of the expected size (Fig. 5H and data not shown). We therefore rule out the possibility that the control-like phenotype from proteolytic domain mutants was due to failure of protein synthesis, concluding that the activity of xHtrA1 depends on the integrity of a functional proteolytic domain.
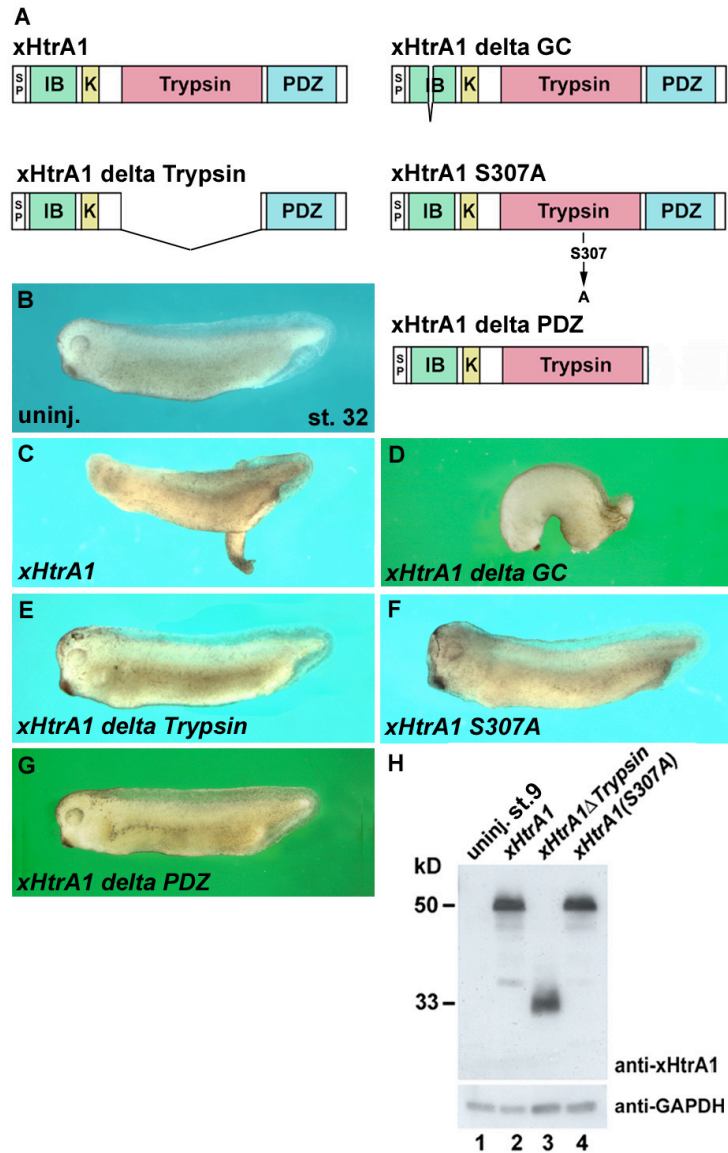
Figure 5. The proteolytic and the PDZ domain are required for the activity of xHtrA1

(A) Schematic diagram of wild type and mutant xHtrA1 protein constructs. (B) Uninjected tailbud embryo. (C) Loss of head structures (111/124) and secondary tail-like outgrowths (44/124) after injection of 80 pg *xHtrA1* mRNA into one ventral blastomere at the four-cell sstage. (D) Anencephaly (43/54) and ectopic tail formation (16/54) induced by 80 pg *xHtrA1ΔGC* mRNA. (E-G) Embryos injected with 80 pg mRNA of *xHtrA1ΔTrypsin* (E, n=406), *xHtrA1 S307A* (F, n=280) or *xHtrA1ΔPDZ* (G, n=86) show normal axial development. (H) Western blot analysis of wild type and mutant xHtrA1 proteins. Embryos were injected at the four-cell stage with 800 pg mRNA of the indicated

constructs, lysed at stage 9 and analyzed by Western blot with an immunopurified antibody derived against the carboxylterminal PDZ domain of xHtrA1 (α-xHtrA1). Note the 50 kD proteins of *xHtrA1*, *xHtrA1S307A*, and the truncated 33 kD protein of *xHtrA1Δtrypsin* synthesized in equal amounts. The low molecular weight 35 kD band in lane 1 is an autocatalytic cleavage product of xHtrA1. That is absent in lane 4, confirming that *xHtrA1S307A* lacks proteolytic activity. Panel A is modified from Hou, 2004. Master Thesis. Panels C, F are from Hou, 2004. Master Thesis.

3.6 Effects of xHtrA1 on embryonic patterning

To study the effects of xHtrA1 on pattern formation, we performed whole mount *in situ* hybridization with region- and tissue-specific molecular markers. At the early gastrula stage, *Otx2* has two distinct expression domains demarcating the anterior ectoderm (prospective cement gland, forebrain and midbrain) and the anterior mesendoderm (prechordal plate) (Fig. 6A; Hou, 2004). *HtrA1* mRNA blocked the anterior ectoderm domain of *Otx2*, but did not affect its mesendodermal expression (Fig. 6B; Hou, 2004). The pan-mesodermal marker *Xbra* demarcates the marginal zone of the gastrula stage embryo (Fig. 6C; Hou, 2004). *HtrA1* greatly expanded *Xbra* expression into the animal hemisphere (Fig. 6D; Hou, 2004), indicating that xHtrA1 may transform ectoderm into mesoderm. At the onset of neurulation, *BF1* demarcates the anterior-most part of the neural plate, which differentiates to the prospective telencephalon (Fig. 6E; Hou, 2004), *Rx2a* labels the eye field and *Krox20* indicates rhombomeres 3 and 5 of the hindbrain (Fig. 6G; Hou, 2004). *xHtrA1*-injected embryos failed to express *BF1*, *Rx2a* and *Krox20* gene expression (Fig. 6F,H; Hou, 2004). *Nkx2.5* marks pre-cardiac mesoderm (Fig. 6 I; Hou, 2004) and *Sizzled* is expressed in the heart and ventral blood islands (Fig. 6K; Hou, 2004). *HtrA1* blocked expression of the heart markers *Nkx2.5* and ventral mesoderm marker *Sizzled* in the anterior part of the embryo (Fig. 6J,L; Hou, 2004). Notably, *HtrA1* expanded the expression domain of *Sizzled* in the ventroposterior mesoderm (Fig. 6L; Hou, 2004). Hence *xHtrA1* suppresses anterior brain and heart development and promotes posterior mesoderm formation.
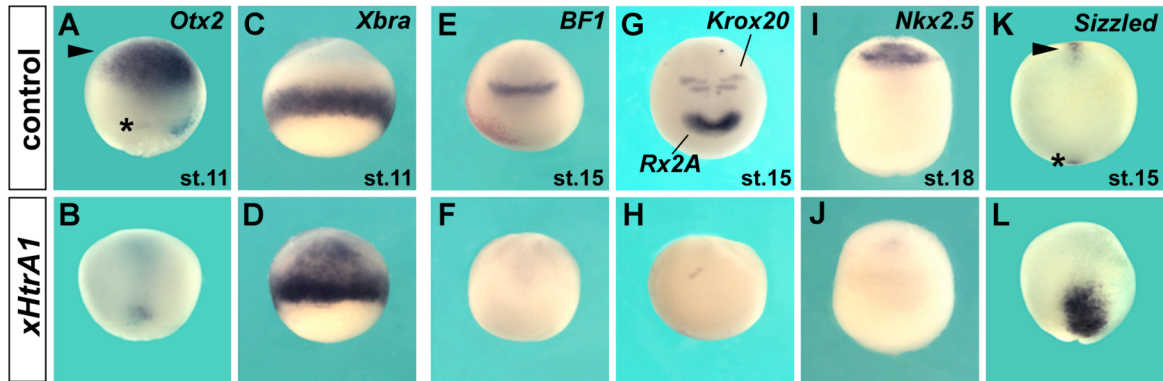
Figure 6. xHtrA1 promotes posterior and mesoderm development

Whole mount *in situ* hybridization of embryos after microinjection of *nlacZ* mRNA as control or *xHtrA1* mRNA into one blastomere at the four-cell stage. (A) Early gastrula embryo (dorsolateral view) with *Otx2* expression in the interior ectoderm (arrowhead) and anterior mesendoderm (star). (B) A single animal injection of *xHtrA1* mRNA (160pg) blocks expression of *Otx2* in the anterior ectoderm (45/45). (C) Sibling embryo (lateral view) with *Xbra* expression in the marginal zone. (D) A single marginal injection of *xHtrA1* (160 pg) expands *Xbra* expression into the animal hemisphere (20/23). (E) Mid-neurula stage embryo (anterior view) with *BF1* expression demarcating the telencephalon. (F) Animally injected *xHtrA1* mRNA blocks expression of *BF1* (22/23). (G) Sibling embryo (anterior view) with *Rx2a* labeling the prospective eye field and *Krox20* rhombomeres 3 and 5 of the hindbrain. (H) Animally injected *xHtrA1* mRNA (160 pg) blocks expression of *Rx2a* (16/20) and *Krox20* (6/20). (I) Late neurula (ventral view) with *Nkx2.5* demarcating the presumptive heart. (J) Animally injected *xHtrA1* leads to loss of *Nkx2.5* expression (28/36). (K) Mid-neurula (ventral view) with *Sizzled* expression in the heart (arrowhead) and ventral mesoderm (star). (L) Marginal injection of *xHtrA1* (80 pg) reduces *Sizzled* signals anteriorly, but expands *Sizzled* gene activity at the posterior end of the embryo (31/36). Panels A-L are from Hou, 2004. Master Thesis.

3.7   xHtrA1 has posteriorizing effect on antero-posterior neural patterning

We further investigated the effects of xHtrA1 on pattern formation of the central nervous system. To this end, we excised the neural plate plus underlying mesoderm and endoderm from late gastrula embryos and subdivided the tissue into four sections roughly corresponding to the future forebrain, midbrain, hindbrain and spinal cord (Fig. 7A). The explants were grown *in vitro* until sibling embryos reached the tailbud stage and analyzed by RT-PCR using region-specific molecular markers (Fig. 7B,C). The most anterior portion of the neural plate (section I) normally expresses the forebrain marker *Rx2a* and the forebrain/ midbrain marker *Otx2*, but not the hindbrain marker *Krox20* (Fig. 7B; lane 2). After microinjection of *xHtrA1* mRNA into animal pole of each blastomere of four-cell stage embryos, the equivalent region of the neural plate showed reduced *Rx2a* and *Otx2* expression, but activation of the hindbrain marker *Krox20* (Fig. 7B; lane 3). The more

43

posterior section II from uninjected neural plate normally expresses *Otx2*, but not the posterior hindbrain/ spinal cord marker *HoxD1* (Fig. 7B; lane 4). *xHtrA1* injection led to a loss of *Otx2* expression and *de novo* induction of the more posterior marker *HoxD1* (Fig. 7B; lane 5). Section III usually is positive for *Krox20* expression, but negative for more posterior spinal cord marker *HoxB9* (Fig. 7B; lane 6). In the presence of *xHtrA1*, the counterpart section lost *Krox20* expression, but induced the more posterior spinal cord marker *HoxB9* instead (Fig. 7B; lane 7). In section IV, expression of *HoxD1* and *HoxB9* was not affected by x*HtrA1* injection (Fig. 7B; lanes 8 and 9). The results indicate that xHtrA1 shifts the overall anteroposterior neural markers anteriorly (Fig. 7C), suggesting that xHtrA1 exerts posteriorizing activity onto the neural plate.
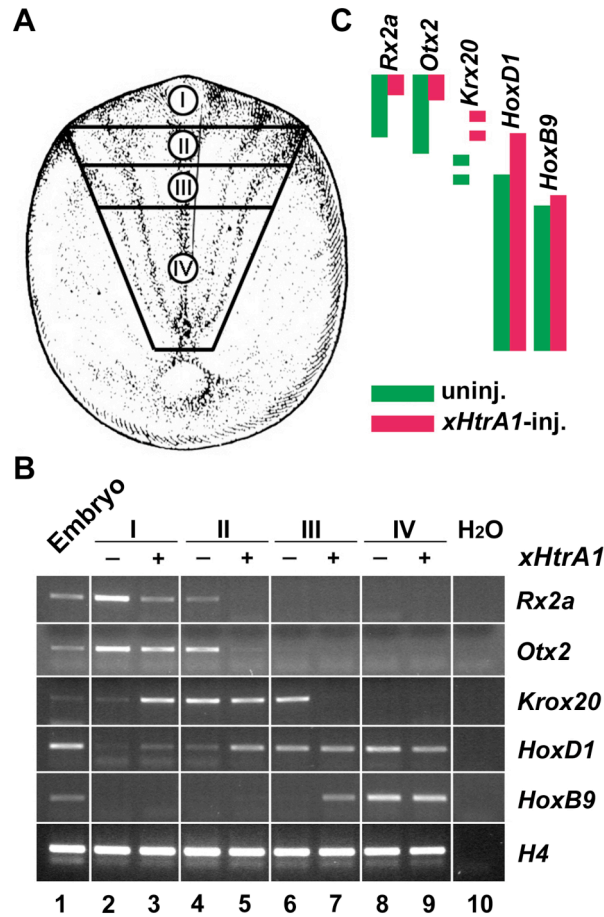
Figure 7. xHtrA1 posteriorizes the neural plate

(A) Experimental design. After injection of *Xenopus* embryos with *xHtrA1* mRNA into the animal pole of each blastomere at the four-cell stage (20 pg total per embryo), embryos were cultured in 0.1 x MBS until siblings reached early neurula stage (stage 13). The neural plate plus underlying mesoderm and endoderm was excised and four sections roughly corresponding to forebrain, midbrain, hindbrain and spinal cord were cultured in 0.8 x MBS. (B) RT-PCR analysis of explants (n=5 per sample) at equivalent of embryonic stage 26 with region-specific neural markers. *Rx2a*, forebrain; *Otx2*, forebrain/midbrain;

Krox20, rhombomeres 3 and 5 of the hindbrain; *HoxD1*, caudal to rhombomere 4 of the hindbrain and spinal cord; *HoxB9*, spinal cord; *H4*, histone4 for normalization. Note that sections I-III progressively lose anterior and gain posterior marker gene expression after *xHtrA1* mRNA injection, while section IV remains unaffected. (C) Regional fate of neural plate in uninjected and *xHtrA1*-injected embryos at stage 13 according to RT-PCR analysis at stage 26. Note the anteriorward shift of molecular markers in response to *xHtrA1* mRNA.

3.8   xHtrA1 dorsalizes the ectoderm and induces neuronal differentiation

Our studies so far focused on the influence of xHtrA1 on anteroposterior development and mesoderm induction of the embryo. Does this molecule also affect ectoderm patterning along the dorsoventral axis? The loss of head structures and the repression of anterior brain markers suggested that *xHtrA1* may interfere with neural plate development. Surprisingly, microinjection of *xHtrA1* mRNA caused significant expansion of the pan-neural marker *Sox2* towards the anterior and lateral side of early neurula embryos (Fig. 8A,B; Hou, 2004). Concomitantly, the neural crest marker *Slug* was severely reduced or lost (Fig. 8C,D; Hou, 2004) and the epidermal marker *Cytokeratin* was ventro-laterally displaced (Fig. 8E,F). At the mid-neurula stage, *xHtrA1* induced supernumerary *N-tubulin*-positive neurons, scattered throughout the epidermis on the lateral and ventral side of the embryo (Fig. 8G,H; Hou, 2004). In sum, xHtrA1 expands the neural plate at the expense of neural crest and epidermis development, and promotes neurogenesis to occur.
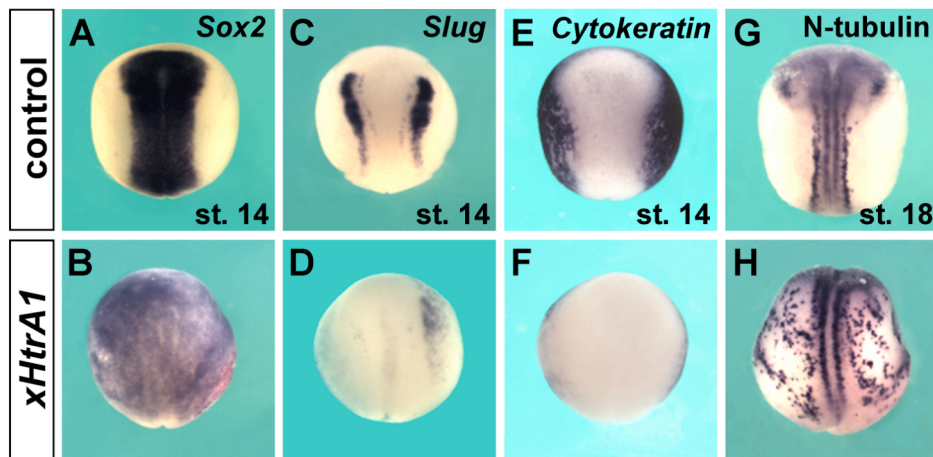
Figure 8. Effects of xHtrA1 on ectodermal patterning

Whole mount *in situ* hybridization analysis of embryos following a single animal injection of *nlacZ* mRNA (control) or *xHtrA1* mRNA at the four-cell stage. (A-F) Early neurula stage embryo in dorsal view. *xHtrA1* mRNA causes anterior and lateral expansion of *Sox2* (A,B, 62/67), reduction of *Slug* (C,D, 19/30) and *Cytokeratin* (E,F, 9/9) expression. (G,H) Mid-neurula embryo in dorsal view. *xHtrA1* mRNA induces ectopic expression of *N-tubulin* (G,H, 34/49) in the lateral and ventral parts of the embryo. Panels A-D, G-H are from Hou, 2004. Master Thesis.

45

3.9   xHtrA1 affects cell migration and promotes cell division

To further study the behaviour of *xHtrA1*-injected cells, we used GFP as a lineage tracer. Microinjection of *GFP* mRNA into one dorsal animal blastomere at the eight-cell stage targets cells in the anterior region and along the dorsal midline of the neural plate (Fig. 9A,A'). The dynamics of GFP labeling in early neurula stage embryos reflects the convergence extension movements characteristic for neural plate cells at this stage (Elul et al., 1998 and data not shown). When co-injected with *xHtrA1* mRNA, GFP-positive cells of the neural plate remain more distant to the dorsal midline (Fig. 9B,B' and data not shown). The failure of *xHtrA1*-injected cells to reach their proper location indicates that xHtrA1 may affect morphogenetic movements.

We next investigated the effect of xHtrA1 on proliferation, using an antibody against phosphorylated Histone3 (pH3, Saka and Smith, 2001) in whole mount embryos. Microinjection of *xHtrA1* mRNA into one animal blastomere at the eight-cell stage did not change the number of pH3-positive nuclei on the dorsal side (Fig. 9C,D). However, the same injection caused a two-fold increase of pH3-labelled cells on the ventral side (Fig. 9E,F,G), indicating that xHtrA1 promotes mitotic activity. In sum, xHtrA1 affects the behaviour of cells in numerous ways including perturbation of cell migration and stimulation of cell proliferation.
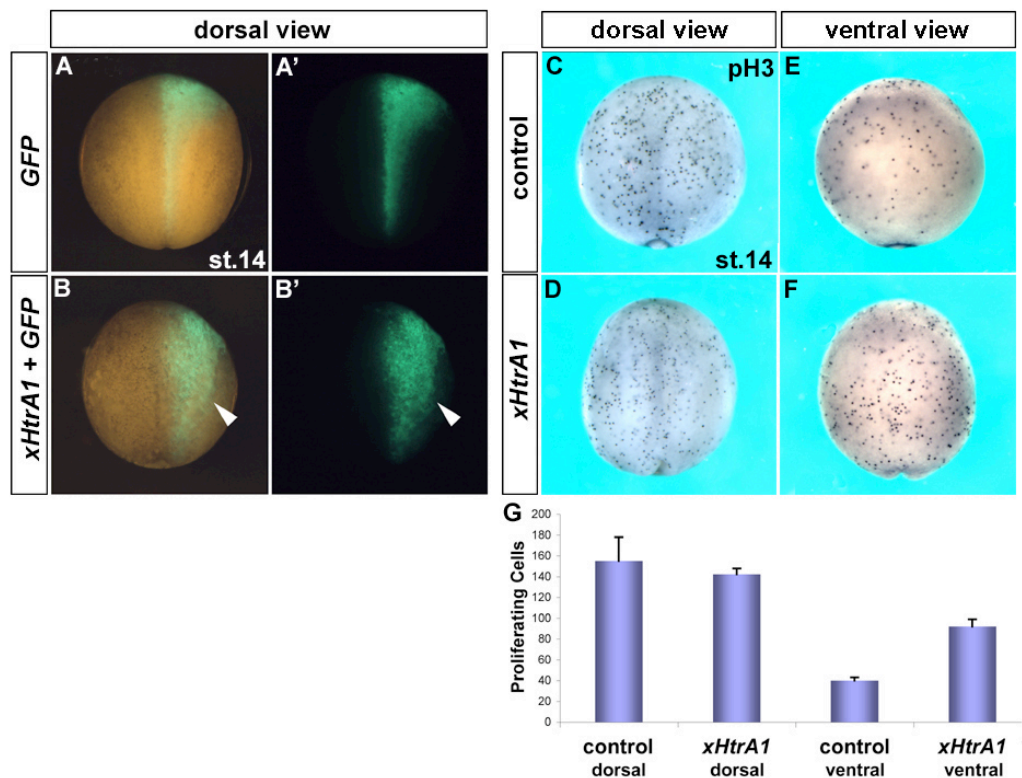
Figure 9. Effects of xHtrA1 on cell migration and proliferation

(A-B´) Early neurula embryos in dorsal view after injection of 230 pg *GFP* mRNA into one dorsal blastomere at the four-cell stage. Embryos are shown in bright and darkfield views (merged pictures, A,B) or darkfield views alone (A',B'). Note that cells co-injected with 80 pg *HtrA1* mRNA do not converge towards the midline, but remain in a more distal position (arrowhead). A minimum of 30 embryos has been analyzed. (C-F) Immunostaining for phosphorylated Histone3 (pH3) in early neurula embryos. Note that a single animal injection of *HtrA1* mRNA does not change the number of proliferating cells on the dorsal side, but increases cell proliferation on the ventral side. (G) Quantification of pH3-positive cells per embryo. For each sample, 3 specimens were evaluated.

3.10 xHtrA1 is essential for proper axial development, mesoderm formation and neuronal differentiation

In order to investigate the endogenous function of xHtrA1, we used an antisense morpholino oligonucleotide to specifically interfere with the protein biosynthesis of xHtrA1 in *Xenopus* embryos (Fig. 10). We designed a 25-mer morpholino sequence against the translation initiation site of the isolated *xHtrA1* gene and a related *xHtrA1* pseudoallel (*xHtrA1*-MO; Fig. 10A). Western blot analysis using an anti-xHtrA1 polyclonal antibody showed that the *xHtrA1*-MO efficiently blocked synthesis of the xHtrA1 protein, whereas a non-specific control morpholino (Co-MO) had no effect on xHtrA1 protein production (Fig. 10B, lanes 1-3). The specificity of the *xHtrA1*-MO was

further demonstrated by its inability to reduce the protein level of a recombinant *xHtrA1* construct that is not targeted by the *xHtrA1*-MO (*xHtrA1**; Fig. 10B, lanes 4 and 5). In xHtrA1*, the aminoterminal signal peptide of xHtrA1 has been replaced by a heterologous signal peptide from the Chordin protein followed by a Flag tag sequence (see Materials and methods). The data indicate that *xHtrA1*-MO is an efficient and specific tool to reduce xHtrA1 protein expression. Microinjection of 8 pmol control-MO into the animal pole at the two-cell stage had no effect compared to non-injected embryos (Fig. 10C and data not shown). In contrast, injection of the same account of *xHtrA1*-MO led to a remarkable reduction of the full body length and enlargement of the head (Fig. 10D; as in Hou, 2004). At the tadpole stage, *xHtrA1*-MO caused reproducibly enlargement of the head, reduction of the eye size and significantly shortened tail (Fig. 10E,F; as in Hou, 2004).

To further examine the effects of the *xHtrA1*-MO, molecular markers were analyzed by whole mount *in situ* hybridization. Strikingly, in gastrula embryos, marginal injection of the *xHtrA1*-MO blocked expression of the pan-mesoderm marker *Xbra* (Fig. 10G,H). In neurula embryos, animally injected *xHtrA1*-MO reduced expression of *N-tubulin* (Fig. 10I,J). *xHtrA1*-MO also erased the posterior expression domain of the ventral mesoderm marker *Sizzled* (Fig. 10K,L; as in Hou, 2004). The effect of the *xHtrA1*-MO was reverted by co-injection of *xHtrA1** mRNA (Fig. 10N). The phenotype of the *xHtrA1*-MO is opposite to those observed in gain-of-function experiments (Figs. 6D,L and Fig. 8H) and suggest an *in vivo* requirement of xHtrA1 for restricting the head territory and allowing tail structures, mesoderm and neurons to form.
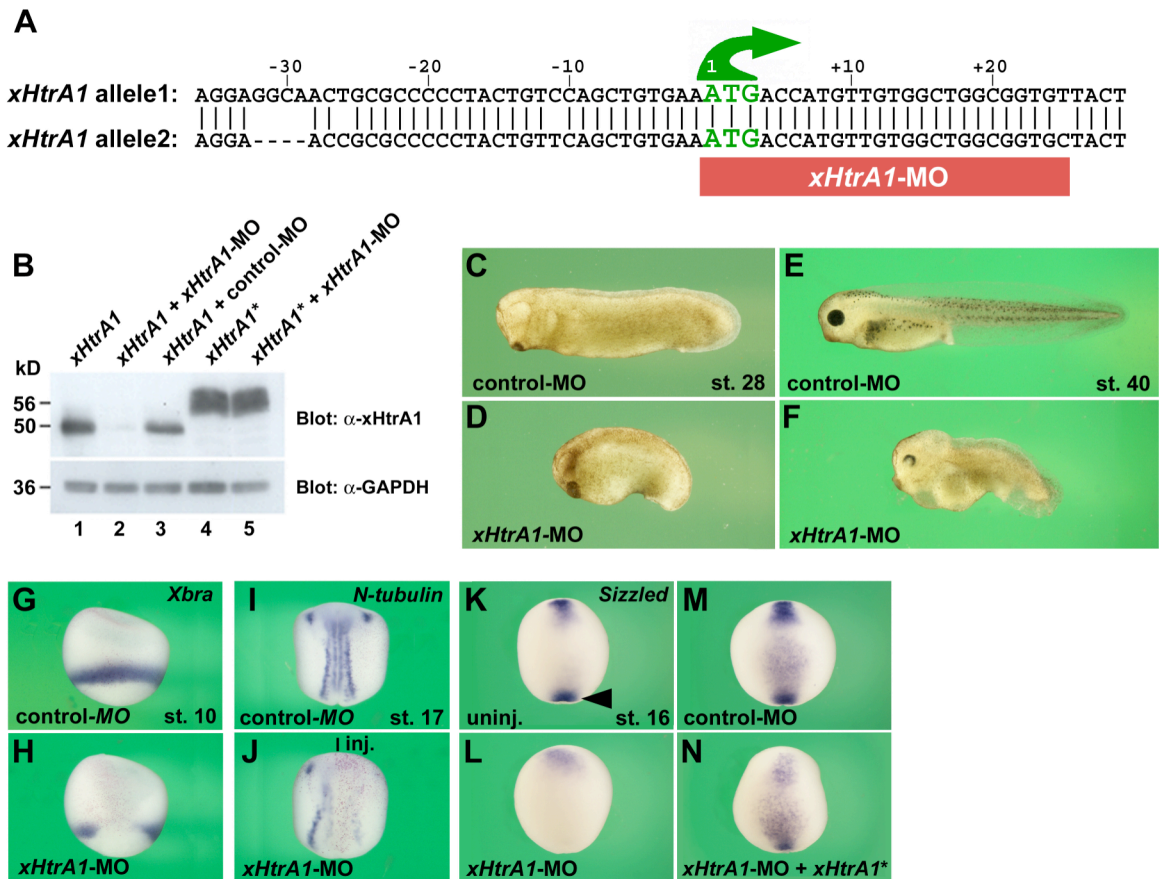
Figure 10. A morpholino oligonucleotide against xHtrA1 enhances anterior development and impairs mesoderm and neuronal differentiation

(A) An antisense morpholino oligonucleotide against *xHtrA1* (*xHtrA1*-MO) targets sequences of both *Xenopus laevis HtrA1* alleles (GenBank accession numbers are EF490997 and BC087471.1). (B) Western blot to verify the efficiency and specificity of the *xHtrA1*-MO. Embryos were microinjected at the two-cell stage with 8 pmol *xHtrA1*-MO or an unspecific control morpholino oligonucleotide (Co-MO), followed by 320 pg mRNA injection at the 4-cell stage of wild-type *xHtrA1* (*xHtrA1*) or of a recombinant *xHtrA1* clone that is not targeted by the *xHtrA1*-MO (xHtrA1*). Extracts from blastula stage embryos were analyzed by Western blotting, using an immunopurified polyclonal anti-xHtrA1 antibody (α-xHtrA1) to detect the xHtrA1 protein. An anti-Glyceraldehyde-3-phosphate dehydrogenase antibody (α-GAPDH) was used as protein loading control. Note that protein synthesis of xHtrA1 is completely blocked by *xHtrA1*-MO (lanes 1 and 2) and largely unaffected by the Co-MO (lane 3). *xHtrA1*-MO does not reduce synthesis of the non-targeted xHtrA1* construct (lanes 4 and 5). (C) Tailbud stage embryo injected animally with a total of 8 pmol control-MO at the two-cell stage (92/92). (D) Microinjection of 8 pmol *xHtrA1*-MO results in reduction of the body length and enlargement of the head territory (60/60). (E) A control-MO-injected tadpole embryo (18/18). (F) A sibling *xHtrA1*-MO-injected embryo has enlarged head, reduced eyes and significantly shortened tail structures (51/51). (G) Early gastrula in lateral view after whole mount *in situ* hybridization with *Xbra*. A single marginal injection of 10 pmol control-MO and 50 pg *nlacZ* mRMA as linage tracer (red nuclei) has no defect on *Xbra* expression (17/19). (H) Sibling embryo injected with 10 pmol *xHtrA1*-MO and 50 pg

49

nlacZ mRNA exhibits a gap in the *Xbra* expression domain at the injected site (red nuclei, 22/28). (I) Mid-neurula embryo in dorsal view labeled with *N-tubulin*. A single animal injection of 10 pmol control-MO and 50 pg *nlacZ* mRNA has no obvious effect on *N-tubulin* expression (15/19). (J) Sibling embryo injected with 10 pmol *xHtrA1*-MO and 50 pg *nlacZ* mRNA diminishes *N-tubulin* expression on the injected side (16/18). (K-N) Mid-neurula stage embryos in ventral view after *in situ* hybridization with *Sizzled* antisense probe. (K) A non-injected neurula stage embryo exhibits *Sizzled* expression at the anterior and posterior end of the embryo (L) Microinjection of 8 pmol *xHtrA1*-MO abolishes the posterior expression domain of *Sizzled* (41/47). (M) A control-MO shows no effect (19/19). (N) Microinjection of 80 pg *xHtrA1** mRNA at the four-cell stage reverts the loss of *Sizzled* posterior expression caused by *xHtrA1*-MO (15/15). Panels C-F, K-L are similar to those in Hou, 2004. Master Thesis.

3.11   A neutralizing antibody against xHtrA1 anteriorizes embryonic development

As an independent test for the requirement of xHtrA1 in axial development, we made use of a neutralizing antibody, which recognizes the PDZ domain of xHtrA1, to block the activity of xHtrA1 in the extracellular space (Fig. 11). Microinjection 100 nl of purified pre-immune serum into the blastocoel cavity of a blastula stage embryo had no detectable effect (Fig. 11B). In contrast, microinjection of the immuno-purified antibody anti-xHtrA1 resulted in an anteriorized phenotype. Typically, the body axis was shortened and the head enlarged at the expense of trunk and tail structures at the advanced tail bud stage (Fig. 11C). The specificity of this effect was underscored by the finding that the anteriorized phenotype of the anti-xHtrA1 antibody was rescued by co-injection of *xHtrA1* mRNA (Fig. 11D). Together the data support a function of xHtrA1 in normal development of the anteroposterior body axis.
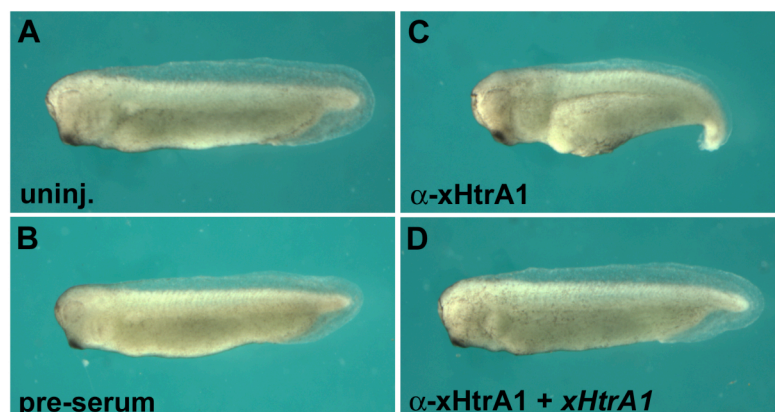
Figure 11. Blastocoel injection of an anti-xHtrA1 antibody promotes anterior development

(A) Uninjected tail bud embryo. (B) Injection of 100 nl of immunopurified pre-serum has no effect (114/121). (C) Enlarged head structures after injection of 100 nl immunopurified

anti-xHtrA1 antibody (α-xHtrA1, 200 ng) into the blastocoel at stage 8 (32/107). (D) Microinjection of 160 pg *xHtrA1* mRNA into blastomeres of the four-cell stage blocks the anteriorizing effect caused by blastocoelic injection of α-xHtrA1 (5/5).

3.12 HtrA1 cooperates with FGF signals

The phenotypic effects observed in *xHtrA1* mRNA-injected embryos are reminiscent of those caused by FGF signals. Microinjection of *FGF4* DNA into one ventral blastomere of four-cell stage embryos resulted in the induction of secondary posterior outgrowths that developed into complex tail-like structures (Fig. 12A; Pownall et al., 1996); radially injected *FGF4* mRNA caused expansion of the mesoderm marker *Xbra* into the animal hemisphere (Fig. 12B; Pownall et al., 1996); *FGF8* mRNA triggered ectopic *N-tubulin*-positive neuronal differentiation (Fig. 12C, Hardcastle et al., 2000). To test whether xHtrA1 and FGFs also cooperate during mesoderm induction, we performed an animal cap assay (Fig. 12D-H). We injected mRNA encoding *FGF4* and *xHtrA1* either alone or in combination into the animal pole of four-cell stage embryos, excised animal caps at the blastula stage and cultured them *in vitro*, until sibling embryos reached the tailbud stage. While uninjected control caps formed spherical structures containing epidermis (Fig. 12D), few caps elongated when injected with *xHtrA1* mRNA (Fig. 12E) or a suboptimal dosis of *FGF4* mRNA (Fig. 12F), indicating formation of mesoderm tissue. Strikingly, co-injection of both *FGF4* and *xHtrA1* mRNA caused a dramatic elongation of all animal caps (Fig. 12G). To confirm mesoderm induction at the molecular level, we analyzed the mesodermal markers *Xbra* and *Xcad3* by RT-PCR analysis when sibling embryos reached the mid-gastrula stage (Fig. 12H). Uninjected animal cap explants showed no *Xbra* and *Xcad3* expression (Fig. 12H, lane 2). Microinjection of *xHtrA1* mRNA mildly activated the expression of *Xbra* and *Xcad3*, giving support to the notion that xHtrA1 induces mesoderm differentiation. As expected, *FGF4* mRNA also activated these mesodermal marker genes (Fig. 12F, lane 4; Pownall et al., 1996). Importantly, co-injection of *xHtrA1* and *FGF4* mRNA further enhanced *Xbra* expression, indicating that xHtrA1 stimulates mesoderm induction by FGF4 (Fig. 12F, lane 5). The results clearly show a cooperative effect between HtrA1 and FGF signals during mesoderm induction.
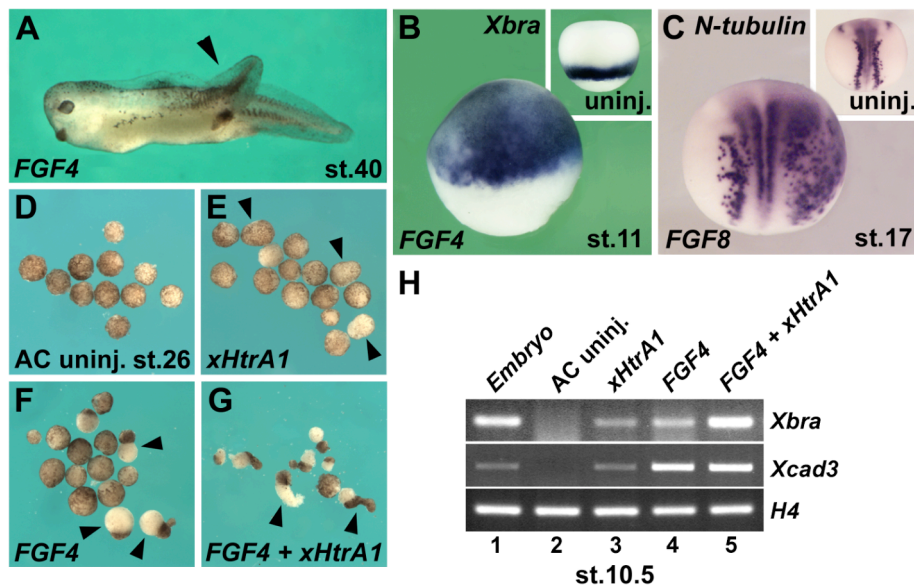
Figure 12. Effects of FGFs on embryonic development and cooperation with xHtrA1 during mesoderm induction

(A) Tadpole embryo with ectopic tail-like outgrowth (arrowhead) induced by microinjection of 4 pg *FGF4* DNA into one ventral blastomere at the four-cell stage (13/66). (B) Significant expansion of the mesoderm marker *Xbra* induced by 1.6 pg *FGF4* mRNA injection into each animal blastomere at the four-cell stage (23/23). Insert shows uninjected sibling embryo. (C) Ectopic *N-tubulin*-positive neurons induced by microinjecting 5 pg *FGF8* mRNA into a single animal blastomere at the four-cell stage (118/120). (D-G) Embryos were injected with mRNA of *xHtrA1* and *FGF4* either alone or in combination, animal caps were excised at stage 8 and cultured until stage 25. (E) Animal caps extend only very slightly when injected with 360 pg *xHtrA1* mRNA. (F) A suboptimal dosis of *FGF4* mRNA (3.2 pg) causes mild elongation in some animal explants. (G) A combination of *xHtrA1* and *FGF4* mRNA showed robust elongation in all animal caps. (H) RT-PCR of animal cap explants at stage 11.

3.13 Role of FGF signals for the activity of xHtrA1

xHtrA1 and FGFs show similar activities in axial development, mesoderm induction and neuronal differentiation. They exhibit cooperative effects on mesoderm induction in animal cap explants. These observations suggest that xHtrA1 and FGF signaling may be linked. To test whether FGF signals are required for the actions of xHtrA1, endogenous FGF signaling was blocked by dominant negative FGF receptor constructs. We used truncated version of the FGFR1 (XFD) and FGFR4a (DnFGFR4a), that each contain an intact extracellular and transmembrane domain, but lack an intracellular tyrosine kinase domain (Amaya et al., 1991; Hugo et al., 1999). Microinjection of *XFD* mRNA enlarged head structures at the expense of trunk and tail development (Fig. 13B, Amaya et al., 1991). Notably, *XFD* blocked the loss of head structures and formation of ectopic tail-like

52

protrusions in embryos co-injected with *xHtrA1* mRNA (Fig. 13C,D). These results suggest that intact FGF signaling is crucial for the effects of xHtrA1 on anterior-posterior axis formation. FGF signals also play a role in mesoderm formation, as shown by the suppression of *Xbra* expression by *XFD* mRNA injection (Fig. 13E,F; Amaya et al., 1991). Importantly, *XFD* abolished ectopic *Xbra* expression induced by *xHtrA1* (Fig. 13G,H), suggesting that FGF signaling is important for *xHtrA1*-mediated mesoderm induction. An involvement of FGF signals in the formation of differentiated neurons is evident from the loss of *N-tubulin* expression by *DnFGFR4a* mRNA (Fig. 13 I,J; Hardcastle et al., 2000). While *xHtrA1* mRNA induced ectopic neurons on both the injected and non-injected contralateral side (Fig. 13K), neurogenesis by *xHtrA1* was blocked by co-injection of *DnFGFR4a* on the injected side (Fig. 13L). In conclusion, multiple patterning activities of xHtrA1 including anterior-posterior patterning, mesoderm formation and neuronal differentiation, rely on intact FGF signaling pathway.
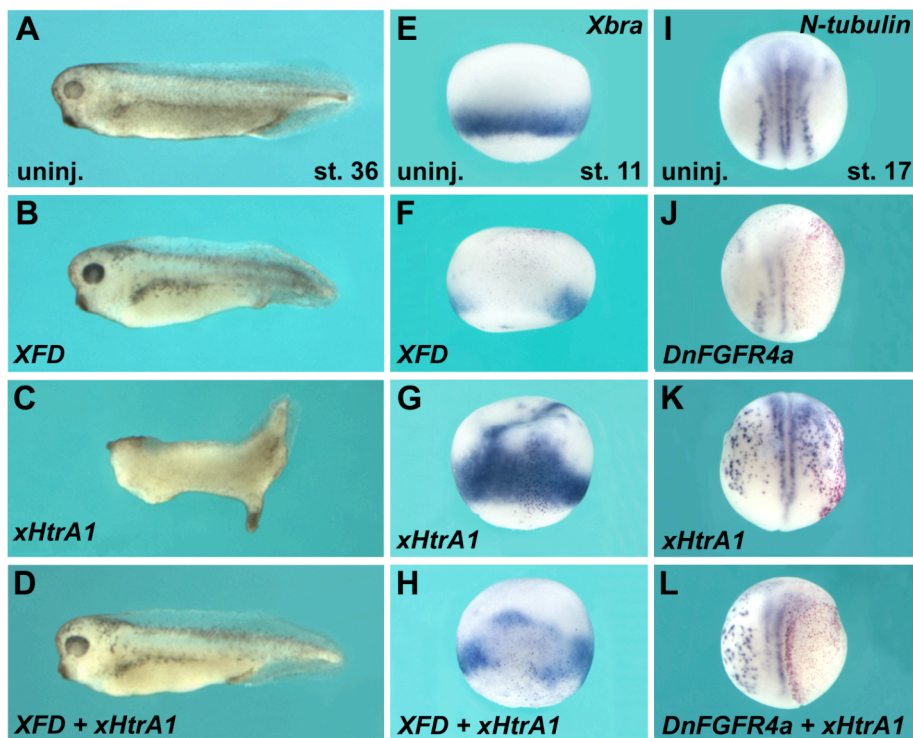
Figure 13. xHtrA1-mediated posteriorization, mesoderm induction and neuronal differentiation require intact FGF signaling

(A) Uninjected tadpole. (B) Microinjection of 110 pg *XFD* mRNA into the animal pole of four-cell stage embryos causes enlargement of head structures and slight shortening of the body length (54/68). (C) Anencephaly and ectopic tail-like outgrowth induced by a single ventral injection of 80 pg *xHtrA1* mRNA (68/80 with reduced heads, 32/80 with ectopic tail-like protrusions). (D) Restoration of head development and suppression of ectopic tail

formation after co-injection of 110 pg *XFD* and 80 pg *xHtrA1* mRNA (13/16). (E) Uninjected embryo at early gastrula stage (lateral view) after whole mount *in situ* hybridization with an *Xbra* antisense probe. (F) Blockage of endogenous *Xbra* expression by a radial injection of 220 pg *XFD* into one blastomere at the four-cell stage (38/47). *nlacZ* mRNA (100 pg) was co-injected as a lineage tracer (red nuclei). (G) Ectopic *Xbra* expression induced by a single marginal injection of 80 pg *xHtrA1* mRNA (13/13). (H) Co-injection of 220 pg *XFD* mRNA inhibits ectopic *Xbra* expression induced by *xHtrA1* mRNA (16/18). (I) Uninjected embryo at mid-neurula stage (dorsal view) after whole mount *in situ* hybridization with *N-tubulin* demarcating trigeminal ganglion cells, motor neurons, intermediate neurons and sensory neurons. (J) Suppression of endogenous *N-tubulin* expression by injection of 110 pg *DnFGFR4a* mRNA into one blastomere at the four-cell stage (18/18). (K) Microinjection of 80 pg *xHtrA1* mRNA induces ectopic *N-tubulin* expression (10/12). Note that supernumerary neurons are not restricted to the injected side (red label), but arise in a non-cell autonomous manner on the contra-lateral side. (L) Co-injection of *DnFGFR4a* and *xHtrA1* mRNA inhibits ectopic *N-tubulin* expression on the injected side (10/10).

3.14   xHtrA1 activates FGF signaling

To investigate whether xHtrA1 directly affects FGF activity, we analysed the activation of the FGF signaling intermediate ERK (extracellular signal regulated protein kinase) by immunoblotting (Fig. 14A). Microinjection of *xHtrA1* mRNA led to an accumulation of diphosphorylated ERK (dpERK; Fig. 14A, lanes 1,2). Compared to control-MO which did not show any effect, the *xHtrA1*-MO blocked ERK phosphorylation (Fig. 14A, lanes 3,4), indicating a requirement for xHtrA1 in the activation of FGF signaling. Whole-mount immunostaining showed that in gastrula embryos, the double phosphorylated form of ERK (dpERK) was restricted to the marginal zone (Fig. 14B; Christen and Slack, 1999). Radial injection of *xHtrA1* mRNA led to expansion of dpERK signals into the animal hemisphere (Fig. 14C). Co-injection of *XFD* not only eliminated endogenous dpERK, but also prevented expansion of dpERK signals by *xHtrA1* (Fig 14D). Whole mount *in situ* hybridization showed that in neurula embryos, microinjection of *xHtrA1* induced ectopic *FGF8* and *FGF4* transcription (Fig. 14E,F,H,I). The ability of *xHtrA1* to activate ectopic FGF gene activity was blocked by co-injection of *XFD* or *DnFGFR4a* mRNA (Fig. 14G,J). This finding suggests that xHtrA1 stimulates ERK phosphorylation and the expression of *FGF8* and *FGF4* via FGF receptor signaling. Based on these and previous data (Fig. 3A), we conclude that xHtrA1 and FGF form a positive feedback loop, in which each component reinforces the gene activity of the other (Fig. 14K).
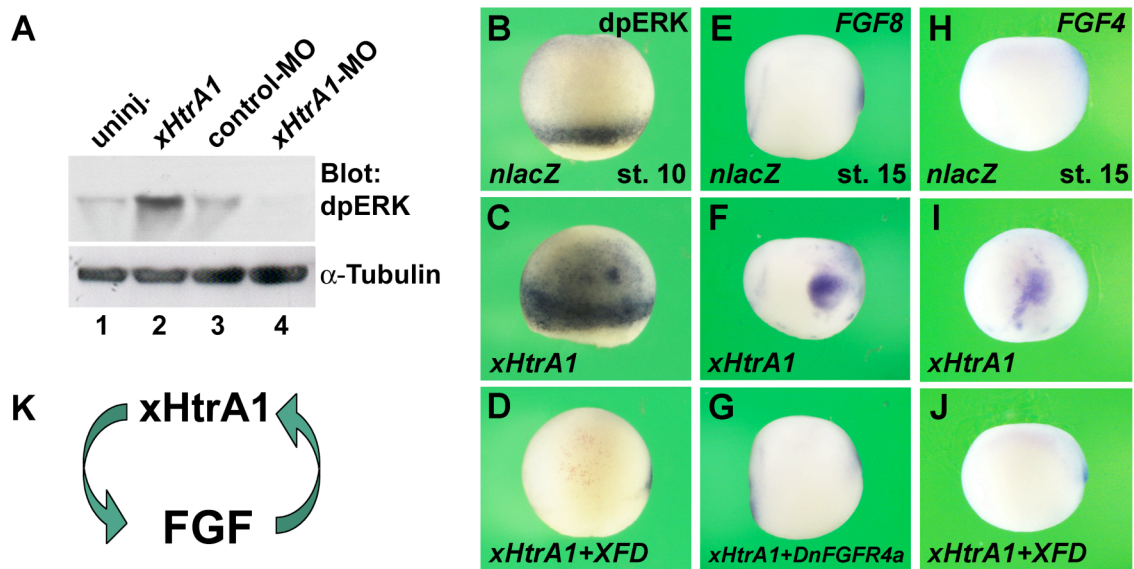
Figure 14. xHtrA1 activates ERK signaling and transcription of *FGF8* and *FGF4*

(A) Western blot analysis for diphosphorylated ERK (dpERK) in stage 14 embryos. *xHtrA1* mRNA (80 pg) was microinjected marginally into each blastomere at the two-cell stage. *xHtrA1*-MO or control-MO (each 4 pmol) was injected into each blastomere at the two-cell stage embryos. At stage 14, embryos were lysed and loaded (approximately three embryos per lane). α-Tubulin was used as loading control. (B-D) Whole mount immunohistochemistry for dpERK in early gastrulae (lateral view). (B) *nlacZ* mRNA-injected control embryo with dpERK activation restricted to the equatorial zone (11/11). (C) Radially injection of 160 pg *xHtrA1* mRNA into one blastomere at the four-cell stage expands dpERK signals into the animal hemisphere (21/21). (D) Co-injection of 220 pg *XFD* mRNA blocks endogenous and *xHtrA1*-induced dpERK expression (26/26). (E-J) Lateral view of early neurula embryos after whole mount *in situ* hybridization (E) *FGF8* expression in *nlacZ* mRNA-injected control embryo at the anterior (left) and posterior end (10/10). (F) Injection of 80 pg *xHtrA1* mRNA into all blastomeres at the four-cell stage induces ectopic expression domain of *FGF8* in the trunk (26/27). (G) Co-injection of 110 pg *DnFGFR4a* mRNA blocks ectopic *FGF8* gene activation by *xHtrA1* (25/27). (H) *FGF4* expression in *nlacZ*-injected control embryo at the anterior and posterior ends (16/16). (I) Injection of 80 pg *xHtrA1* mRNA leads to ectopic expression of *FGF4* in the trunk (12/12). (J) The effect of *xHtrA1* on *FGF4* expression is reverted by co-injection of 220 pg *XFD* (10/12). (K) Diagram showing that HtrA1 and FGF form a positive feedback loop, in which each component reinforces the gene activity of the other.

3.15 xHtrA1 stimulates FGF signaling at distance

We next studied whether xHtrA1 promotes long-range FGF signaling using an animal cap conjugate assay. Animal caps from embryos injected with *FGF4*, *xHtrA1* and *nlacZ* mRNA as lineage tracer ("inducer" caps) were first combined with uninjected "responder" caps, incubated *in vitro* for 4.5 hours and analyzed by *in situ* hybridization for *Xbra* expression (Fig. 15A, upper half). Control conjugates injected with *nlacZ* mRNA alone

were flat and did not express *Xbra* (Fig. 15B). Following microinjection of *FGF4* mRNA, the responding hemisphere slightly elongated and showed weak *Xbra* expression restricted to the interface with the inducer hemisphere (Fig. 15C). *xHtrA1* mRNA on its own exhibited only a little effect, with slight elongation of animal cap conjugates but without detectable *Xbra* expression (Fig. 15D). However, when *xHtrA1* was in combination with *FGF4* mRNA, it triggered a robust outgrowth of both the inducer and the responder caps. Importantly, the levels of *Xbra* expression were greatly elevated and expanded to locations far away from the sites of FGF4 secretion (Fig. 15E). In an independent experiment, we examined of how signaling was affected, when the sources of FGF4 and xHtrA1 were spatially segregated. We recombined *FGF4* mRNA-injected inducer caps with *xHtrA1* mRNA-injected responder caps (Fig. 15A, lower half). *nlacZ*-injected control inducer caps combined with *xHtrA1*-treated responder caps induced only slight elongation without *Xbra* staining (Fig. 15F). In contrast, juxtaposition of *FGF4* and *xHtrA1* sources triggered elongation of both hemispheres and resulted in strong and widespread *Xbra* expression (Fig. 15G). The fact that *nlacZ*-labeled cells from the inducer cap did not intermingle with responder cap cells indicates that the effect of xHtrA1 was not due to cell movements. The results demonstrate that xHtrA1 stimulates long-range signaling of FGF.
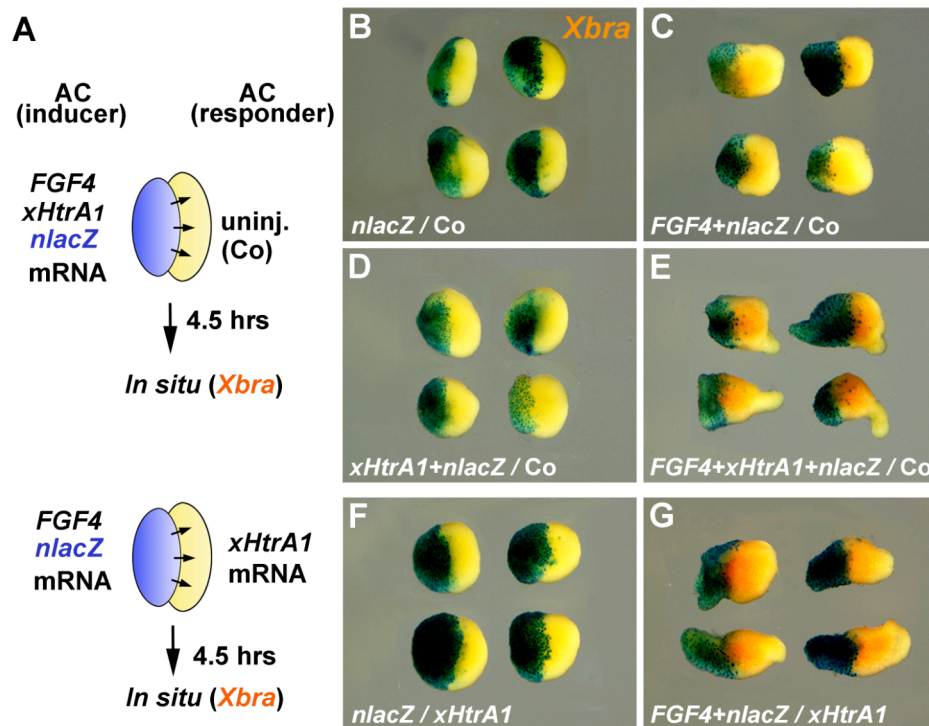

Figure 15. xHtrA1 promotes long-range FGF signaling in the animal cap conjugate assay

(A) Experimental design. "Inducer" animal cap explants from blastula stage embryos were injected with 16 pg *FGF4* alone or in combination with 160 pg *xHtrA1* mRNA and juxtaposed to uninjected „responder" animal caps (upper panel). Alternatively, an *FGF4*-injected inducer cap was recombined with an *xHtrA1*-injected responder cap (lower panel). The inducer caps were co-injected with 100 pg *nlacZ* mRNA as lineage tracer (blue X-Gal staining) to distinguish them from the responder caps. The animal cap conjugates were cultured for 4.5 hours at room temperature until sibling embryos reached the mid-gastrula stage, fixed and analyzed by whole-mount *in situ* hybridization for the expression of the FGF-responsive *Xbra* gene (orange staining). (B) Control animal cap conjugates with *nlacZ*-injected inducer cap (blue) and uninjected responder cap remain flat and do not express *Xbra*. (C) Slight elongation and narrow *Xbra* expression (red) in the responder cap at the interface to the *FGF4*-injected inducer cap. (D) *xHtrA1* in the inducer cap does not cause significant elongation and detectable *Xbra* expression in the responder cap. (E) A combination of *FGF4* and *xHtrA1* induces significant elongation and robust *Xbra* expression in the responder cap. (F) *xHtrA1* in the responder cap has no apparent effects on the conjugate. (G) *xHtrA1* in the responder cap juxtaposed to an *FGF4*-injected inducer cap causes strong elongation and *Xbra* expression far away from the signaling source.

3.16 xHtrA1 causes proteolytic degradation of Biglycan, Syndecan4, and Glypican4

Proteoglycans are important regulators of FGF signaling that control the spread and activity of FGF ligands in the extracellular space (Trowbridge and Gallo, 2002; Kramer and Yost, 2003). It has previously been reported that an aminoterminally truncated mouse HtrA1 construct consisting of only the trypsin and PDZ domains degrades bovine Biglycan (Tocharus et al., 2004). *Xenopus* Biglycan (xBgn) as well as the heparan sulfate proteoglycans Syndecan4 (xSyn4) and Glypican4 (xGpn4) are expressed in the early embryo (Galli et al., 2003; Moreno et al., 2005; Munoz et al., 2006). We transfected full-length xHtrA1 cDNA together with Flag-tagged xBgn, xSyn4, and xGpn4 constructs into HEK293 cells. Western blot analysis showed that xHtrA1 caused degradation of all three proteoglycans (Fig. 16A). In order to confirm this result *in vivo* in *Xenopus* embryos, mRNA of Flag-tagged *Xenopus Biglycan* (*Flag-xBgn*) was microinjected alone or together with *xHtrA1* into each blastomere of four-cell stage embryos. In addition, control-MO or *xHtrA1*-MO was microinjected into all blastomeres at the two-cell stage, followed by another injection of *xHtrA1* mRNA into all blastomeres at the four-cell stage. When the control embryos reached mid-neurula stage, total proteins were extracted, fractionated on 12% SDS-PAGE gel, and subjected to Western blot analysis with an anti-Flag antibody. In *Xenopus* embryos, microinjection of *xHtrA1* mRNA decreased the protein levels of Flag-xBgn. In contrast, *xHtrA1*-MO but not control-MO, led to the accumulation of the

full-length Flag-xBgn. It is of interest that the low molecular weight band at 55 kD in uninjected or control-MO-injected embryos disappeared in *xHtrA1*-MO-injected embryos, suggesting that this xBgn fragment may arise through proteolysis by endogenous xHtrA1 (Fig. 16B). This result shows that exogenously applied as well as endogenous xHtrA1 cleaves xBgn *in vivo*. We also observed that injected *xHtrA1* mRNA degraded Flag-xSyn4 (Fig. 16C). Overexpression of *xHtrA1* did not appear to affect xGpn4-Flag, but *xHtrA1*-MO led to an accumulation of this protein in the embryo (Fig. 16D), indicating that endogenous xHtrA1 may largely degrade xGpn4-Flag. Together, the results suggest that xBgn, xSyn4 and xGpn4 are proteolytic targets of xHtrA1 activity.

Biglycan contains one or two dermatan/chondroitin sulfate chains that are covalently linked to the core protein (Trowbridge and Gallo, 2002). Dermatan sulfate arises from chondroitin sulfate through epimerization of glucuronic into iduronic acid (Maccarana et al., 2006). As dermatan sulfate, but not chondroitin sulfate, binds to and activates FGF ligands (Taylor et al., 2005), we assessed the nature of the glycosaminoglycan in *xBgn* in *Xenopus* embryos. Flag-tagged *xBgn* was injected into *Xenopus* embryos, all glycosylated proteins were extracted from late neurula stage embryos and purified using an anion-exchange column. Treatment of purified proteoglycans with Chondroitinase B, which specifically degrades DS sugar chains, caused a mobility shift of Flag-tagged Biglycan (Fig. 16E), strongly indicating the presence of dermatan sulfate chains in *Xenopus* Biglycan.
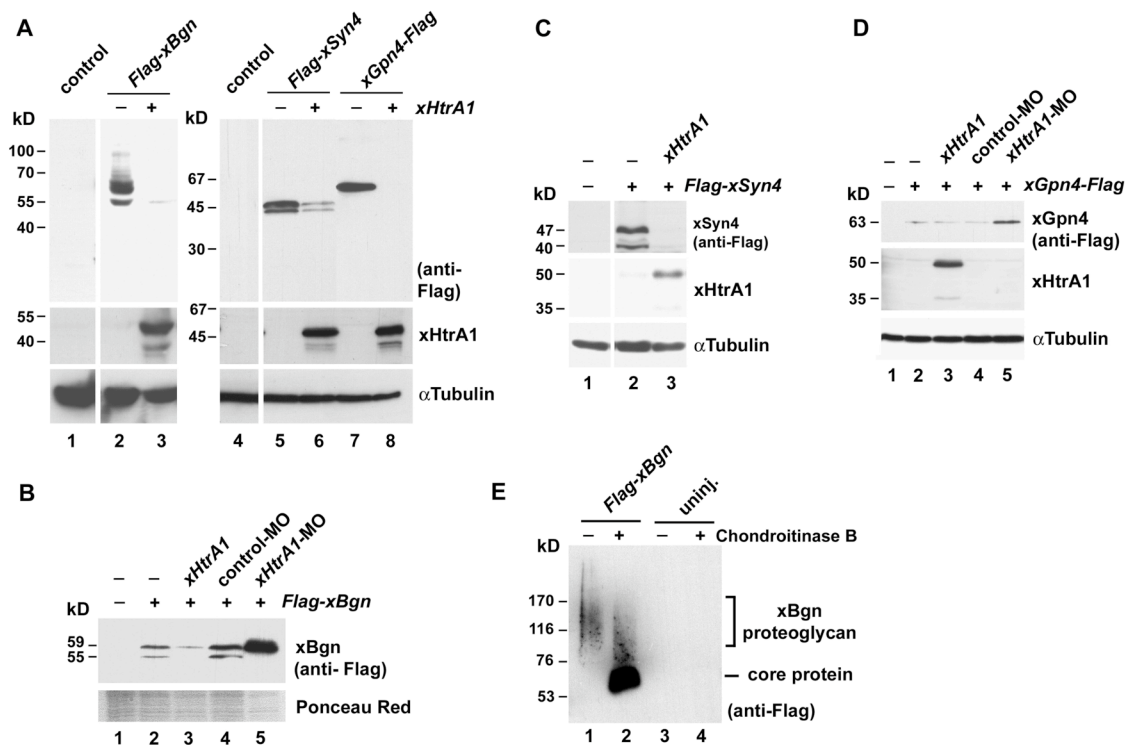
Figure 16. xHtrA1 causes proteolytic cleavage of *Xenopus* Biglycan, Syndecan4 and Glypican4

(A) HEK293 cells in 6-well plate were transfected with 3 μg Flag-tagged proteoglycan substrates including Flag-xBgn, Flag-xSyn4 and xGpn4-Flag, either alone or together with 2.5 μg xHtrA1. The cell medium was exchanged to serum-free conditioning medium after one day, cells were harvested three days after transfection and lysed in RIPA buffer. The cell lysates were separated by 12% SDS-PAGE gel. Western blot analysis was done with anti-Flag antibody (upper panel). After stripping, the same membrane was probed with anti-xHtrA1 antibody (middle panel), and after another round of stripping, probed with anti α-Tubulin antibody (lower panel). xHtrA1 specifically cleaves Flag-tagged xBgn (lanes 2,3), Flag-xSyn4 (lanes 5,6) and xGpn4-Flag (Lanes 7,8). (B) *Xenopus* embryos injected with *Flag-tagged xBgn* mRNA (500 pg) alone or together with *xHtrA1* mRNA (300 pg) into four-cell stage embryos. Embryos were harvested at stage 14 and proteins extracted and separated by 12% SDS-PAGE. Ponceau red staining was used as loading control. (C,D) *Xenpus* embryos were injected at the two-cell stage with control-MO or *xHtrA1*-MO (8 pmol per embryo) and at the four-cell stage with *Flag-xSyn4* (150 pg), *xGpn4-Flag* (60 pg) or *xHtrA1* mRNA (180 pg). Injected embryos were harvested at stage 20 and subjected to Western blot analysis. (E) *Flag-xBgn* mRNA (100 pg) was injected at the four-cell stage and embryos harvested at stage 22. Extraction of proteoglycans, anion-exchange purification and treatment with Chondroitinase B were kindly performed by Dr. Marco Maccarana (Univ. Lund).

3.17 Heparan sulfate and dermatan sulfate induce posteriorization, mesoderm and neuronal differentiation in an FGF-dependent manner

Biglycan contains 1-2 dermatan sulfate (DS) chains that are released upon digestion of the protein core (Trowbridge and Gallo, 2002), Syndecan4 and Glypican4 contain heparan

sulfate. We compared the biological activities of exogenously added heparan sulfate (HS), dermatan sulfate (DS), and the chondroitin sulfates CSE and CSA in early *Xenopus* embryos. DS contains a high proportion of iduronic acid, which is absent in chondroitin sulfates (Trowbridge and Gallo, 2002). CSE has additional 6-O-sulfate compared with CSA. Upon injection into the blastocoel, HS caused loss of head structures (Fig. 17a,b). Likewise, DS at a hundred-fold higher dosis resulted in anencephaly and occasional induction of secondary tails (Fig. 17c). In contrast, CSE had little and CSA no effect on head development and failed to induce ectopic tail-like structures (Fig. 17d,e). Importantly, defects in head development were reversed when embryos had been injected with *XFD* mRNA (Fig. 17a'-e'), indicating that the posteriorizing effect of polysaccharides depends on a functional FGF receptor. In addition, HS and DS, but not CSE and CSA, caused robust expansion of the mesodermal marker *Xbra* (Fig. 17f-j). While HS strongly induced ectopic neurons, DS, CSE and CSA only moderately expanded the neuronal marker *N-tubulin* expression territory (Fig 17 k-o). *XFD* and *DnFGFR4* mRNA obscured ectopic mesoderm induction and neuronal differentiation, respectively (Fig. 17f'-j', k'-o'), indicating that the glycosaminoglycans require an intact FGF signaling pathway to exert their activities. These effects are strikingly similar to those induced by FGF signals (Fig. 12) and by xHtrA1 (Fig. 13), suggesting a functional interaction between HS, DS, xHtrA1, and FGF.
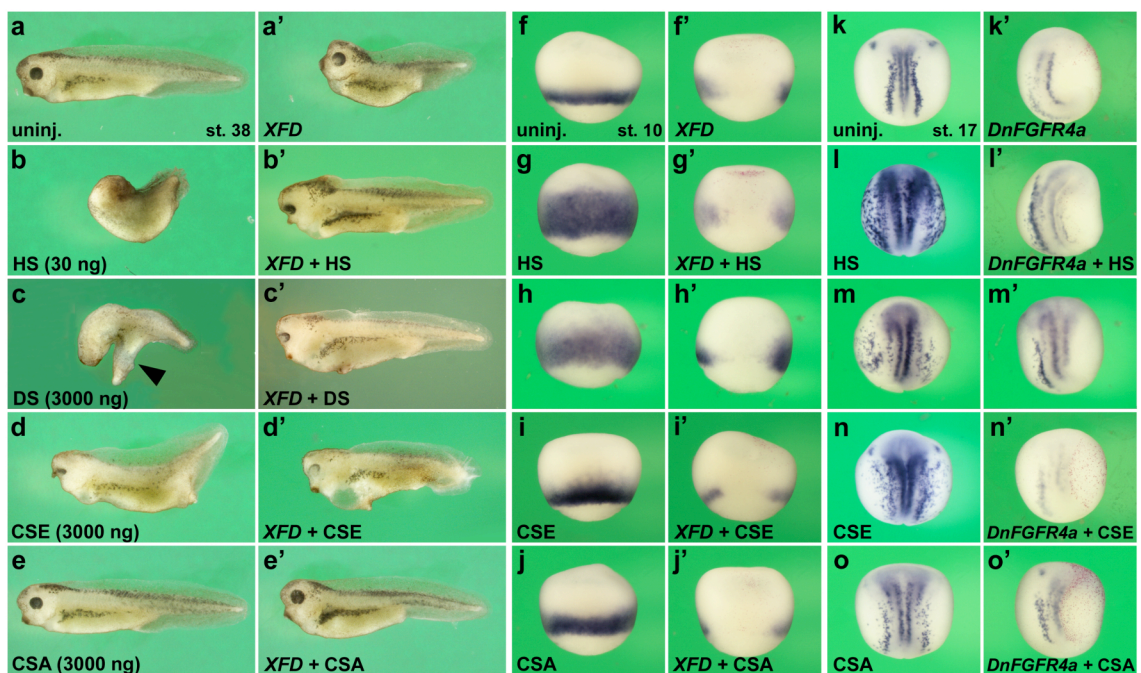
Figure 17. Heparan sulfate and dermatan sulfate induce posteriorization, mesoderm and neuronal differentiation in an FGF-dependent manner

(a-e) Heparan sulfate (HS, 30 ng), dermatan sulfate (DS, 3000 ng), and the chondroitin sulfates CSE and CSA (each 3000 ng) were injected into the blastocoel at stage 8 embryos. Note the loss or reduction of head structures by HS, DS and CSE, and the induction of an ectopic tail-like outgrowth by DS (arrowhead). (a'-e') Injection of 110 pg *XFD* mRNA at the four-cell stage reverts the posteriorizing effects of HS, DS and CSE. (f-j) HS and DS injected at stage 6.5 significantly expand *Xbra* expression. (f'-j') Expansion of *Xbra* by polysaccharides is blocked by injection of 220 pg *XFD* mRNA into the four-cell stage embryos. (k-o) HS, DS, CSE, and CSA injected into the blastocoel cavity at stage 8 expand *N-tubulin* expression. Note that HS significantly induces ectopic *N-tubulin*, whereas DS, CSE and CSA only mildly expand *N-tubulin* expression. (k'-o') Microinjection of 110 pg *DnFGFR4a* mRNA blocks *N-tubulin* expansion caused by polysaccharides. Frequency of embryos with the indicated phenotype was: b, 63/63; c, 98/110 (anencephaly) and 20/110 (ectopic tail); d, 47/47; e, 53/53; b', 11/11; c', 7/7; d', 5/6; e', 9/13; g, 29/30; h, 30/40; i, 10/20 with slight expansion of *Xbra;* j, 9/9; g', 46/46; h', 25/37; i', 50/50; j', 43/43; l, 63/63; m, 14/21; n, 32/36 with slight expansion; o, 27/34 with slight expansion; l', 22/22; m', 9/17; n', 35/35; o', 16/17.

4. Discussion

In this study, we characterize the secreted serine protease HtrA1 in the *Xenopus* embryo. Microinjection of *xHtrA1* mRNA resulted in the loss of head tissue and induction of ectopic tail-like structures. Apart from patterning the anteroposterior axis, *xHtrA1* affects additional important processes, including mesoderm induction, dorsoventral patterning of the ectoderm, neuronal differentiation, regulation of the cell motility and proliferation. Using specific morpholino oligonucleotides or neutralizing antibodies against xHtrA1, we show that this protease plays an important role in proper head and tail development, mesoderm induction and neuronal differentiation. Importantly, *xHtrA1* is transcriptionally activated by *FGF8* and *FGF4*, cooperates with FGF signals to activate mesoderm markers, and the activity of xHtrA1 depends on an intact FGF signaling pathway.

4.1 Interaction with IGF and BMP antagonism are not sufficient to explain the activities of xHtrA1

The presence of an aminoterminal IGF binding domain in the HtrA1 protein (Fig. 1; Hou, 2004) suggests a possible interaction with insulin-like growth factor (IGF) signals. It has been suggested that HtrA1 may regulate the availability of the IGFs by cleaving IGF binding proteins (Zumbrunn and Trueb, 1996). Indeed, a recent study has shown that purified human HtrA1 protein modulates Insulin-like growth factor (IGF) signalling by cleaving the IGFBP5, (IGF binding protein 5; Hou et al., 2005). In *Xenopus* embryos, overexpressing IGFBP5 phenocopies IGFs to promote anterior neural structures (Pera et al., 2001). Hence, one may speculate that by cleaving IGFBP5, xHtrA1 may attenuate IGF signals. Downregulation of IGF signaling suppresses head development (Pera et al., 2001; Richard-Parpaillon et al., 2002), reminiscent of the anencephaly that results from *xHtrA1* mRNA injection (Fig. 4; Hou, 2004). However, the dorsalization of the ectoderm, induction of neuronal differentiation and stimulation of cell proliferation by *xHtrA1* (Fig. 8; Hou, 2004 and Fig.9) are characteristic for an activation of IGF signaling (Pera et al., 2001; 2003; Richard-Parpaillon et al., 2002). One way to reconcile the findings is to assume that xHtrA1 may function as a positive or negative regulator of IGF signaling in a context-dependent manner. However, the induction of secondary tail structures by xHtrA1 (Fig. 4; Hou, 2004) cannot be explained by either positive or negative regulation of IGF signals.

Previous studies in the mouse showed that HtrA1 binds to a wide range of TGFβ family proteins including BMP4, TGFβ1, TGFβ2, activin and GDF5, and blocks the activity of BMP4 and TGFβ1 in cell culture experiments (Oka et al., 2004). The dorsalization of ectoderm by xHtrA1, e.g. the expansion of the neural plate at the expense of neural crest and epidermis tissue, together with ectopic neuronal differentiation by xHtrA1 (Fig. 8; Hou, 2004) is consistent with inhibition of BMP signals. Soluble antagonists of BMP ligands, such as Chordin, Noggin and Follistatin, similarly dorsalize the ectoderm and promote neural development (De Robertis and Kuroda, 2004). However, other effects of xHtrA1 observed in *Xenopus* embryos cannot be explained by inhibition of TGFβ or BMP signaling. First, xHtrA1 eliminates anterior neural markers including *Otx2*, *BF1*, *Rx2a*, when injected into whole embryos (Fig. 6; Hou, 2004). Whereas inhibition of the BMP pathway, e.g. by Chordin, promotes anterior neural marker gene expression (Sasai et al., 1994,1995). Second, xHtrA1 robustly expands the posterior expression domain of *Sizzled* (Fig. 6L; Hou, 2004). The BMP antagonist Chordin downregulates *Sizzled* expression. In contrast, elevation of BMP signals by knockdown of Chordin protein synthesis or overexpression of the metalloprotease Xolloid-related protein (Xlr), upregulates *Sizzled* gene activity (Lee et al., 2006). Third, xHtrA1 stimulates mesoderm development (Fig. 6D; Hou, 2004, Fig. 12H). However, blocking the TGFβ pathway, e.g. by dominant negative activin receptor or Nodal inhibitor Cerberus-short, impairs with mesoderm formation (Clements et al., 1999; Agius et al., 2000). Hence, anti-TGFβ activity does not account for the positive effect of xHtrA1 on mesoderm development. Indeed, active BMP or TGFβ signals lead to ectopic mesoderm formation (Dale et al., 1992; Hemmati-Brivanlou and Thomsen, 1995). Fourth, the induction of ectopic tail-like structures by xHtrA1 (Fig. 4; Hou, 2004) cannot be explained by antagonism of BMP, as secondary axes induced by BMP antagonists only contain trunk and head structures (Glinka et al, 1997). Several lines of evidence argue instead for an active role of BMP signaling in tail development. Ectopic expression of BMP4, a constitutively active BMP receptor, or an activated form of the BMP signaling intermediate Smad5 in the posterior neural plate of an early *Xenopus* neurula results in the formation of extra tail-like structures (Beck et al., 2001). Reduced BMP signaling, caused by e.g. injection of morpholino oligonucleotides against *BMP7* and *Twisted gastrulation*, leads to a loss of posterior ventral mesoderm and truncation of tail structures (Zakin et al., 2005). In the mouse mutant, depletion of BMP signals impairs tail development (Winnier et al, 1995). Hence BMP signaling is both

necessary and sufficient for tail outgrowth in vertebrates. Fifth, Oka and co-workers showed that mouse mutant HtrA1 construct that carries a point mutation, in which catalytic serine residue is substituted with alanine, still binds to and attenuates TGFβ signals in cell culture assays. In *Xenopus*, blocking of TGFβ signaling suppresses mesoderm development (Clements et al., 1999) and blocking BMP signals promotes neural development (De Robertis and Kuroka, 2004). However, similar xHtrA1 mutant *xHtrA1S307A* did not show phenotypic effect in mRNA-injected *Xenopus* embryos and failed to suppress the mesodermal marker *Xbra* and expand the neural marker *Sox2* (data not shown). Taken together, BMP antagonism is not sufficient to explain the activities of xHtrA1 during *Xenopus* embryonic development.

4.2   xHtrA1 is a novel regulator of FGF signaling

Several lines of evidence from our study support a specific link between xHtrA1 and FGF signaling in *Xenopus* embryonic development. The early expression pattern of *xHtrA1* (Fig. 2) overlaps with known sites of FGF activity, as revealed by the transcription of crucial components of the FGF signaling pathway, including *FGF8* (Christen and Slack, 1997), *XFLRT3* (Böttcher et al., 2004), *Sef* (Fürthauer et al., 2002; Tsang et al., 2002) and *Sprouties* (Fürthauer et al., 2001, 2004), and the phosphorylation of the extracellular signal-regulated protein kinase (dpERK; Christen and Slack, 1999). Common expression was observed in the blastopore ring, posterior mesoderm, anterior neural plate, midbrain-hindbrain boundary, neural fold, and branchial arch region. It has been suggested that genes sharing expression sites form a synexpression group and as such may functionally interrelate (Niehrs and Meinhardt, 2002). Microinjection of *FGF8* and *FGF4* into ectoderm explants activates *de novo* expression of *xHtrA1*, although interference of FGF signaling through dominant negative FGF receptors does not reduce *xHtrA1* transcripts in marginal zone explants (Fig. 3). This indicates that FGF signals are sufficient, but not required for the induction of *xHtrA1*. Thus, *xHtrA1* is a FGF target gene that like *Sprouties*, *Sef* and *XFLRT3*, is expressed in response to FGF signaling (Fürthauer et al., 2001, 2002, 2004; Tsang et al., 2002; Böttcher et al., 2004). xHtrA1 and FGF signals have several common activities. First, anencephaly and ectopic tail-like structures, as induced by *xHtrA1* mRNA injection (Figs. 4,12), have also been observed after misexpression of FGF ligands or signaling intermediates of the FGF-MAPK pathway. Microinjection of *FGF4* DNA or mRNAs encoding a constitutively active FGFR1, activated Ras, the

transmembrane protein XFLRT3, the Src-family kinase Laloo, or the Ets-type transcription factor ER81 induce microcephaly and ectopic tail-like structures (Isaacs et al., 1994; Pownall et al., 1996; Weinstein et al., 1998; Chen et al., 1999; Böttcher et al., 2004). Overexpression of *FGF8* also leads to reduction of anterior structures, a trunk bent to the ventral side and an expanded proctodeum (Christen and Slack, 1997), reminiscent of the phenotype induced by xHtrA1 (Fig. 4; Hou, 2004). Second, like FGF signals (Pownall et al., 1996; Umbhauer et al., 2000; Liu et al., 2001; Bel-Vialar et al., 2002), xHtrA1 also acts as a posteriorizing agent for the central nervous system (Fig. 7). In mRNA-injected neural plate explants, xHtrA1 suppresses rostral neural markers and enhances more caudal markers instead, e.g. in the anterior-most neural plate section, the gene expression of the eye marker *Rx2a* and forebrain marker *Otx2* was reduced, whereas the hindbrain marker *Krox20* and the posterior hindbrain/spinal cord marker *HoxD1* was induced upon microinjection of a low dosis of *xHtrA1* mRNA (Fig. 7). When a higher dosis of *xHtrA1* mRNA was injected, the expression of rostral neural markers including *Krox20* were even completely erased in whole embryos (Fig. 6; Hou, 2004). Third, xHtrA1 stimulates mesoderm development, as shown by the formation of secondary notochord and somite tissue in mRNA-injected embryos (Fig. 4; Hou, 2004), expansion of the pan-mesodermal marker *Xbra* from the marginal zone into the animal hemisphere (Fig. 6; Hou, 2004), and *de novo*-induction of the mesodermal marker genes *Xbra* and *Xcad3* in isolated animal cap explants (Fig. 12). Mesoderm induction is also caused by overexpression of *FGF4* (Isaacs et al., 1994) and other activators of FGF/MAPK signaling (Pownall et al., 1996; Weinstein et al., 1998; Böttcher et al., 2004). Fourth, xHtrA1 markedly expands the neural plate at the expense of neural crest and epidermal tissue, and stimulates neuronal differentiation (Fig. 8; Hou, 2004), a phenotype that also results from misexpression of *FGF8* (Hardcastle et al., 2000; Pera et al., 2003). Previous studies in chick, zebrafish and *Xenopus* have shown that FGFs, through the control of BMP activity, affect dorsoventral patterning in the ectoderm. FGF/MAPK signaling promotes the induction of neural fate by inhibiting BMP gene expression (Wilson et al., 2000; Fürthauer et al., 2004) or by phosphorylating and inactivating the BMP signaling intermediate Smad1 (Pera et al., 2003; Kuroda and De Robertis, 2004). Fifth, HtrA1 perturbs convergence-extension movements of the neural plate (Fig. 9). In *Xenopus*, the chick and the mouse, FGF signaling has been shown to directly affect morphogenetic cell movements during gastrulation (Ciruna et al., 1997; Nutt et al., 2001; Yang et al., 2002) through a mechanism that is distinct from the

Ras/MAPK pathway and depends on PLC-γ activation (Sivak et al., 2005). Sixth, xHtrA1 causes excessive cell proliferation (Fig. 9), as also observed upon activation of FGF signaling (Powers et al., 2000). In sum, the abnormalities caused by xHtrA1 are indistinguishable from those caused by FGF signals, strongly suggesting that xHtrA1 may act through activating FGF signaling.

Moreover, loss-of-function experiments suggest that xHtrA1 and FGF may share common functions. Knockdown of xHtrA1 by microinjection of specific morpholino oligonucleotides or of a neutralizing antibody resulted in enlarged head structures, reduced tail formation and deficient mesoderm development (Fig. 10 and data not shown). This phenotype also arises after injecting molecules that disrupt FGF/MAPK signaling, including a dominant negative FGF receptor (Amaya et al., 1991), a dominant negative Raf1 mutant (MacNicol et al., 1993), a MAPK-specific phosphatase (Umbhauer et al., 1995), a dominant-inhibitory Laloo mutant (Weinstein et al., 1998), or the FGF/MAPK antagonist Sef (Tsang et al., 2002). Microinjection of *xHtrA1*-MO also blocked expression of the differentiated neuron marker *N-tubulin* (Fig. 10), which also results from misexpression of DnFGFR4a, a dominant negative FGF receptor that mediates FGF8 signaling (Hardcastle et al., 2000). Downregulation of xHtrA1 eliminated phosphorylation and activation of the MAPK pathway intermediate ERK in whole embryos (Fig. 14), which is also observed in dissociated animal cap explants treated with the MEK inhibitor U0126 (Kuroda et al., 2005). These loss-of-function data indicate that xHtrA1 may play a role in allowing FGFs to signal.

Our animal cap explants experiment shows that xHtrA1 cooperates with FGF4 to induce mesoderm markers (Fig. 12), supporting the view that xHtrA1 may converge with the FGF signaling pathway. Abrogation of FGF signaling by injecting dominant negative FGF receptors blocks the posteriorization of the embryonic axis, induction of mesoderm and stimulation of neuronal differentiation caused by xHtrA1 (Fig. 13). This epistatic experiment shows that xHtrA1-mediated activities rely on intact FGF signaling. Importantly, xHtrA1 induced ectopic activation of the FGF signaling intermediate MAPK/ERK and induction of *FGF4* and *FGF8* expression (Fig. 14), suggesting that xHtrA1 acts upstream of FGF signals and is able to stimulate the FGF pathway *in vivo*. Our experiments indicate that xHtrA1 and FGF engage in a positive feedback loop, in

which FGF signals induce the transcription of *xHtrA1* (Fig. 3), and vice versa, xHtrA1 transcriptionally activates FGF genes and promotes FGF signaling (Fig. 14). The autoinduction of positive and negative modulators is a reoccuring theme in growth factor signaling, and the FGF8 synexpression group provides a good example therefore (Niehrs and Meinhardt, 2002; Tsang and Dawid, 2004). The transmembrane protein XFLRT3, whose gene expression is activated by FGFs, binds to the FGF receptor at the cell surface and similarly as xHtrA1 stimulates FGF signalling (Böttcher et al., 2004). On the other hand, the membrane-bound Sef and cytosolic Sprouty and Spred proteins block the FGF pathway intracellularly and establish a negative feedback loop (Fuerthauer et al., 2002; Tsang et al., 2002; Sivak et al., 2005). Hence, xHtrA1 adds to an intricate network of feedback-regulated factors that modulates the activity of this important signaling pathway. In *Xenopus*, FGF4 induces *Xbra* expression via the transcription factor Ets2 and, in turn, *Xbra* induces *FGF4* expression (Isaacs et al., 1994; Kawachi et al., 2003). Our results suggest that xHtrA1 is integrated in this positive feed-forward network. It has been proposed that such a self-regulated biological signalling loop contributes to the establishment of local organizing centers (Tsang and Dawid, 2004). This system of regulation may explain of how misexpression of xHtrA1, FGF4 or Ets-type transcription factors eventually leads to complex secondary tail-like outgrowths.

4.3   A model for the regulation of FGF signals in the extracellular space

FGF signaling is regulated at the cell surface and in the extracellular matrix by proteoglycans (PGs) of the heparan sulfate (HS) and dermatan sulfate (DS) families (Bernfield et al., 1999; Ornitz, 2000; Trowbridge and Gallo, 2002). Secreted FGFs tightly bind to HSPGs through interaction with their glycosaminoglycan (GAG) moieties. In this way, HSPGs restrict the diffusion of FGFs in the extracellular space. GAGs also stabilize the interaction of FGF with the FGF receptor, thereby increasing signal transduction. The protein core of the cell-associated HSPG is sensitive to degradation by a large spectrum of serine proteases, including chymotrypsin and trypsin. Cleavage at a labile region between the GAG attachment site and the membrane anchor releases the GAG-containing portion of HSPG from the cell surface (Rapraeger and Bernfield, 1985). Previous *in vitro* studies have shown that the secreted serine protease plasmin releases FGF2 that is bound to the extracellular matrix of cultured endothelial cells (Saksela and Rifkin, 1990). When released by plasmin, the growth factor is recovered from the medium as a complex with a

partly degraded HSPG. Interestingly, FGF2 is able to increase plasminogen activator activity in these cells, allowing for a positive feedback loop (Saksela et al., 1987).

In this study, we could show that xHtrA1 triggers the proteolytic cleavage of *Xenopus* Biglycan, Syndecan4 and Glypican4 in transfected cells and *Xenopus* embryos (Fig. 16). This finding supports a previous *in vitro* observation that identified bovine Biglycan as a substrate of N-terminally truncated mouse HtrA1 (Tocharus et al., 2004). It remains to be shown whether Syndecan4 or Glypican4 are directly cleaved by xHtrA1 or by other proteases that are activated by xHtrA1. To this end, purified xHtrA1 protein is needed to show *in vitro* proteolytic cleavage of isolated Syndecan4, and Glypican4 proteins. Interestingly, Glypican4 binds FGF2 and modulates FGF signaling in *Xenopus* (Galli et al., 2003), underscoring the notion that proteoglycans may mediate the stimulatory effect of xHtrA1 on FGF activity.

Using blastocoelic injections, we could demonstrate that HS and DS trigger posteriorization of the primary embryonic axis, mesoderm induction and neuronal differentiation (Fig. 17). Not only are the effects of heparan sulfate and dermatan sulfate reminiscent of those caused by FGF signals, but they also occur in an FGF-dependent manner. Interestingly, the biological potency of a given glycosaminoglycan (GAG) correlates with its reported affinity to FGFs. HS and DS, but not chondroitin sulfate, share a high content of iduronic acid, which renders conformational flexibility to the GAG chain and facilitates tight binding to FGF and its receptor (Trowbridge et al., 2002; Kramer and Yost, 2003). Previous *in vitro* studies have shown that DS binds to FGF2 and FGF7 and stimulate their activity during cellular proliferation (Penc et al., 1998; Trowbridge et al., 2002; Taylor et al., 2005). Our findings now strongly point towards an *in vivo* link between HS/DS and FGF signaling.

Based on these results, we propose a model that explains of how the secreted serine protease xHtrA1 may stimulate FGF signals in the extracellular space (Fig. 4.1). As FGFs have high affinities for GAG side-chains of proteoglycans, the FGFs are normally sequestered on or nearby to cells from which they are secreted, consistent with their function as short-range intercellular signaling molecules (Häcker et al., 2005; Bülow and Hobert, 2006). The secreted serine protease xHtrA1 triggers the cleavage of

proteoglycans, such as Biglycan, Syndecan4 and Glypican4, thereby releasing soluble FGF-GAG complexes. In this way, FGFs are able to reach cells far away from their site of synthesis and activate FGF receptors at distance. Since GAGs strengthen the binding of FGF ligands to their receptors, the FGF-GAG complexes also increase the overall signaling intensity.
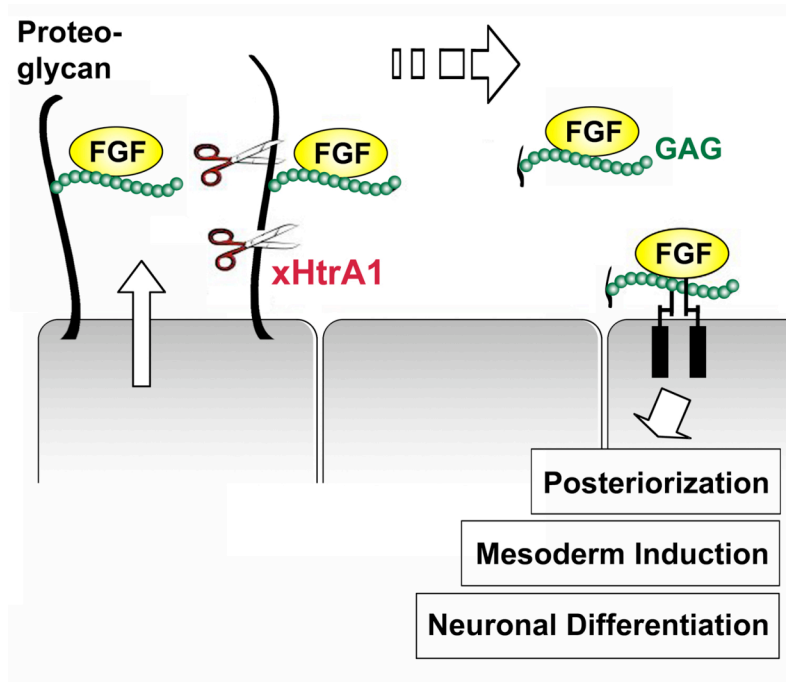
Figure 4.1 Model for the stimulation of long-range FGF signaling by the secreted serine protease xHtrA1.
xHtrA1 cleaves the protein moiety of proteoglycans and releases biologically active FGF bound to glycosaminoglycan (GAG). The FGF-GAG complex activates the FGF receptor on cells distant to its site of origin.

In support of this „proteolytic spread" model, we could show that xHtrA1 has non-cell autonomous activity in the embryo. In lineage tracing experiments, we could show that molecular marker genes are induced in a non-cell autonomous manner (Fig. 8; Hou, 2004). Secondary tail-like structures arose on the ventral side although injected *xHtrA1* mRNA is restricted to dorsal parts of the embryo (Fig. 4). Similarly, ectopic neuronal differentiation is induced on the contralateral side of *xHtrA1* mRNA injection (Fig. 13). Using an animal cap conjugate experiment, we could demonstrate that *xHtrA1* allows ectopic mesoderm induction far away from the source of FGF signals, indicating that xHtrA1 promotes long-range FGF signaling (Fig. 15).

In an attempt to demonstrate that xHtrA1 facilitates diffusion of FGF ligands in the extracellular space, we studied the distribution of exogenously added and fluorescently labeled FGFs in *Xenopus* embryonic explants using two different strategies. First, animal cap explants injected with *FGF4-GFP*/*FGF8-GFP* alone or in combination with *xHtrA1* mRNA were juxtaposed to non-injected animal cap explants on coverslips and analysed by confocal microscopy. No clear difference could be observed between samples injected with or without *xHtrA1* due to technical difficulties, including unequal distribution of injected mRNAs, release of FGF-GFP proteins during cutting and mounting of the explants and imperfect contact between explants in the conjugates. In addition, xHtrA1 may have caused the release of FGF-GFP ligands before explants were excised, leading to a relative decease of FGF-GFP protein in *xHtrA1*-injected samples. In order to overcome these drawbacks, we used heparin beads soaked with Alex Fluor 488-labeled FGF8 protein and embedded them in the center of animal cap explants that were non-injected or injected with *xHtrA1* mRNA. Confocal microscopy revealed that the signals within and around the beads were too weak to unambiguously trace the distribution of labeled FGF8 protein in explant tissues. Together, our confocal microscopy experiments do not allow to draw a conclusion about the diffusion of FGF signals in response to xHtrA1 treatment. However, the observation that xHtrA1 promotes the intensity and range of *Xbra* expression in *FGF4* mRNA-injected animal cap conjugates clearly shows that xHtrA1 promotes long-range FGF signaling (Fig. 15).

4.4 Specificity of xHtrA1-mediated regulation of FGF signaling

HSPGs not only bind FGFs, but also other growth factors of the TGFβ and Wnt families (Iozzo 1998). Our model is consistent with the idea that xHtrA1 may also release and activate these factors. However, the activities and functions exhibited by xHtrA1 are most reminiscent of those shown by FGFs, supporting the interpretation that xHtrA1 predominantly activates FGF signaling in *Xenpus* embryos. One explanation could be that FGFs are probably unique in their requirement of HS for the ligand-receptor interaction (Rapraeger et al., 1991; Itoh and Sokol, 1994) and DS appears to interact with FGFs and their receptors (Penc et al., 1998; Trowbridge et al., 2002; Taylor et al., 2005).

The specific activation of FGF signaling in the embryo raises the question whether components of the FGF signaling pathway may be directly affected by xHtrA1? The

TGFα /EGF homologue Spitz in *Drosophila* is proteolytically activated by the serine protease Rhomboid-1 (Urban et al., 2001). *Xenopus* FGF3 has been reported to undergo proteolytic cleavage by the secreted serine protease plasmin to produce an N-terminally truncated product (Antoine et al., 2000). The processed 27 kD glycoprotein (gp27) has stronger biological activity than the full-length gp31 protein, as judged by their higher affinity to FGF receptors, enhanced ability to transform NIH3T3 cells and increased mitogenic activity. In addition, two aminoterminally processed isoforms of human FGF4 have higher affinity to FGF receptors and increased mitogenicity compared to the wild-type protein (Bellosta et al., 1993). It will be of interest to test whether xHtrA1 may process FGF ligands and render them hyperactive. Our preliminary results indicate that xHtrA1 appears to cleave Flag-tagged FGF4 protein in transfected HEK293 cells (data not shown).

4.5   Implication of HtrA1 for mammalian development and disease

Does the link between HtrA1 and FGF as reported here for the *Xenopus* embryo apply to other aspects of vertebrate development? During skeletal development, mouse HtrA1 overlaps with FGFs and their cognate receptors in precartilage condensations, ossification centers and the bone matrix (Oka et al., 2004; Ornitz, 2005). In addition to the previously described function of HtrA1 as regulator of TGFβ signaling (Oka et al., 2004), its co-localization with FGF signaling components suggests an additional link between HtrA1 and FGF during growth, differentiation and remodeling of bones. There are striking parallels between FGF signaling and proteoglycans in skeletal disease syndromes. For example, human hypochondroplasia can be caused by FGFR3 mutations (Ornitz, 2005) or by mutations in the Colony stimulating factor 1 receptor that prevent specific sulfation of GAG chains on proteoglycans (Hastbacka et al., 1994). Furthermore, a progeroid variant of the Ehlers-Danlos syndrome, characterized by short stature and skeletal malformations, results from mutations in the gene for galactosyltransferase-1 that lead to a selective loss of GAG synthesis of the dermatan sulfate proteoglycans Biglycan and Decorin (Quentin et al., 1990). Biglycan is very abundant in bone, and Biglycan-deficient mice develop an osteoporosis-like phenotype suggesting an essential role in bone formation (Xu et al., 1998). HtrA is a major virulence factor of *Streptococcus pneumoniae* that induces inflammation in the lung (Ibrahim et al., 2004). FGFs participate in inflammation, repair and regeneration during wound healing (Powers et al., 2000), and dermatan sulfate is

highly enriched in wound fluids (Trowbridge and Gallo, 2002). Finally, age-related macular degeneration, which is the most common cause of blindness in aged people, is associated with upregulation of HtrA1 due to a promoter polymorphism (DeWan et al., 2006; Yang et al., 2006) and increased FGF gene expression (Kitaoka et al., 1997), suggesting a pathophysiological link for HtrA1 and angiogenic FGF signals in this eye neovascular disorder. Thus, our finding of a functional link between HtrA1, FGFs may not only be relevant to answer questions related to early development, but also contribute to understand other aspects including bone formation, wound repair and the etiology of a common cause of blindness.

5.   Conclusion

In this study, we describe the secreted serine protease xHtrA1 as a novel positive modulator of FGF signaling. xHtrA1 contains an N-terminal signal peptide, an IGF binding domain, a Kazal-type serine protease inhibitor domain, a Trypsin-like serine protease domain and a PDZ domain. xHtrA1 is co-expressed with FGF8 at several sites, and its expression is activated by FGF signals. Microinjection of *xHtrA1* mRNA into *Xenopus* embryos results in loss of head structures, induction of ectopic tails and expansion of mesoderm. *xHtrA1* also enlarges the neural plate at the expense of neural crest and epidermal tissue and induced ectopic neurons. An analysis of mutant protein constructs indicates a crucial role of the proteolytic domain, the catalytic serine residue and the PDZ domain for the activity of xHtrA1. In loss-of-function experiments, an antisense morpholino oligonucleotide or a neutralizing antibody against xHtrA1 enlarges head structures and reduces tail development. *xHtrA1*-MO also impairs mesoderm formation and neuronal differentiation. In whole embryos, a dominant-negative FGF receptor (XFD) blocks the ability of xHtrA1 to inhibit head development, to induce secondary tails and to stimulate mesoderm formation. Moreover, a dominant-negative FGF receptor-4a (DnFGFR4a) impairs ectopic neuronal differentiation by xHtrA1, suggesting that xHtrA1 relies on intact FGF signaling pathway to exert its activities. xHtrA1 is sufficient and required for FGF/ERK signaling and activates the transcription of *FGF4* and *FGF8*, suggesting a positive feedback regulation between xHtrA1 and FGF. xHtrA1 is shown to cleave the dermatan sulfate proteoglycan Biglycan and the heparan sulfate proteoglycans Syndecan4 and Glypican4. Blastocoelic injection of heparan sulfate and dermatan sulfate leads to posteriorization, ectopic mesoderm induction and neuronal differentiation in an FGF-dependent manner. Based on these experiments, a mechanism for the regulation of FGF by xHtrA1 is suggested. The secreted serine protease xHtrA1 cleaves proteoglycans such as Biglycan, Syndecan4 and Glypican4 and thereby releases FGF-glycosaminoglycan complexes, that allow long-range FGF signaling in a key inductive and morphogenetic phases of embryogenesis.

Bibliography

Abreu J. G., Ketpura N. I., Reversade B., De Robertis, E. M. (2002). Connective-tissue growth factor (CTGF) modulates cell signalling by BMP and TGF-beta. Nat Cell Biol, 4, 599-604.

Agius E., Oelgeschlager M., Wessely O., Kemp C. & De Robertis E. M. (2000). Endodermal Nodal-related signals and mesoderm induction in *Xenopus*. Development, 127, 1173-83.

Amaya E., Musci T.J., Kirschner M.W. (1991). Expression of a dominant negative mutant of the FGF receptor disrupts mesoderm formation in *Xenopus* embryos. Cell 66, 257-270.

Amaya E., Stein P.A., Musci T.J., Kirschner M.W. (1993). FGF signalling in the early specification of mesoderm in *Xenopus*. Development. 118, 477-487.

Antoine M., Daum M., Kohl R., Blecken V., Close M. J., Peters G., Kiefer P. (2000). NH2-terminal cleavage of xenopus fibroblast growth factor 3 is necessary for optimal biological activity and receptor binding. Cell Growth Differ, 11, 593-605.

Baker J. C., Beddington R. S., Harland R. M. (1999). Wnt signaling in *Xenopus* embryos inhibits bmp4 expression and activates neural development. Genes Dev, 13, 3149-59.

Baldi A., De Luca A., Morini M., Battista T., Felsani A., Baldi F., Catricala C., Amantea A., Noonan D.M., Albini A., Natali P.G., Lombardi D., Paggi M.G. (2002). The HtrA1 serine protease is down-regulated during human melanoma progression and represses growth of metastatic melanoma cells. Oncogene 21, 6684-6688.

Beck C. W., Whitman M., Slack J. M. (2001). The role of BMP signaling in outgrowth and patterning of the *Xenopus* tail bud. Dev Biol, 238, 303-14.

Bell E., Munoz-Sanjuan I., Altmann C. R., Vonica A. Brivanlou A. H. (2003). Cell fate specification and competence by Coco, a maternal BMP, TGFβ and Wnt inhibitor. Development, 130, 1381-9.

Bellosta P., Talarico D., Rogers D., Basilico C. (1993). Cleavage of K-FGF produces a truncated molecule with increased biological activity and receptor binding affinity. J Cell Biol, 121, 705-13.

Bel-Vialar S, Itasaki N., Krumlauf R. (2002). Initiating Hox gene expression: in the early chick neural tube differential sensitivity to FGF and RA signaling subdivides the HoxB genes in two distinct groups. Development 129, 5103-5115.

Bernfield M., Gotte M., Park P. W., Reizes O., Fitzgerald M. L., Lincecum J., Zako M. (1999). Functions of cell surface heparan sulfate proteoglycans. Annu Rev Biochem, 68, 729-77.

Birsoy B., Kofron M., Schaible K., Wylie C., Heasman J. (2006). Vg 1 is an essential signaling molecule in *Xenopus* development. Development, 133, 15-20.

Blume-Jensen P., Hunter T. (2001). Oncogenic kinase signalling. Nature, 411, 355-65.

Böttcher R.T., Pollet N., Delius H., Niehrs C. (2004). The transmembrane protein XFLRT3 forms a complex with FGF receptors and promotes FGF signalling. Nat Cell Biol. 6, 38-44.

Böttcher R.T., Niehrs C. (2005). Fibroblast growth factor signaling during early vertebrate development. Endocr Rev. 26, 63-77.

Bouwmeester T., Kim S., Sasai Y., Lu B., De Robertis, E. M. (1996). Cerberus is a head-inducing secreted factor expressed in the anterior endoderm of Spemann's organizer. Nature, 382, 595-601.

Brannon M., Kimelman D. (1996). Activation of Siamois by the Wnt pathway. Dev Biol, 180, 344-7.

Bülow H.E., Hobert O. (2006). The molecular diversity of glycosaminoglycans shapes animal development. Annu. Rev. Cell Dev. Biol. 22, 375-407.

Chang C. & Hemmati-Brivanlou A. (1999). *Xenopus* GDF6, a new antagonist of noggin and a partner of BMPs. Development, 126, 3347-57.

Casellas R., Brivanlou A. H. (1998). *Xenopus* Smad7 inhibits both the activin and BMP pathways and acts as a neural inducer. Dev Biol, 198, 1-12.

Chen Y., Hollemann T., Grunz H., Pieler T. (1999). Characterization of the Ets-type protein ER81 in Xenopus embryos. Mech Dev. 80, 67-76.

Chien J, Staub J, Hu SI, Erickson-Johnson MR, Couch FJ, Smith DI, Crowl RM, Kaufmann SH, Shridhar V. (2004). A candidate tumor suppressor HtrA1 is downregulated in ovarian cancer. Oncogene 23, 1636-1644.

Christen B., Slack J.M. (1997). FGF-8 is associated with anteroposterior patterning and limb regeneration in *Xenopus*. Dev Biol. 192, 455-466.

Christen B., Slack J.M. (1999). Spatial response to fibroblast growth factor signalling in *Xenopus* embryos. Development 126, 119-125.

Ciruna B.G., Schwartz L., Harpal K., Yamaguchi T.P., Rossant J. (1997). Chimeric analysis of fibroblast growth factor receptor-1 (Fgfr1) function: A role for FGFR1 in morphogenetic movement through the primitive streak. Development 124, 2829-2841.

Clausen T., Southan C., Ehrmann M. (2002). The HtrA family of proteases: implications for protein composition and cell fate. Mol Cell 10, 443-455.

Clements D., Friday R. V., Woodland H. R. (1999). Mode of action of VegT in mesoderm and endoderm formation. Development, 126, 4903-11.

Cornell R. A., Musci T. J., Kimelman D. (1995). FGF is a prospective competence factor for early activin-type signals in *Xenopus* mesoderm induction. Development, 121, 2429-37.

Cox W. G., Hemmati-Brivanlou, A. (1995). Caudalization of neural fate by tissue recombination and bFGF. Development, 121, 4349-58.

Crossley P. H., Martinez S., Martin G. R. (1996). Midbrain development induced by FGF8 in the chick embryo. Nature, 380, 66-8.

Dale L., Howes G., Price B. M., Smith J. C. (1992). Bone morphogenetic protein 4: a ventralizing factor in early *Xenopus* development. Development, 115, 573-85.

Dale L., Jones C. M. (1999). BMP signalling in early *Xenopus* development. Bioessays, 21, 751-60.

Dale L., Matthews G., Colman A. (1993). Secretion and mesoderm-inducing activity of the TGF-β-related domain of *Xenopus* Vg1. Embo J, 12, 4471-80.

Delaune E., Lemaire P., Kodjabachian L. (2005). Neural induction in *Xenopus* requires early FGF signalling in addition to BMP inhibition. Development, 132, 299-310.

De Robertis E.M., Kuroda H. (2004). Dorsal-ventral patterning and neural induction in *Xenopus* embryos. Annu Rev Cell Dev Biol. 20, 285-308.

De Robertis E.M. (2006). Spemann's organizer and self-regulation in amphibian embryos. Nature Rev Mol Cell Biol. 7, 296-302.

DeWan A., Liu M., Hartman S., Zhang S., Liu D.T., Zhao C., Tam P.O., Chan W.M., Lam D.S., Snyder M. et al.,(2006). HTRA1 Promoter Polymorphism in Wet Age-Related Macular Degeneration. Science 314, 989-992.

Dohrmann C. E., Hemmati-Brivanlou A., Thomsen G. H., Fields A., Woolf T. M., Melton D. A. (1993). Expression of activin mRNA during early development in *Xenopus laevis*. Dev Biol, 157, 474-83.

Dominguez I., Green J. B. (2000). Dorsal downregulation of GSK3b by a non-Wnt-like mechanism is an early molecular consequence of cortical rotation in early Xenopus embryos. Development, 127, 861-8.

Doniach T. (1995). Basic FGF as an inducer of anteroposterior neural pattern. Cell, 83, 1067-70.

Dono R. (2003). Fibroblast growth factors as regulators of central nervous system development and function. Am J Physiol Regul Integr Comp Physiol. 284, R867-81.

Dupont S., Zacchigna L., Cordenonsi M., Soligo S., Adorno M., Rugge M., Piccolo S. (2005). Germ-layer specification and control of cell growth by Ectodermin, a Smad4 ubiquitin ligase. Cell, 121, 87-99.

Elinson R. P., Rowning, B. (1988). A transient array of parallel microtubules in frog eggs: potential tracks for a cytoplasmic rotation that specifies the dorso-ventral axis. Dev Biol, 128, 185-97.

Esposito V., Campioni M., De Luca A., Spugnini E.P., Baldi F., Cassandro R., Mancini A., Vincenzi B., Groeger A., Caputi M., Baldi A. (2006). Analysis of HtrA1 serine protease expression in human lung cancer. Anticancer Res. 26, 3455-3459.

Farr G. H., 3rd, Ferkey D. M., Yost C., Pierce S. B., Weaver C., Kimelman D. (2000). Interaction among GSK-3, GBP, axin, and APC in *Xenopus* axis specification. J Cell Biol, 148, 691-702.

Freeman M., Gurdon J.B. (2002). Regulatory principles of developmental signaling. Annu Rev Cell Dev Biol. 18, 515-539.

Fukui A., Nakamura T., Uchiyama H., Sugino K., Sugino H., Asashima M. (1994). Identification of activins A, AB, and B and follistatin proteins in *Xenopus* embryos. Dev Biol, 163, 279-81.

Fukui A., Shiurba R., Asashima M. (1999). Activin incorporation into vitellogenic oocytes of *Xenopus laevis*. Cell Mol Biol, 45, 545-54.

Fürthauer M., Lin W., Ang S. L., Thisse B., Thisse C. (2002). Sef is a feedback-induced antagonist of Ras/MAPK-mediated FGF signalling. Nat Cell Biol, 4, 170-4.

Fürthauer M., Reifers F., Brand M., Thisse B., Thisse C. (2001). sprouty4 acts *in vivo* as a feedback-induced antagonist of FGF signaling in zebrafish. Development, 128, 2175-86.

Fürthauer M., Van Celst J., Thisse C.,Thisse B. (2004). Fgf signalling controls the dorsoventral patterning of the zebrafish embryo. Development, 131, 2853-64.

Galli A, Roure A, Zeller R, Dono R. (2003). Glypican4 modulates FGF signalling and regulates dorsoventral forebrain patterning in *Xenopus* embryos. Development 130, 4919-4929.

Gamse J. T., Sive, H. (2001). Early anteroposterior division of the presumptive neurectoderm in *Xenopus*. Mech Dev, 104, 21-36.

Garcia-Garcia M.J., Anderson K.V. (2003). Essential role of glycosaminoglycans in Fgf signaling during mouse gastrulation. Cell. 114, 727-737.

Glinka A., Wu W., Delius H., Monaghan A. P., Blumenstock C., Niehrs, C. (1998). Dickkopf-1 is a member of a new family of secreted proteins and functions in head induction. Nature, 391, 357-62.

Glinka A., Wu W., Onichtchouk D., Blumenstock C., Niehrs, C. (1997). Head induction by simultaneous repression of Bmp and Wnt signalling in *Xenopus*. Nature, 389, 517-9.

Gilbert S. F. (2003). Developmental Biology 7th Ed. Sunderland (MA), Sinauer Associates, Inc.

Godsave S. F., Isaacs H. V., Slack J. M. (1988). Mesoderm-inducing factors: a small class of molecules. Development, 102, 555-66.

Godsave S. F., Slack J. M. (1989). Clonal analysis of mesoderm induction in *Xenopus laevis*. Dev Biol, 134, 486-90.

Graff J. M., Thies R. S., Song J. J., Celeste A. J., Melton D. A. (1994). Studies with a *Xenopus* BMP receptor suggest that ventral mesoderm-inducing signals override dorsal signals in vivo. Cell, 79, 169-79.

Grau S., Baldi A., Bussani R., Tian X., Stefanescu R., Przybylski M., Richards P., Jones S.A., Shridhar V., Clausen T., Ehrmann M. (2005). Implications of the serine protease HtrA1 in amyloid precursor protein processing. Proc Natl Acad Sci U S A. 102, 6021-6026.

Green J. B., Howes G., Symes K., Cooke J., Smith J. C. (1990). The biological effects of XTC-MIF: quantitative comparison with *Xenopus* bFGF. Development, 108, 173-83.

Grose R., Dickson C. (2005). Fibroblast growth factor signaling in tumorigenesis. Cytokine Growth Factor Rev, 16, 179-86.

Grunz H., Tacke L. (1990). Extracellular matrix components prevent neural differentiation of disaggregated *Xenopus* ectoderm cells. Cell Differ Dev, 32, 117-23.

Hardcastle Z., Chalmers A.D., Papalopulu N. (2000). FGF-8 stimulates neuronal differentiation through FGFR-4a and interferes with mesoderm induction in *Xenopus* embryos. Curr Biol. 10, 1511-1514.

Hastbacka J., de la Chapelle A., Mahtani M.M., Clines G., Reeve-Daly M.P., Daly M., Hamilton B.A., Kusumi K., Trivedi B., Weaver A., et al. (1994). The diastrophic dysplasia gene encodes a novel sulfate transporter: positional cloning by fine-structure linkage disequilibrium mapping. Cell. 78, 1073-1087.

Häcker U., Nybakken K., Perrimon N. (2005). Heparan sulphate proteoglycans: the sweet side of development. Nat. Rev. Mol. Cell Biol. 6, 530-541.

Hansen C. S., Marion C. D., Steele K., George S., Smith W. C. (1997). Direct neural induction and selective inhibition of mesoderm and epidermis inducers by Xnr3. Development, 124, 483-92.

Hata A., Lagna G., Massague J., Hemmati-Brivanlou A. (1998). Smad6 inhibits BMP/Smad1 signaling by specifically competing with the Smad4 tumor suppressor. Genes Dev, 12, 186-97.

Hawley S. H., Wunnenberg-Stapleton K., Hashimoto C., Laurent M. N., Watabe T., Blumberg B. W., Cho, K. W. (1995). Disruption of BMP signals in embryonic *Xenopus* ectoderm leads to direct neural induction. Genes Dev, 9, 2923-35.

Hemmati-Brivanlou A., Kelly O. G., Melton D. A. (1994). Follistatin, an antagonist of activin, is expressed in the Spemann organizer and displays direct neuralizing activity. Cell, 77, 283-95.

Hemmati-Brivanlou A., Melton, D. A. (1992). A truncated activin receptor inhibits mesoderm induction and formation of axial structures in *Xenopus* embryos. Nature, 359, 609-14.

Hemmati-Brivanlou A., Thomsen G. H. (1995). Ventral mesodermal patterning in *Xenopus* embryos: expression patterns and activities of BMP-2 and BMP-4. Dev Genet, 17, 78-89.

Hollemann T., Chen Y., Grunz H., Pieler, T. (1998). Regionalized metabolic activity establishes boundaries of retinoic acid signalling. Embo J, 17, 7361-72.

Hongo I., Kengaku M., Okamoto H. (1999). FGF signaling and the anterior neural induction in *Xenopus*. Dev Biol. 216, 561-581.

Hou J., Clemmons D.R., Smeekens S. (2005). Expression and characterization of a serine protease that preferentially cleaves insulin-like growth factor binding protein-5. J. Cell Biochem. 94, 470-484.

Hou S. (2004). Master Thesis. A secreted serine protease with IGF binding motif involved in anterior-posterior patterning of *Xenopus* embryos. University Goettingen.

Hu S.I., Carozza M., Klein M., Nantermet P., Luk D., Crowl R.M. (1998). Human HtrA, an evolutionarily conserved serine protease identified as a differentially expressed gene product in osteoarthritic cartilage. J Biol Chem. 273, 34406-34412.

Huang P., Stern M.J. (2005). FGF signaling in flies and worms: More and more relevant to vertebrate biology. Cytokine Growth Factor Rev. 16, 151-158.

Hyde C. E., Old R. W. (2000). Regulation of the early expression of the *Xenopus* nodal-related 1 gene, Xnr1. Development, 127, 1221-9.

Ibrahim Y.M., Kerr A.R., McCluskey J., Mitchell T.J. (2004). Role of HtrA in the virulence and competence of Streptococcus pneumoniae. Infect Immun., 72, 3584-3591.

Iozzo R.V. (1998). Matrix proteoglycans: from molecular design to cellular function. Annu Rev Biochem. 67, 609-652.

Isaacs H. V., Tannahill D., Slack J. M. (1992). Expression of a novel FGF in the *Xenopus* embryo. A new candidate inducing factor for mesoderm formation and anteroposterior specification. Development, 114, 711-20.

Isaacs H.V., Pownall M.E., Slack J.M. (1994). eFGF regulates Xbra expression during *Xenopus* gastrulation. EMBO J. 13, 4469-4481.

Itoh K., Sokol S. Y. (1994). Heparan sulfate proteoglycans are required for mesoderm formation in *Xenopus* embryos. Development, 120, 2703-11.

Jones J.M., Datta P., Srinivasula S.M., Ji W., Gupta S., Zhang Z., Davies E., Hajnoczky G., Saunders T.L., Van Keuren M.L., Fernandes-Alnemri T., Meisler M.H., Alnemri E.S. (2003). Loss of Omi mitochondrial protease activity causes the neuromuscular disorder of mnd2 mutant mice. Nature 425, 721-727.

Jones C. M., Lyons K. M., Lapan P. M., Wright C. V., Hogan B. L. (1992). DVR-4 (bone morphogenetic protein-4) as a posterior-ventralizing factor in *Xenopus* mesoderm induction. Development, 115, 639-47.

Kawachi K., Masuyama N., Nishida E. (2003). Essential role of the transcription factor Ets-2 in *Xenopus* early development. J Biol Chem. 278, 5473-5477.

Kengaku M., Okamoto H. (1993). Basic fibroblast growth factor induces differentiation of neural tube and neural crest lineages of cultured ectoderm cells from *Xenopus* gastrula. Development, 119, 1067-78.

Kengaku M., Okamoto H. (1995). bFGF as a possible morphogen for the anteroposterior axis of the central nervous system in *Xenopus*. Development, 121, 3121-30.

Kimelman D., Abraham J. A., Haaparanta T., Palisi T. M., Kirschner M. W. (1988). The presence of fibroblast growth factor in the frog egg: its role as a natural mesoderm inducer. Science, 242, 1053-6.

Kimelman D., Kirschner M. (1987). Synergistic induction of mesoderm by FGF and TGF-β and the identification of an mRNA coding for FGF in the early *Xenopus* embryo. Cell, 51, 869-77.

Kimelman D. (2006). Mesoderm induction: from caps to chips. Nat Rev Genet, 7, 360-72.

Kitaoka T., Morse L.S., Schneeberger S., Ishigooka H., Hjelmeland L.M. (1997). Expression of FGF5 in choroidal neovascular membranes associated with ARMD. Curr. Eye Res. 16, 396-399.

Kofron M., Demel T., Xanthos J., Lohr J., Sun B., Sive H., Osada S., Wright C., Wylie C., Heasman J. (1999). Mesoderm induction in *Xenopus* is a zygotic event regulated by maternal VegT via TGF-β growth factors. Development, 126, 5759-70.

Koster M., Plessow S., Clement J. H., Lorenz A., Tiedemann H., Knochel W. (1991). Bone morphogenetic protein 4 (BMP-4), a member of the TGF-β family, in early embryos of *Xenopus laevis*: analysis of mesoderm inducing activity. Mech Dev, 33, 191-9.

Kramer K.L., Yost H.J. (2003). Heparan sulfate core proteins in cell-cell signaling. Annu Rev Genet. 2003; 37:461-84.

Kretzschmar M., Doody J., Massague J. (1997). Opposing BMP and EGF signalling pathways converge on the TGF-β family mediator Smad1. Nature, 389, 618-22.

Kroll K. L., Salic A. N., Evans L. M., Kirschner M. W. (1998). Geminin, a neuralizing molecule that demarcates the future neural plate at the onset of gastrulation. Development, 125, 3247-58.

Kuroda H., Wessely O., De Robertis E. M. (2004). Neural induction in *Xenopus*: requirement for ectodermal and endomesodermal signals via Chordin, Noggin, β-Catenin, and Cerberus. PLoS Biol, 2, E92.

Kuroda H., Fuentealba L., Ikeda A., Reversade B., De Robertis E. M. (2005). Default neural induction: neuralization of dissociated *Xenopus* cells is mediated by Ras/MAPK activation. Genes Dev, 19, 1022-7.

LaBonne C., Whitman M. (1994). Mesoderm induction by activin requires FGF-mediated intracellular signals. Development, 120, 463-72.

Lamb T. M., Harland R. M. (1995). Fibroblast growth factor is a direct neural inducer, which combined with noggin generates anterior-posterior neural pattern. Development, 121, 3627-36.

Lamb T. M., Knecht A. K., Smith W. C., Stachel S. E., Economides A. N., Stahl N., Yancopolous G. D., Harland R. M. (1993). Neural induction by the secreted polypeptide noggin. Science, 262, 713-8.

Launay C., Fromentoux V., Shi D. L., Boucaut J. C. (1996). A truncated FGF receptor blocks neural induction by endogenous *Xenopus* inducers. Development, 122, 869-80.

Laurent M. N., Blitz I. L., Hashimoto C., Rothbacher U., Cho K. W. (1997). The *Xenopus* homeobox gene twin mediates Wnt induction of goosecoid in establishment of Spemann's organizer. Development, 124, 4905-16.

Lee H.X., Ambrosio A.L., Reversade B., De Robertis E.M. (2006). Embryonic dorsal-ventral signaling: secreted frizzled-related proteins as inhibitors of tolloid proteinases. Cell.124 (1):147-59.

Li L., Yuan H., Weaver C. D., Mao J., Farr G. H., 3rd, Sussman D. J., Jonkers J., Kimelman D., Wu D. (1999). Axin and Frat1 interact with dvl and GSK, bridging Dvl to GSK in Wnt-mediated regulation of LEF-1. Embo J, 18, 4233-40.

Li W., Srinivasula S.M., Chai J., Li P., Wu J.W., Zhang Z., Alnemri E.S., Shi Y. (2002). Structural insights into the pro-apoptotic function of mitochondrial serine protease HtrA2/Omi. Nat Struct Biol. 9, 436-441.

Lin X., Buff E.M., Perrimon N., Michelson A.M. (1999). Heparan sulfate proteoglycans are essential for FGF receptor signaling during *Drosophila* embryonic development. Development. 126, 3715-3723.

Lipinska B., Zylicz M., Georgopoulos C. (1990). The HtrA (DegP) protein, essential for Escherichia coli survival at high temperatures, is an endopeptidase. J Bacteriol. 172, 1791-1797.

Liu J.P., Laufer E., Jessell T.M. (2001). Assigning the positional identity of spinal motor neurons: rostrocaudal patterning of Hox-c expression by FGFs, Gdf11, and retinoids. Neuron 32, 997-1012.

Logan C. Y. & Nusse R. (2004). The Wnt signaling pathway in development and disease. Annu Rev Cell Dev Biol, 20, 781-810.

Lustig, K. D., Kroll, K. L., Sun, E. E. & Kirschner, M. W. (1996). Expression cloning of a *Xenopus* T-related gene (Xombi) involved in mesodermal patterning and blastopore lip formation. Development, 122, 4001-12.

Maccarana M., Olander B., Malmstrom J., Tiedemann K., Aebersold R., Lindahl U., Li J.P., Malmström A. (2006). Biosynthesis of dermatan sulfate: chondroitin-glucuronate C5-epimerase is identical to SART2. J Biol Chem. 281, 11560-11568.

MacNicol A.M., Muslin A.J., Williams L.T. (1993). Raf-1 kinase is essential for early *Xenopus* development and mediates the induction of mesoderm by FGF. Cell 73, 571-583.

Maden M. (2002). Retinoid signalling in the development of the central nervous system. Nat Rev Neurosci, 3, 843-53.

Massague J. (2003). Integration of Smad and MAPK pathways: a link and a linker revisited. Genes Dev, 17, 2993-7.

Martin G. R. (1998). The roles of FGFs in the early development of vertebrate limbs. Genes Dev, 12, 1571-86.

Meyers E. N., Lewandoski M., Martin G. R. (1998). An Fgf8 mutant allelic series generated by Cre- and Flp-mediated recombination. Nat Genet, 18, 136-41.

Miller J. R., Hocking A. M., Brown J. D., Moon R. T. (1999). Mechanism and function of signal transduction by the Wnt/β-catenin and Wnt/Ca2+ pathways. Oncogene, 18, 7860-72.

Mizuseki K., Kishi M., Matsui M., Nakanishi S., Sasai Y. (1998). *Xenopus* Zic-related-1 and Sox-2, two factors induced by chordin, have distinct activities in the initiation of neural induction. Development, 125, 579-87.

Mizuseki K., Kishi M., Shiota K., Nakanishi S., Sasai Y. (1998). SoxD: an essential mediator of induction of anterior neural tissues in *Xenopus* embryos. Neuron, 21, 77-85.

Moreno M., Munoz R., Aroca F., Labarca M., Brandan E., Larrain J. (2005). Biglycan is a new extracellular component of the Chordin-BMP4 signaling pathway. EMBO J. 24, 1397-1405.

Munoz R., Moreno M., Oliva C., Orbenes C., Larrain J. (2006). Syndecan4 regulates non-canonical Wnt signalling and is essential for convergent and extension movements in *Xenopus* embryos. Nat Cell Biol. 8, 492-500.

Niehrs C., Meinhardt H. (2002). Modular feedback. Nature 417, 35-36.

Nieuwkoop P. D. The formation of the mesoderm in urodelean amphibians I. The induction by the endoderm. (1969). *W. Roux´Arch. Ent. Org.* 162, 341-373.

Nieuwkoop P. D. and Faber J. (1994) Normal table of Xenopus leavis (Daudin) A systematical and chronological survey of the development from the fertilized egg till the end of metamorphosis.

Nishimatsu S., Suzuki A., Shoda A., Murakami K., Ueno N. (1992). Genes for bone morphogenetic proteins are differentially transcribed in early amphibian embryos. Biochem Biophys Res Commun, 186, 1487-95.

Nutt S.L., Dingwell K.S., Holt C.E., Amaya E. (2001). *Xenopus* sprouty2 inhibits FGF-mediated gastrulation movements but does not affect mesoderm induction and patterning. Genes and Development 15, 1152-1166

Oda S., Nishimatsu S., Murakami K., Ueno N. (1995). Molecular cloning and functional analysis of a new activin beta subunit: a dorsal mesoderm-inducing activity in *Xenopus*. Biochem Biophys Res Commun, 210, 581-8.

Oka C., Tsujimoto R., Kajikawa M., Koshiba-Takeuchi K., Ina J., Yano M., Tsuchiya A., Ueta Y., Soma A., Kanda H., Matsumoto M., Kawaichi M. (2004). HtrA1 serine protease inhibits signaling mediated by Tgfβ family proteins. Development 131, 1041-1053.

Onichtchouk D., Gawantka V., Dosch R., Delius H., Hirschfeld K., Blumenstock C., Niehrs C. (1996). The Xvent-2 homeobox gene is part of the BMP-4 signalling pathway controlling dorsoventral patterning of *Xenopus* mesoderm. Development, 122, 3045-53.

Ornitz D.M. (2000) FGFs, heparan sulfate and FGFRs: complex interactions essential for development. Bioessays 22, 108-112.

Ornitz D.M. (2005). FGF signaling in the developing endochondral skeleton. Cytokine Growth Factor Rev. 16, 205-213.

Penc S. F., Pomahac B., Winkler T., Dorschner R. A., Eriksson E., Herndon M., Gallo R. L. (1998). Dermatan sulfate released after injury is a potent promoter of fibroblast growth factor-2 function. J Biol Chem, 273, 28116-21.

Peng Y., Jiang B. H., Yang P. H., Cao Z., Shi X., Lin M. C., He M. L., Kung H. F. (2004). Phosphatidylinositol 3-kinase signaling is involved in neurogenesis during *Xenopus* embryonic development. J Biol Chem, 279, 28509-14.

Pera E.M., Wessely O., Li S.Y., De Robertis E.M. (2001). Neural and head induction by insulin-like growth factor signals. Dev Cell. 1, 655-665.

Pera E.M., Ikeda A., Eivers E., De Robertis E.M. (2003). Integration of IGF, FGF, and anti-BMP signals via Smad1 phosphorylation in neural induction. Genes Dev. 17, 3023-3028.

Pera E.M., Hou S., Strate I., Wessely O., De Robertis E.M. (2005). Exploration of the extracellular space by a large-scale secretion screen in the early *Xenopus* embryo. Int J Dev Biol. 49, 781-796.

Powers C.J., McLeskey S.W., Wellstein A. (2000). Fibroblast growth factors, their receptors and signaling. Endocr Relat Cancer 7, 165-197.

Pownall M.E., Tucker A.S., Slack J.M., Isaacs H.V. (1996). eFGF, Xcad3 and Hox genes form a molecular pathway that establishes the anteroposterior axis in *Xenopus*. Development 122, 3881-3892.

Presta M., Dell'Era P., Mitola S., Moroni E., Ronca R., Rusnati M. (2005). Fibroblast growth factor/fibroblast growth factor receptor system in angiogenesis. Cytokine Growth Factor Rev, 16, 159-78.

Quentin E., Gladen A., Roden L., Kresse H. (1990). A genetic defect in the biosynthesis of dermatan sulfate proteoglycan: galactosyltransferase I deficiency in fibroblasts from a patient with a progeroid syndrome. Proc Natl Acad Sci U S A. 87, 1342-1346.

Rapraeger A., Bernfield, M. (1985). Cell surface proteoglycan of mammary epithelial cells. Protease releases a heparan sulfate-rich ectodomain from a putative membrane-anchored domain. J Biol Chem, 260, 4103-9.

Rapraeger A.C., Krufka A., Olwin B.B. (1991). Requirement of heparan sulfate for bFGF-mediated fibroblast growth and myoblast differentiation. Science 252, 1705-1708.

Rebagliati M. R., Dawid, I. B. (1993). Expression of activin transcripts in follicle cells and oocytes of *Xenopus laevis*. Dev Biol, 159, 574-80.

Reifers F., Bohli H., Walsh E. C., Crossley P. H., Stainier D. Y., Brand M. (1998). Fgf8 is mutated in zebrafish acerebellar (ace) mutants and is required for maintenance of midbrain-hindbrain boundary development and somitogenesis. Development, 125, 2381-95.

Richard-Parpaillon L., Heligon C., Chesnel F., Boujard D., Philpott A. (2002). The IGF pathway regulates head formation by inhibiting Wnt signaling in *Xenopus*. Dev Biol. 244, 407-417.

Riou J. F., Delarue M., Mendez A. P., Boucaut J. C. (1998). Role of fibroblast growth factor during early midbrain development in *Xenopus*. Mech Dev, 78, 3-15.

Reversade B., De Robertis E.M. (2005). Regulation of ADMP and BMP2/4/7 at opposite

embryonic poles generates a self-regulating morphogenetic field. Cell. 2005 Dec 16;123(6):1147-60.

Reversade B., Kuroda H., Lee H., Mays A., De Robertis E.M. (2005). Depletion of Bmp2, Bmp4, Bmp7 and Spemann organizer signals induces massive brain formation in Xenopus embryos. Development. 2005 Aug;132(15):3381-92. Epub 2005 Jun 23.

Saka Y., Smith J.C. (2001). Spatial and temporal patterns of cell division during early *Xenopus* embryogenesis. Dev Biol. 229, 307-318.

Saksela O., Moscatelli D., Rifkin D. B. (1987). The opposing effects of basic fibroblast growth factor and transforming growth factor beta on the regulation of plasminogen activator activity in capillary endothelial cells. J Cell Biol, 105, 957-63.

Saksela O., Rifkin D.B. (1990). Release of basic fibroblast growth factor-heparan sulfate complexes from endothelial cells by plasminogen activator-mediated proteolytic activity. J Cell Biol. 110, 767-775.

Salic A., Lee E., Mayer L., Kirschner M. W. (2000). Control of beta-catenin stability: reconstitution of the cytoplasmic steps of the wnt pathway in *Xenopus* egg extracts. Mol Cell, 5, 523-32.

Sasai Y., Lu B., Steinbeisser H., De Robertis E.M. (1995). Regulation of neural induction by the Chd and Bmp-4 antagonistic patterning signals in *Xenopus*. Nature. Oct 26;377(6551):757.

Sasai Y., Lu B., Piccolo S., De Robertis E. M. (1996). Endoderm induction by the organizer-secreted factors chordin and noggin in *Xenopus* animal caps. Embo J, 15, 4547-55.

Sasai Y. (1998). Identifying the missing links: genes that connect neural induction and primary neurogenesis in vertebrate embryos. Neuron, 21, 455-8.

Sato S. M., Sargent T. D. (1989). Development of neural inducing capacity in dissociated *Xenopus* embryos. Dev Biol, 134, 263-6.

Saxén L., Toivonen S. (1962). Primary Embryonic Induction (London: Academic Press Inc. Ltd.), pp. 119-135.

Shridhar V., Sen A., Chien J., Staub J., Avula R., Kovats S., Lee J., Lillie J., Smith D.I. (2002). Identification of underexpressed genes in early- and late-stage primary ovarian tumors by suppression subtraction hybridization. Cancer Res. 62, 262-270.

Schroeder K. E., Condic M. L., Eisenberg L. M., Yost H. J. (1999). Spatially regulated translation in embryos: asymmetric expression of maternal Wnt-11 along the dorsal-ventral axis in *Xenopus*. Dev Biol, 214, 288-97.

Sivak J.M., Petersen L.F., Amaya E. (2005). FGF signal interpretation is directed by Sprouty and Spred proteins during mesoderm formation. Dev Cell. 8, 689-701.

Sive H., Bradley L. (1996). A sticky problem: the *Xenopus* cement gland as a paradigm for anteroposterior patterning. Dev Dyn, 205, 265-80.

Skorko-Glonek J., Wawrzynow A., Krzewski K., Kurpierz K., Lipinska B. (1995). Site-directed mutagenesis of the HtrA (DegP) serine protease, whose proteolytic activity is indispensable for Escherichia coli survival at elevated temperatures. Gene 163, 47-52

Slack J. M., Darlington B. G., Heath J. K., Godsave S. F. (1987). Mesoderm induction in early *Xenopus* embryos by heparin-binding growth factors. Nature, 326, 197-200.

Smith J. C., Price B. M., Van Nimmen K., Huylebroeck D. (1990). Identification of a potent *Xenopus* mesoderm-inducing factor as a homologue of activin A. Nature, 345, 729-31.

Sokol S. Y., Klingensmith J., Perrimon N., Itoh K. (1995). Dorsalizing and neuralizing properties of Xdsh, a maternally expressed *Xenopus* homolog of dishevelled. Development, 121, 1637-47.

Souchelnytskyi S., Nakayama T., Nakao A., Moren A., Heldin C. H., Christian J. L., ten Dijke P. (1998). Physical and functional interaction of murine and Xenopus Smad7 with bone morphogenetic protein receptors and transforming growth factor-beta receptors. J Biol Chem, 273, 25364-70.

Spemann H., Mangold H. (1924). Ueber Induktion von Embryonalanlagen durch Implantation artfremder Organisatoren. Roux's Arch. Entw. Mech. Org. 100, 599-638. Reprinted and transl. Int. J. Dev. Biol. 45, 13-18.

Stennard F., Carnac G., Gurdon J. B. (1996). The *Xenopus* T-box gene, Antipodean, encodes a vegetally localised maternal mRNA and can trigger mesoderm formation. Development, 122, 4179-88.

Streit A., Berliner A. J., Papanayotou C., Sirulnik A., Stern C. D. (2000). Initiation of neural induction by FGF signalling before gastrulation. Nature, 406, 74-8.

Sun B. I., Bush S. M., Collins-Racie L. A., LaVallie E. R., DiBlasio-Smith E. A., Wolfman N. M., McCoy J. M., Sive H. L. (1999). derriere: a TGF-β family member required for posterior development in *Xenopus*. Development, 126, 1467-82.

Sun X., Meyers E.N., Lewandoski M., Martin G.R. (1999). Targeted disruption of Fgf8 causes failure of cell migration in the gastrulating mouse embryo. Genes Dev. 13, 1834-1846.

Suzuki A., Thies R. S., Yamaji N., Song J. J., Wozney J. M., Murakami K., Ueno N. (1994). A truncated bone morphogenetic protein receptor affects dorsal-ventral patterning in the early *Xenopus* embryo. Proc Natl Acad Sci U S A, 91, 10255-9.

Suzuki A., Ueno N., Hemmati-Brivanlou A. (1997). *Xenopus* msx1 mediates epidermal induction and neural inhibition by BMP4. Development, 124, 3037-44.

Suzuki A., Chang C., Yingling J. M., Wang X. F., Hemmati-Brivanlou A. (1997a). Smad5 induces ventral fates in *Xenopus* embryo. Dev Biol, 184, 402-5.

Suzuki A., Kaneko E., Ueno N., Hemmati-Brivanlou A. (1997b). Regulation of epidermal induction by BMP2 and BMP7 signaling. Dev Biol, 189, 112-22.

Takahashi S., Yokota C., Takano K., Tanegashima K., Onuma Y., Goto J., Asashima M. (2000). Two novel nodal-related genes initiate early inductive events in *Xenopus* Nieuwkoop center. Development, 127, 5319-29.

Tannahill D., Melton D. A. (1989). Localized synthesis of the Vg1 protein during early *Xenopus* development. Development, 106, 775-85.

Tao Q., Yokota C., Puck H., Kofron M., Birsoy B., Yan D., Asashima M., Wylie C. C., Lin X., Heasman J. (2005). Maternal wnt11 activates the canonical wnt signaling pathway required for axis formation in *Xenopus* embryos. Cell, 120, 857-71.

Taylor K.R., Rudisill J.A., Gallo R.L. (2005). Structural and sequence motifs in dermatan sulfate for promoting fibroblast growth factor-2 (FGF-2) and FGF-7 activity. J Biol Chem. 7, 5300-5306.

Teel A.L., Yost H.J. (1996). Embryonic expression patterns of *Xenopus* syndecans. Mech Dev. 59, 115-127.

Thomsen G., Woolf T., Whitman M., Sokol S., Vaughan J., Vale W., Melton D. A. (1990). Activins are expressed early in *Xenopus* embryogenesis and can induce axial mesoderm and anterior structures. Cell, 63, 485-93.

Thomsen G. H., Melton D. A. (1993). Processed Vg1 protein is an axial mesoderm inducer in *Xenopus*. Cell, 74, 433-41.

Tocharus J., Tsuchiya A., Kajikawa M., Ueta Y., Oka C., Kawaichi M. (2004). Developmentally regulated expression of mouse HtrA3 and its role as an inhibitor of TGF-β signaling. Dev Growth Differ. 46, 257-274.

Trowbridge J.M., Rudisill J.A., Ron D., Gallo R.L. (2002). Dermatan sulfate binds and potentiates activity of keratinocyte growth factor (FGF-7). J. Biol. Chem. 277, 42815-42820.

Trowbridge J.M., Gallo R.L. (2002). Dermatan sulfate: new functions from an old glycosaminoglycan. Glycobiology. 12, 117R-25R.

Tsang M., Friesel R., Kudoh T., Dawid I.B. (2002). Identification of Sef, a novel modulator of FGF signalling. Nat Cell Biol. 4, 165-169.

Tsang M., Dawid I.B. (2004). Promotion and attenuation of FGF signaling through the Ras-MAPK pathway. Sci STKE. 228, 1-5.

Umbhauer M., Marshall C.J., Mason C.S., Old R.W., Smith J.C. (1995). Mesoderm induction in *Xenopus* caused by activation of MAP kinase. Nature 376, 58-62.

Umbhauer M., Penzo-Mendez A., Clavilier L., Boucaut J., Riou J. (2000). Signaling specificities of fibroblast growth factor receptors in early *Xenopus* embryo. J Cell Sci. 113, 2865-2875.

Urban S., Lee J. R., Freeman M. (2001). *Drosophila* rhomboid-1 defines a family of putative intramembrane serine proteases. Cell, 107, 173-82.

Vonica A., Brivanlou A. H. (2006). An obligatory caravanserai stop on the silk road to neural induction: inhibition of BMP/GDF signaling. Semin Cell Dev Biol, 17, 117-32.

Wang S., Krinks M., Kleinwaks L., Moos M., Jr. (1997). A novel *Xenopus* homologue of bone morphogenetic protein-7 (BMP-7). Genes Funct, 1, 259-71.

Weaver C., Farr G. H., 3rd, Pan W., Rowning B. A., Wang J., Mao J., Wu D., Li L., Larabell C. A., Kimelman D. (2003). GBP binds kinesin light chain and translocates during cortical rotation in *Xenopus* eggs. Development, 130, 5425-36.

Weaver C., Kimelman D. (2004). Move it or lose it: axis specification in *Xenopus*. Development, 131, 3491-9.

Weeks D. L., Melton D. A. (1987). A maternal mRNA localized to the vegetal hemisphere in *Xenopus* eggs codes for a growth factor related to TGF-β. Cell, 51, 861-7.

Weinstein D.C., Marden J., Carnevali F., Hemmati-Brivanlou A. (1998). FGF-mediated mesoderm induction involves the Src-family kinase Laloo. Nature 394, 904-908.

Wessely O., Agius E., Oelgeschlager M., Pera E. M., De Robertis E. M. (2001). Neural induction in the absence of mesoderm: β-catenin-dependent expression of secreted BMP antagonists at the blastula stage in *Xenopus*. Dev Biol, 234, 161-73.

Wilken C., Kitzing K., Kurzbauer R., Ehrmann M., Clausen T. (2004). Crystal structure of the DegS stress sensor: How a PDZ domain recognizes misfolded protein and activates a protease. Cell 117, 483-494.

Wilson P. A., Hemmati-Brivanlou A. (1995). Induction of epidermis and inhibition of neural fate by Bmp-4. Nature, 376, 331-3.

Wilson P. A., Lagna G., Suzuki A., Hemmati-Brivanlou A. (1997). Concentration-dependent patterning of the *Xenopus* ectoderm by BMP4 and its signal transducer Smad1. Development, 124, 3177-84.

Wilson S. I., Graziano E., Harland R., Jessell T. M., Edlund T. (2000). An early requirement for FGF signalling in the acquisition of neural cell fate in the chick embryo. Curr Biol, 10, 421-9.

Wilson S. I., Rydstrom A., Trimborn T., Willert K., Nusse R., Jessell T. M., Edlund T. (2001). The status of Wnt signalling regulates neural and epidermal fates in the chick embryo. Nature, 411, 325-30.

Winnier G., Blessing M., Labosky P. A., Hogan B. L. (1995). Bone morphogenetic protein-4 is required for mesoderm formation and patterning in the mouse. Genes Dev, 9, 2105-16.

Xanthos J. B., Kofron M., Wylie C., Heasman J. (2001). Maternal VegT is the initiator of a molecular network specifying endoderm in *Xenopus laevis*. Development, 128, 167-80.

Xu T., Bianco P., Fisher L.W., Longenecker G., Smith E., Goldstein S., Bonadio J., Boskey A., Heegaard A.M., Sommer B., et al. 1998. Targeted disruption of the biglycan gene leads to an osteoporosis-like phenotype in mice. Nat Genet. 20, 78-82.

Xu R. H., Kim J., Taira M., Lin J. J., Zhang C. H., Sredni D., Evans T., Kung H. F. (1997). Differential regulation of neurogenesis by the two *Xenopus* GATA-1 genes. Mol Cell Biol, 17, 436-43.

Yang X., Dormann D., Munsterberg A.E., Weijer C.J. (2002). Cell movement patterns during gastrulation in the chick are controlled by positive and negative chemotaxis mediated by FGF4 and FGF8. Developmental Cell 3, 425-437.

Yost C., Farr G. H., 3rd, Pierce S. B., Ferkey D. M., Chen M. M., Kimelman D. (1998). GBP, an inhibitor of GSK-3, is implicated in *Xenopus* development and oncogenesis. Cell, 93, 1031-41.

Zakin L., Reversade B., Kuroda H., Lyons K. M., De Robertis E. M. (2005). Sirenomelia in Bmp7 and Tsg compound mutant mice: requirement for Bmp signaling in the development of ventral posterior mesoderm. Development, 132, 2489-99.

Zhang J., King M. L. (1996). *Xenopus* VegT RNA is localized to the vegetal cortex during oogenesis and encodes a novel T-box transcription factor involved in mesodermal patterning. Development, 122, 4119-29.

Zhang Y., Chang C., Gehling D. J., Hemmati-Brivanlou A., Derynck, R. (2001). Regulation of Smad degradation and activity by Smurf2, an E3 ubiquitin ligase. Proc Natl Acad Sci U S A, 98, 974-9.

Zhu H., Kavsak P., Abdollah S., Wrana J. L., Thomsen G. H. (1999). A SMAD ubiquitin ligase targets the BMP pathway and affects embryonic pattern formation. Nature, 400, 687-93.

Zumbrunn J., Trueb B. (1996). Primary structure of a putative serine protease specific for IGF-binding proteins. FEBS Lett. 398, 187-192.

Curriculum Vitae

Name:	Shirui Hou
Date of birth:	Dec. 11, 1978
Place of birth:	Beijing, P. R. China
Nationality:	Chinese
Address:	Lund Stem Cell Center,
	BMC, B13, Klinikgatan 26,
	S-22184 Lund, Sweden
Telephone:	+46-46-22-23929
Fax:	+46-46-22-20899
E-mail:	conniehou@yahoo.com

Education

2007(expected)	**Ph.D,** International MSc/Ph.D Molecular Biology Program, Max Planck Research School, Georg August University Goettingen, Germany
04/2004	**MSc,** International MSc/Ph.D Molecular Biology Program, Max Planck Research School, Department of Developmental Biochemistry, Georg August University Goettingen, Germany
10/2002-10/2003	International MSc/Ph.D Molecular Biology program, Max Planck Research School, Georg August University Goettingen, Germany
06/2001	**BSc,** Department of Biology, College of Life Sciences, Nankai University, Tianjin, China

Research Experience

11/2005-current	**Lund Strategic Research Center for Stem Cell Biology and Cell Therapy, Lund, Sweden**

Ph.D candidate

Supervisor: Dr. Edgar Pera

Project: Regulation of FGF signaling by proteolysis in
the extracellular space

05/2004-11/2005   **Department of Developmental Biochemistry,**

Georg August University Goettingen, Germany

Ph.D candidate

Supervisor: Dr. Edgar Pera and Prof. T. Pieler

Project: Regulation of FGF signaling by proteolysis in
the extracellular space

10/2003-04/2004   **Department of Developmental Biochemistry,**

Georg August University Goettingen, Germany

MSc candidate

Supervisor: Dr. Edgar Pera and Prof. T. Pieler

Master project: A secreted serine protease with IGF binding motif
involved in anterior-posterior patterning of *Xenopus*
embryos

11/2001-08/2002   **Laboratory of Plant Biotechnology,**

Institute of Microbiology,

Chinese Academy of Sciences, Beijing, China

Research Assistant

Supervisor: Associate Prof. Xiaoying Chen

Project: Generation of transgenic rice using the agribacteria
method

09/1997-06/2001   **Department of Biology, College of Life Sciences,**

Nankai University, Tianjin, China

Supervisor: Prof. Qiang Chen

Project: The current status of biosensor and preparation of selective
modified electrode

Awards and Fellowships

05/2004-03/2006   Georg Lichtenberg fellowship,

Ministry for Science and Culture of Lower Saxony, Germany

10/2002-08/2003   Stipend International Max Planck Research School

10/2000-06/2001   Procter & Gamble (P&G) Academic Scholarship

10/1998-10/2000   Academic Scholarship of Nankai University

1998 - 2001   All Excellent Student of Nankai University

Publications

1. Hou S., Maccarana M., Min T. H., Strate I., and Pera E. M. The secreted serine protease HtrA1 acts as a positive feedback modulator of FGF signaling in *Xenopus* embryos. (accepted for publication in *Dev. Cell*).

2. Pera E. M., Hou S., Strate I., Wessely O., and De Robertis E. M. (2005). Exploration of the extracellular space by a large-scale secretion screen in the early *Xenopus* embryo. *International Journal of Developmental Biology* 49, 781-796.